The Effects of High Glucose Exposure on Endothelial Microparticles

Maddison Turner

A thesis submitted in partial fulfillment of the requirements for the

Masters of Science degree.

Cellular and Molecular Medicine

Faculty of Medicine

University of Ottawa

Abstract

Individuals with diabetes have an increased mortality due to the macro- and micro-vascular complications, which are commonly preceded by endothelial dysfunction. We have shown that endothelial microparticles (eMPs) are markers and mediators of vascular injury and pathology. However, their utility as a biomarker of hyperglycemia-induced endothelial damage and their influence on the vasculature remains unclear. We hypothesized that high glucose (HG) exposure alters eMPs protein composition, making them reflective of active signalling processes characteristic of a hyperglycemic environment. In addition, HG alters eMPs bioactivity, making them more potent inducers of oxidative stress, thrombosis and endothelial damage. Therefore, we assessed the exclusive effects of HG on eMPs formation, composition, and signalling. **Results:** Exposure of endothelial cells to high glucose for 24 hours caused a 3-fold increase in eMPs formation, increased mean vesicle size and their absolute electronegativity. Proteomic analysis of eMPs identified 1,212 independent proteins, with 68 exclusive to HG and associated with signalling processes related to metabolic processes, oxidation-reduction reactions, hemostasis and thrombosis and cellular interactions at the vascular wall. Compared to eMPs formed under normal conditions, eMPs formed in response to HG possess a ~3-fold greater pro-coagulant activity, induced a greater production of cellular ROS and were more potent inhibitors of endothelial-dependent relaxation. **Conclusions/Interpretation:** Taken together our results indicate HG alters the composition of eMPs, making them more potent mediators of endothelial damage. With similar changes in bioactivity being evident in the protein composition and the associated enriched biological processes, eMPs protein content may provide insight into the pathophysiological status of the cells in a hyperglycemic environment and provide use clinically, to identify dysregulated pathways for therapeutic targeting.

Table of Contents

Acknowledgements

I would like to take the time to thank the many people who helped and encouraged me during my M.Sc. For starters, I am very grateful for the opportunity to complete an M.Sc. with Dr. Dylan Burger. When I began as an undergraduate student I had very little scientific experience; thank you for taking the time to teach me the ins and outs of research. Your guidance, support and encouragement during my time at the KRC was greatly appreciated. Thank you for being tolerant with me following the centrifuge fiasco and patient during the many bouts of contamination, when your backups for your backups definitely came in handy! I would also like to thank you for the many conference opportunities you provided me with; presenting at the International Society of Hypertension in Seoul was an amazing experience that I will treasure. Besides my advisor, this M.Sc. would not have been possible without Mr. Anthony Carter, you vouched for me and introduced me to Dr. Burger while I was an undergraduate student and I am extremely appreciative of this opportunity.

I would also like to thank my co-supervisor Dr. Chris Kennedy and my thesis advisory committee Dr. Alexander Sorisky and Dr. Nuch Tanphaichitr for their encouragement, insightful comments, challenging questions and above all, taking the time to advise me on my thesis. My sincerest thanks go to Lawrence Puente, Arkadiy Reunov and Julie Zhu for their help and guidance on LC-MS/MS, TEM and wire myography experiments.

Thank you to the Italian Night Committee and the Kidney Foundation of Canada for generously providing me with the Agostino Monteduro Endowment Fund. This scholarship enabled me to travel to Chicago and present my research at the American Society of Nephrology Kidney Week to leading researchers in the field of kidney disease, diabetes and hypertension.

I would also like to thank my fellow lab mates; Mercedes Munkonda, Fengxia Xiao, Shareef Akbari, Suzy Sun, Larissa Reid and Jude Sanon, for the support, encouragement and entertainment that you provided. My time in the Burger lab was very enjoyable and I can say for certain, without our stimulating scientific discussions or more importantly, chatting about the latest gossip, I would have not enjoyed my time at the KRC quite as much. I am also forever in debt to both Mercedes and Fengxia, who kept backup HUVEC cultures, for when my cells became contaminated, which as you all know was a common occurrence and can finally be laughed about.

I cannot forget to thank my dearest friends and siblings. Whether you were living here in Ottawa, visiting me or facetiming me from across the pond or back home in London you've all helped me complete this M.Sc. in some way or another. I am extremely blessed to have you all in my life and to call you my friends.

And finally, I would like to express my profound gratitude to both Justin Richards and my parents, Dawn and Scott Turner. Justin, you came in to my life a little over a year ago and since then have pushed me to excel in every aspect of my life. My M.Sc. was definitely a rollercoaster and I am happy I had you by myside. You supported me and comforted me, motivated me and celebrated with me, worked at the lab on weekends with me and travelled to conferences with me; but most importantly, you never let me give up. Our trip to South Korea was amazing! Thank you for sitting in our tiny window-less hotel room for hours, listening to me practice my presentation and then celebrating with me afterwards, Gangnam style!

To my parents, words cannot describe how thankful I am to have you two in my life. You have been extremely generous and supportive throughout my educational endeavors. Even though neither of you have a research or scientific background you both went above and beyond

to help me when needed and I am eternally grateful! This M.Sc. would not be possible without the two of you!

"Perhaps they are not stars in the sky, rather opening where our loved ones shine through to let us know they are happy and safe."

In loving memory of Doris MacArthur.

Thank you for motivating and encouraging me to persevere through university. You were a strong advocate for the empowerment of women and firm believer in post-secondary education.

This is for you, Grandma!

List of Figures

List of Tables

List of Abbreviations

2-HE	2-Hydroxyethidium
ABs	Apoptotic Bodies
ApoE-/-	Apolipoprotein E Deficient
BSA	Bovine Serum Albumin
cMPs	Circulating Microparticles
CRP	C-Reactive Protein
DCF	2',7'-Dichlorofluorescein
DCFDA	7′-dichlorofluorescein diacetate fluorescence
DHE	Dihydroethidium
DM	Diabetes Mellitus
DMT	Danish Myo Technology
DTPA	Diethylenetriaminepentaacetic acid
ECs	Endothelial Cells
EDCFs	Endothelium Derived Contracting Factors
EDRFs	Endothelium Derived Relaxation Factors
eEVs	Endothelial Extracellular Vesicles
ELISA	Enzyme Linked Immunosorbent Assay
eMPs	Endothelial Microparticles
$eMPs^{HG}$	eMPs Cultured in 25mM D-Glucose (High Glucose)
$eMPs^{LG}$	eMPs Cultured in 25mM L-Glucose (Osmotic Control)
$eMPs^{NG}$	eMPs Cultured in 5.6mM D-Glucose (Normal Glucose)
EMS-18	EndoMAX Supplement 18
eNOS	Endothelial Nitric Oxide Synthase
erMPs	Erythrocyte Microparticles
ESRD	End Stage Renal Disease
Eth	Ethidium
EVs	Extracellular Vesicles
EXOs	Exosomes
FBS	Fetal Bovine Serum
FXa	Activated Factor X
HbA1C	Glycated Hemoglobin
HCAECs	Human Coronary Artery Endothelial Cells
HG	High D-Glucose
HMECs	Human Microvascular Endothelial Cells
HPLC	High Performance Liquid Chromatography
HUVECs	Human Umbilical Vein Endothelial Cells
ICAM	Intracellular Adhesion Molecular

IL-6	Interleukin-6
JEV	Journal of Extracellular Vesicles
KPSS	Potassium Physiological Saline Solution
LC-MS/MS	Liquid Chromatography-Tandem Mass Spectrometry
LG	L-Glucose
lMPs	Leukocyte Microparticles
MAEC	Mouse Aortic Endothelial Cells
mMPs	Monocyte Microparticles
MPs	Microparticles
NG	Normal Glucose
NO	Nitric Oxide
NTA	Nanoparticle Tracking Analysis
PAI-1	Plasminogen Activator Inhibitor-1
PBS	Phosphate Buffered Saline Solution
PGI_2	Prostacyclin
pMPs	Platelet Microparticles
PS	Phosphatidylserine
PSS	Physiological Saline Solution
RIPA	Radioimmunoprecipitation Assay Buffer
ROCK1	Rho Associated Kinase 1
ROS	Reactive Oxygen Species
T1DM	Type 1 Diabetes Mellitus
T2DM	Type 2 Diabetes Mellitus
TEM	Transmission Electron Microscopy
TF	Tissue Factor
TNF-α	Tumor Necrosis Factor-α
TNFR1	Tumor Necrosis Factor Receptor 1
TRAIL	TNF-Related Apoptosis-Inducing Ligand
TSG 101	Tumor Susceptibility Gene 101
VCAM	Vascular Cell Adhesion Molecule
VSMCs	Vascular Smooth Muscle Cells
vWF	vonWillbrand Factor

List of Publications

A portion of this thesis was published in Diabetalogia (2017). Permission to present my findings in this thesis can be found in section 7.0. Copyright Releas.

Burger D., **Turner M**., Xiao F., Munkonda MN., Akbari S., & K.D. Burns. (2017). High glucose increases the formation and pro-oxidative activity of endothelial microparticles. *Diabetologia* doi: 10.1007/s00125-017-4331-2.

1.0. Introduction

1.1. Diabetes

Diabetes Mellitus (DM) is a group of metabolic disorders characterized by the body's inability to properly produce or use insulin. In 2016, approximately 3.5 million Canadians (20-79 years of age) were living with DM[1]. In the past, DM predominantly affected westernized and higher income countries; however with growing obesity and population rates, the prevalence in low-to middle-income countries is on the rise[2]. The World Health Organization estimates roughly 422 million adults worldwide (age = 18+) were living with DM in 2014, a 3.9 fold increase since 1980, when there were only 108 million worldwide[3]. Specifically, with respect to Canadians, the prevalence of DM in adults aged 20-79 is predicted to increase to 4.9 million by 2026[1], a 40% increase from 2016.

1.1.1. Insulin

Insulin is a 51 amino acid peptide hormone produced by beta cells in the pancreatic islets. It is an anabolic hormone required for the uptake, storage and metabolism of circulating glucose in adipose tissue, liver and skeletal muscle. At basal glucose levels, insulin is not produced or secreted and therefore glucose uptake at these tissues is slow. However, as blood glucose levels rise post-prandium, pancreatic beta cells produce and secrete insulin into the blood to stimulate glucose uptake. Insulin circulates to the target tissues, binds to insulin receptors and signals storage vesicles to mobilize glucose transporters (GLUT) 4 to the plasma membrane, resulting in a quicker more efficient uptake. Unfortunately, in DM the body is either deficient in insulin or

resistant to the hormone resulting in impaired glucose uptake and high circulating levels of glucose.

1.1.2. Insulin Deficiency, Resistance and Prediabetes

Insulin deficiency, the key characteristic of type 1 diabetes (T1DM) comprises approximately 5-10% of all DM diagnoses[4]. It is the consequence of an autoimmune dysfunction, whereby autoantibodies destroy the insulin secreting pancreatic beta cells, leaving the body unable to produce the hormone.

Insulin resistance, a main characteristic of type 2 diabetes (T2DM) occurs when target cells become desensitized and fail to respond to the hormone. With the reduced responsiveness, glucose levels remain elevated, signalling the beta cells to hypersecrete insulin. Over time this intense stress can lead to beta cell death and insulin deficiency[5]. Unlike T1DM, T2DM traditionally manifests in adulthood and its onset is associated with the presence of cardiovascular risk factors such as obesity, hyperglycemia, dyslipidemia, hypercoagulability, hypertension and smoking. However with the rise in childhood obesity and sedentary lifestyles, Canada's youth and adolescents are increasingly diagnosed with insulin resistance or prediabetes. Prediabetes is a state of slightly elevated blood glucose, which predisposing one to insulin resistance and future T2DM diagnoses. The Public Health Agency of Canada estimates in 2015, 5.7 million people (20+ years of age) were in a pre-diabetic state[1], a statistic estimated to increase to 6.4 million by 2025[1], creating a national cause for concern.

Blood glucose levels are routinely assessed over a 3-month period by quantifying one's glycated haemoglobin (HbA_{1C}) levels. Normal glucose HbA_{1C} readings are below

6.0%, whereas readings between 6.0-6.9% are classified as prediabetic and readings exceeding 7.0% are diagnosed with DM.

1.2. The Vascular System

The vascular system is composed of a network of blood vessels responsible for the transportation of nutrients, oxygen, hormones and cellular waste. Blood vessels are broadly characterized based on size (macro- versus micro-vessels) and function into 3 categories, arteries (arterioles), veins (venules) and capillaries. Arteries and veins consist of 3 circumferential tissue layers; the tunica adventitia, a tough outer layer consisting mainly of connective tissue, the tunica media, a middle layer of smooth muscle (vascular smooth muscle cells, VSMCs) and an inner monolayer of endothelial cells (ECs) called the endothelium, or tunica intima[6]. Oxygenated blood flows to target tissues and organs through large arteries, while deoxygenated blood flows away, through large veins, both of which make up the macro-vasculature. At the target tissue/organ, arteries and veins branch into smaller vessels, called arterioles and venules, which are part of the microvasculature. These smaller vessels are connected through a capillary network and are the smallest of vessel types, making up the rest of the microvasculature. They are composed solely of an endothelium, allowing for efficient nutrient and gas exchange between the blood and tissue[6].

1.2.1. The Endothelium

The endothelium is a type of epithelial tissue composed of a monolayer of cells, ECs that surround the inner lumen. ECs function varies depending on its vessel type, however broadly speaking they act as a selective barrier between the circulating blood and the surrounding tissue. They maintain vascular homeostasis and regulate a host of biological activities by controlling the expression of vasoconstrictors and vasodilators,

pro-coagulants and anti-coagulants, inflammatory and anti-inflammatory, and oxidizing and anti-oxidizing molecules. With a main goal of controlling blood flow, fluidity and pressure while also reducing the inflammatory and thrombotic signals in hopes of maintaining a quiescent state[6–9].

1.2.2. Endothelial Function

Prior to the seminal work by Furchgott *et al.*[10], the endothelium was thought of as a static barrier. This belief was proven false when Furchgott et *al.* observed the requirement of ECs for acetylcholine induced vascular relaxation, which lead to the discovery of endothelium-derived relaxing factors (EDRFs)[9–11].

Accordingly, a main function of the endothelium is to control blood flow and fluidity by regulating vascular tone. This is accomplished through the production of EDRFs and active regulatory mechanisms controlling the output of endothelial derived contracting factors (EDCFs). NO, a potent vasodilator is a highly reactive signalling molecule produced in ECs by endothelial NO synthase (eNOS)[8]. Once activated, eNOS oxidizes L-arginine to L-citrilline, producing NO as a by-product[8]. As NO is produced, it quickly diffuses from ECs into VSMCs, activating soluble guanylate cyclase (sGC), which converts cyclic guanosine triphosphate (cGTP) into cyclic guanosine monophosphate (cGMP), to induce smooth muscle relaxation (Figure 1)[12].

Prostacyclin (PGI_2), a member of the prostanoid group, is another potent vasodilator and regulator of homeostasis. PGI_2 is produced by ECs and works independent of NO. Its vasoactive actions are mediated through the prostacyclin receptor (IP), upon binding; there is an increase in cyclic adenosine monophosphate (cAMP) and

protein kinase A, resulting in a decrease in intracellular Ca^{2+} and ultimately smooth muscle relaxation[13].

1.2.3. Assessing Endothelial Function

Endothelial function is clinically assessed by measuring its ability to react to vasoactive substances or shear stress and used as an indicator of endothelial health in vascular pathology. Currently, ultrasound flow mediated dilation (FMD) and myograph assessment of a gluteal biopsy are being used.

Ultrasound FMD of the brachial artery is a measure of vascular reactivity from the change in brachial artery diameter in response to shear stress induced NO production[14]. A clinician wraps a pneumatic cuff around the patient's forearm, which is inflated to stop blood flow for 5 minutes. Upon deflation, the shear stress caused by the increase in blood flow induces eNOS-mediated NO production and subsequent smooth muscle relaxation. This change in vessel diameter is measured with an ultrasound machine to infer vessel reactivity[14]. Although non-invasive, this test is labour intensive and lacks reproducibility and reliability because it is operator and patient dependent.

A more invasive technique to assess endothelial function and rarely used in the clinical setting entails a myograph assessment of a micro-vessel obtained through gluteal biopsy. This requires a clinician to invasively obtain a biopsy sample from the patient's subcutaneous fat of the gluteal region to dissect out a resistance artery [15]. This vessel is then mounted on a myograph, pharmacologically stimulated to contract and the endothelium's ability to respond to vaso-active substances are assessed. In addition to the invasive nature of this technique, it is also time consuming and lacks intra-patient reproducibility. In light of this, there is a need for a clinical assessment of endothelial

function that is reproducible, reliable, translatable to the clinical setting, minimally invasive and an early indicator of cell stress and damage.

1.2.3. Endothelial Dysfunction

As mentioned, accompanying the high output of EDRFs, regulatory mechanisms actively reduce EDCF levels and function to maintain a quiescent anti-inflammatory and anti-thrombotic phenotype. However when the endothelium is chronically exposed to low-grade inflammation and oxidative stress, the endothelial phenotype shifts, becoming pro-constrictive (increased EDCF production), pro-oxidative, pro-inflammatory and pro-thrombotic (increased expression and secretion of pro-inflammatory and pro-adhesive factors) (Figure 1)[9,16–18].

1.2.3.1. The Effects of Oxidative Stress

ROS are highly reactive, oxygen containing molecules formed naturally, as by-products of oxygen metabolism. Initially, oxygen is reduced to superoxide (O_2^-) a potent ROS. This in turn can be dismutated to form hydrogen peroxide (H_2O_2), which is then partially reduced to hydroxyl radical (OH^-)[19]. A variety of reduction-oxidation reactions mediate their formation, such as xanthine oxidase, the mitochondrial electron transport chain, nicotine adenine dinucleotide phosphate (NADPH) oxidase, amino acid oxidase and metabolic reaction-induced peroxisome activity. Under physiological conditions, levels remain low with the help of enzymatic and non-enzymatic mechanisms[19]. Superoxide dismutase (SOD), catalase and glutathione peroxidase are enzymes that catalyze either the dismutation of O_2^- or the reduction of H_2O_2 to water. Non-enzymatically, vitamin C scavenges O_2^-, vitamin E defends and repairs against membrane oxidation,

glutathione monitors oxidative damage and detoxify enzymes and b-carotene inhibits downstream pro-oxidative signals such as NF- κB activation and tumor necrosis factor-α (TNF-α) production.

Basal ROS play a role in the host defense system and cell signalling. However under pathological conditions, antioxidant mechanisms cannot control the increased production. Therefore at high levels, ROS scavenge NO to produce peroxynitrate (a deleterious reactive nitrogen species), while also inactivating eNOS, thus decreasing the overall bioavailability of NO and negatively effecting vascular tone[8]. In addition, elevated ROS cause lipid peroxidation, disrupting the membrane lipid bi-layer and altering cell permeability and structure[19]. High ROS also stress and activate ECs, increasing the expression and secretion of pro-inflammatory, pro-adhesive and pro-thrombotic factors, such as vascular cell adhesion molecule (VCAM), intracellular adhesion molecule (ICAM), E-selectin, C-reactive protein (CRP), TNF-α, interleukin-6 (IL-6), plasminogen activator inhibitor (PAI-1), vonWillebrand factor (vWF) and P-selectin[19]. These factors enhance leukocyte, monocyte and platelet recruitment and adhesion to the vascular wall, compounding the stress and damage imposed on the endothelium[20,21]. Lastly, elevated ROS directly induce apoptosis through a various death receptors, such as Fas, TNF receptor type 1 (TNFR1) and receptors specific to TNF-related apoptosis-inducing ligand (TRAIL) type 1 and 2, in ECs[22,23]. With ECs death, cells detach, exposing the basement membrane to circulating blood[20]. The basement membrane is rich with proteoglycans, phospholipids, collagen and fibroblasts; when exposed to circulating blood it becomes the ideal surface for platelets to adhere and aggregate.

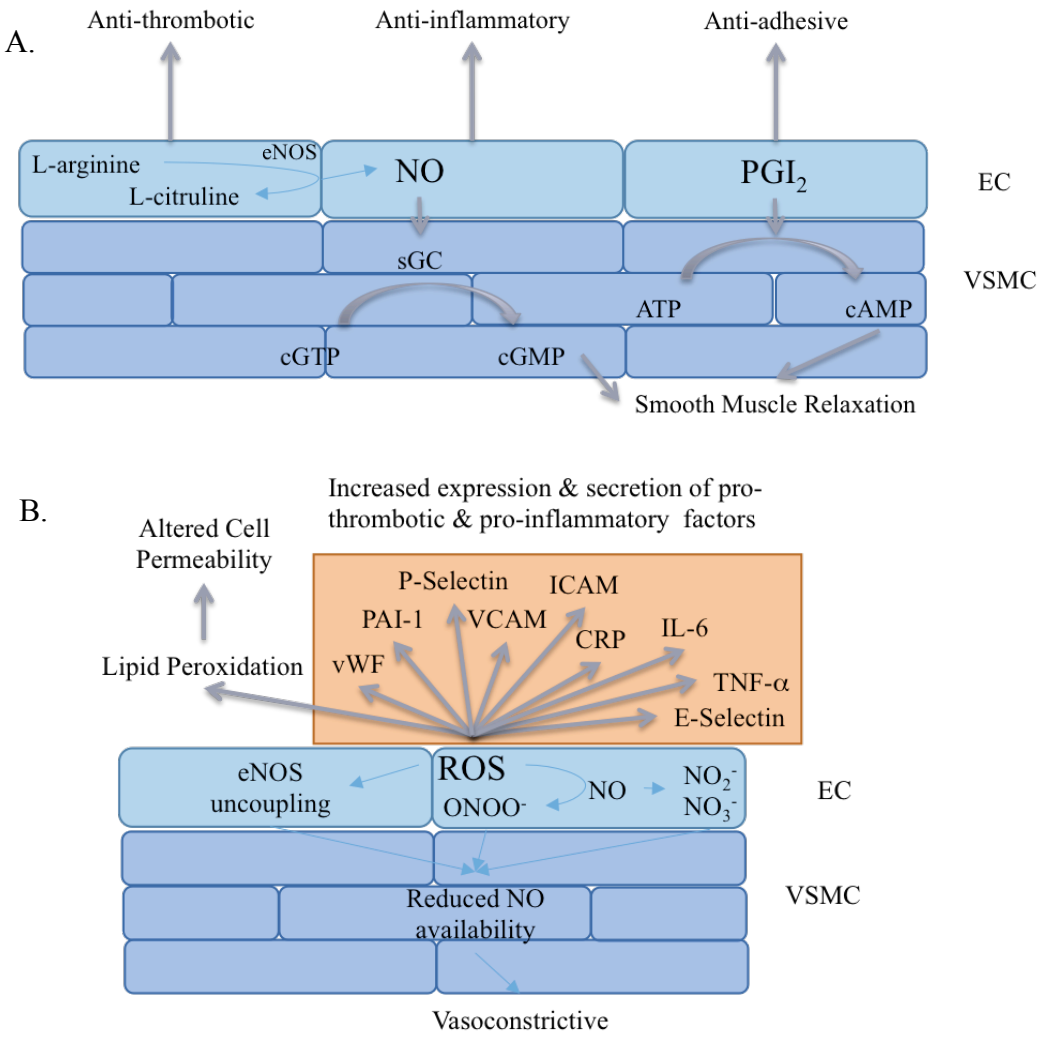

Figure 1: Endothelial function (a) and the molecular changes in response to endothelial damage (b).

1.2.3.2. Coagulation and Thrombosis

Under normal conditions, hemostatic mechanisms are in place to reduce blood loss and repair vascular injury via a fibrin clot. There are two pathways responsible for this, the intrinsic and extrinsic coagulation pathways that ultimately converge into one common pathway (Figure 2). The extrinsic cascade occurs in response to vascular injury and the release of tissue factor (TF), a cofactor for the activation of Factor X (FXa). While the intrinsic pathway,

otherwise known as the contact activation pathway, is initiated when circulating blood, more specifically Factor XII, encounters a negatively charged surface, a characteristic of an exposed basement membrane. This contact, initiates a cascade of activations converging with the extrinsic pathway (the common pathway) at the activation of Factor X (FXa) (Figure 2). Factor Xa activates prothrombin, converting it to thrombin; a reaction that requires the prothrombinase complex (phospholipids, phosphatidylserine (PS), Ca^{2+}, factors Va, Xa and prothrombin)[24,25]. In turn, thrombin converts fibrinogen peptides into fibrin, which accumulate at the site of injury as a fibrin clot. Blood coagulation and thrombus formation are the body's natural mechanisms to reduce bleeding following injury, however when the vasculature is chronically stressed, there is an increase in the expression of TF, pro-fibrotic factors pro-adhesive and pro-thrombotic factors as well as an increased externalization of PS (a negatively charged phospholipid), amplifying the adherence and aggregation of activated platelets ultimately leading to macro- and micro-vascular damages[24,25].

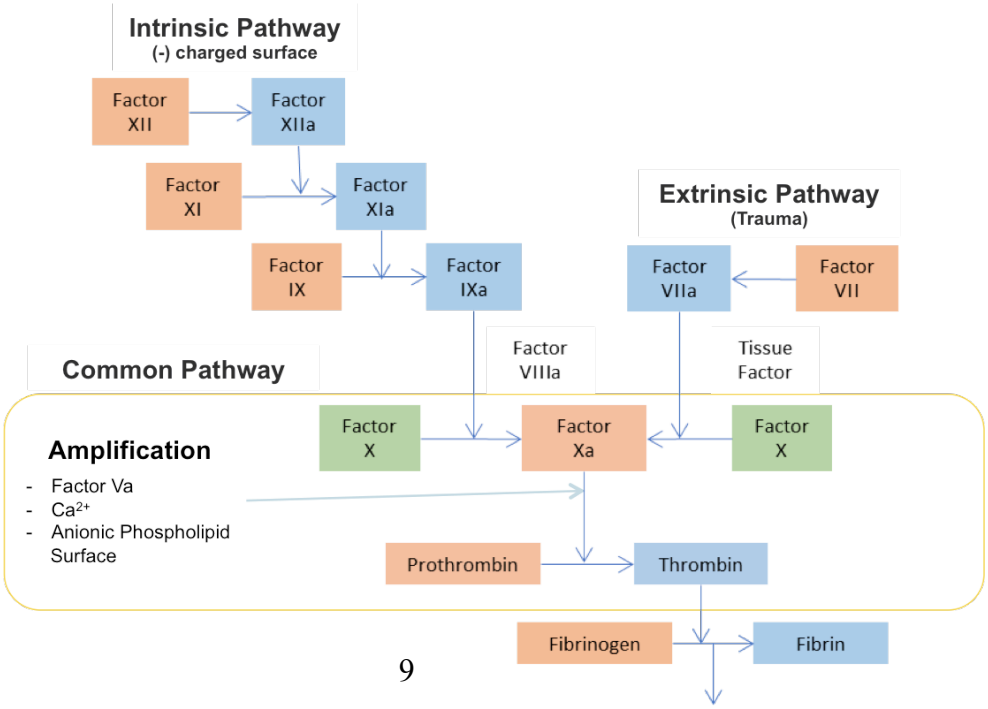

Figure 2: Coagulation and thrombus formation

1.3. Hyperglycemia and Vascular Damage

Macrovascular damages lead to the development and acceleration of large vessel atherosclerosis, commonly manifesting as coronary artery disease, peripheral vascular disease or cerebrovascular disease and stroke. While microvascular damages affect the microcirculation and commonly manifest as retinopathy (damage to the eyes), nephropathy (damage to the kidneys) and neuropathy (damage to the nerves)[26,27]. Among these complications, ECs injury appears to be an early hallmark, preceding the observable onset of macro-and micro-vascular complications. Not surprisingly, markers of ECs injury correlate with HbA_{1C} levels and future DM diagnoses[28,29].

While endothelial dysfunction is multifactorial, hyperglycemia is considered to play a significant causative role in damaging the vasculature. At the cellular level, glucose is taken up by ECs via insulin-independent facilitated diffusion and not tightly controlled[30]. Consequently, inadequate glucose uptake in target tissues leads to the accumulation of glucose and its metabolites in ECs, inducing intense metabolic stress.

At basal glucose levels, ECs glucose metabolism is primarily accomplished through glycolytic pathways due to the reduced quantity of mitochondria. However, at high glucose levels, glycolytic mechanisms cannot compensate for the intense influx. Excess glucose causes modifications to glyceraldehyde-3-phosphate dehydrogenase (GAPDH), resulting in a stall in glycolysis and an increase in glucose metabolites[31]. These metabolites and excess glucose are shunted into glycolysis side pathways leading to increased protein glycosylation, ROS production, eNOS uncoupling, and advanced

glycation end product (AGEs) productione[31]. As fructose-6-phophate accumulates, it is shunted down the hexosamine biosynthesis pathway, increasing protein glycosylation. More specifically, eNOS uncouples upon o-glycosylation leading to reduced NO production. Excess glucose is converted to sorbitol and in the processes depletes NADPH by converting it to $NADP^-$, increasing ROS production. In addition to this, sorbitol can be further converted to fructose, increasing the formation of AGEs, which are potent pro-inflammatory mediators contributing to vascular damage. Lastly, increased glucose stimulate arginase activity, the enzyme that consumes arginine, ultimately uncoupling eNOS and producing O_2^- instead[31].

In response to this influx of metabolic and oxidative stress, there is an increase in membrane lipid peroxidation, pro-inflammatory and pro-thrombotic gene expression and the endothelium gradually shifts its vaso-dilatory phenotype to become vaso-constrictive[12,31–34]. Not surprisingly, proper glycemic control slightly improves endothelial health and reduces micro- and macro- vascular complications in patients with DM [29,35,36]. Unfortunately, by the time DM is identified and therapeutic actions are taken to control glucose levels, endothelial function has been compromised and already increasing ones risk for cardiovascular complications. Therefore an early indicator of cell stress and endothelial damage is in need.

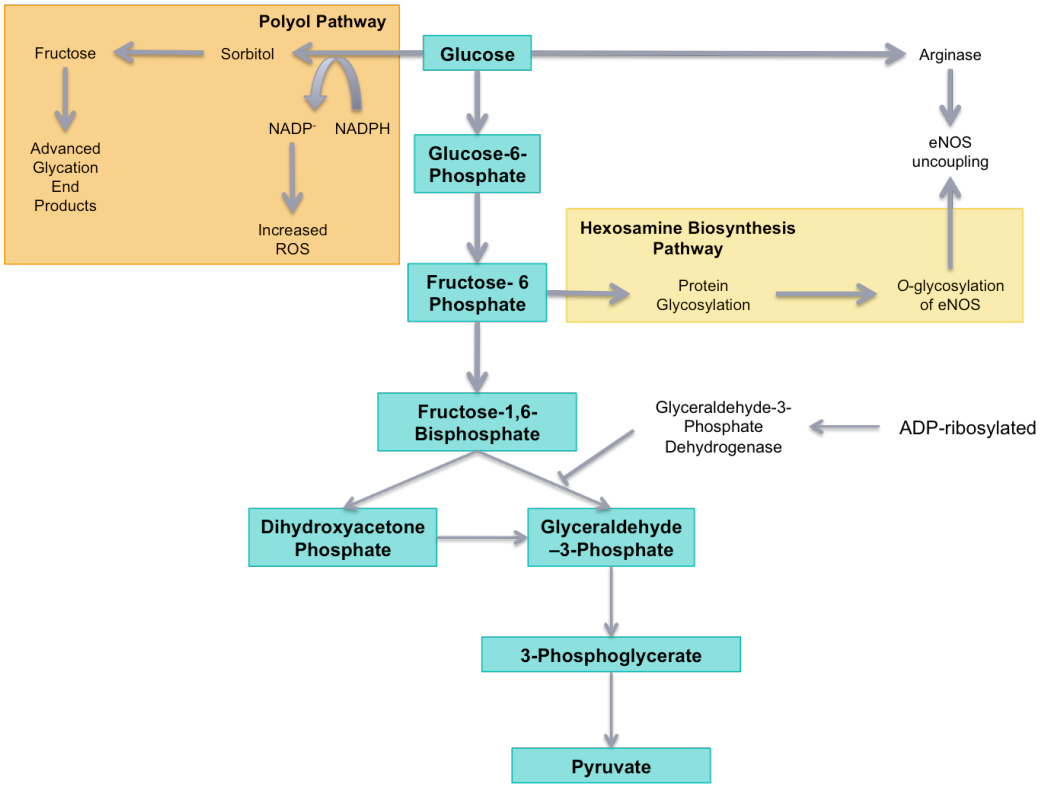

Figure 3: The effects of elevated glucose concentrations on glycolytic processes.

1.4. Extracellular Vesicles

Extracellular vesicles (EVs) are cell fragments ubiquitously released and found in bodily fluids, such as blood, lymph, cerebrospinal fluid or excreted in tears, saliva, urine, feces and breast milk[37–42]. While nomenclature is inconsistent, there are three types of vesicles that have been widely described: apoptotic bodies (ABs), microparticles (MPs) and exosomes (EXOs), which differ in size, mechanism of formation, composition and function[43,44].

ABs are formed during apoptosis, when the cell shrinks and fragments They are large cell fragments (>1000 nm in size) containing nuclear material, proteins, RNA and cell organelles[45,46]. Upon their release, ABs undergo phagocytosis, becoming engulfed and removed from the blood by phagocytic cells.

On the other side of the spectrum are exosomes, ranging from 40-100nm in size[46,47]. They are formed through inward membrane budding and enveloped by multi-vesicular bodies, which

fuse with lysosomes for proteolytic degradation or migrate to the cell membrane to release the vesicle contents into the extracellular milieu as exosomes[46]. Unlike ABs, EXOs do not contain nuclear material, rather, they are characterized by the presence of endosomal sorting proteins, tumor susceptibility gene 101 (TSG101), tetraspanins (CD63, CD81 and CD9) and membrane transport and fusion proteins[47]. EXOs are highly involved in intracellular communication and generally proposed as promoters of vascular homeostasis. They have the ability to inhibit cell senescence and apoptosis and aid in vascular development[46,48,49].

1.4.1. Microparticles

MPs, which range from 100-1000nm in size and are formed via external membrane budding and shedding in response to cell stress and activation and during the early stages of apoptosis[46]. They are small membrane blebs ubiquitously released and observed in all biological fluids in both healthy and disease states. Plasma has been extensively studied and found to contain a variety of circulating MPs (cMPs) originating from different cell types, such as endothelial- (eMPs), leukocyte- (lMPs), monocyte- (mMPs), platelet- (pMPs) and erythrocyte- (erMPs) derived MPs[46,50–53].

Many stimuli are responsible for MPs release. Specifically, eMPs formation is stimulated by cytokines, thrombin, PAI-1, CRP, angiopoietin-II, high glucose (HG) and shear stress[45,46]. Although, the exact molecular mechanism induced via these stressors remains unclear, they all elicit an increase in intracellular Ca^{2+}(Figure 4). Ca^{2+} influx activates calpain, a proteolytic enzyme, cytoskeletal proteins, such as spectrin and actin, and protein kinases like Rho associated kinase 1 (ROCK-1). These proteins are all crucial mediators in cytoskeletal reorganization and proteolysis [46,51]. In addition, the influx of Ca^{2+} activates floppase enzymes while inhibiting flippase enzymes, both of which are

ATP-dependent phospholipid membrane transporters responsible for outward (floppase) and inward (flippase) translocation. PS, a negatively charged phospholipid typically found on the inner portion of a healthy membrane, is one of the phospholipids translocated in response to Ca^{2+} influx. PS rapidly gets externalized by activated floppases and with flippase inhibition there is no compensatory internalization mechanism[51,54]. Thus, externalized PS becomes incorporated into the membrane blebs and is characteristic of MPs.

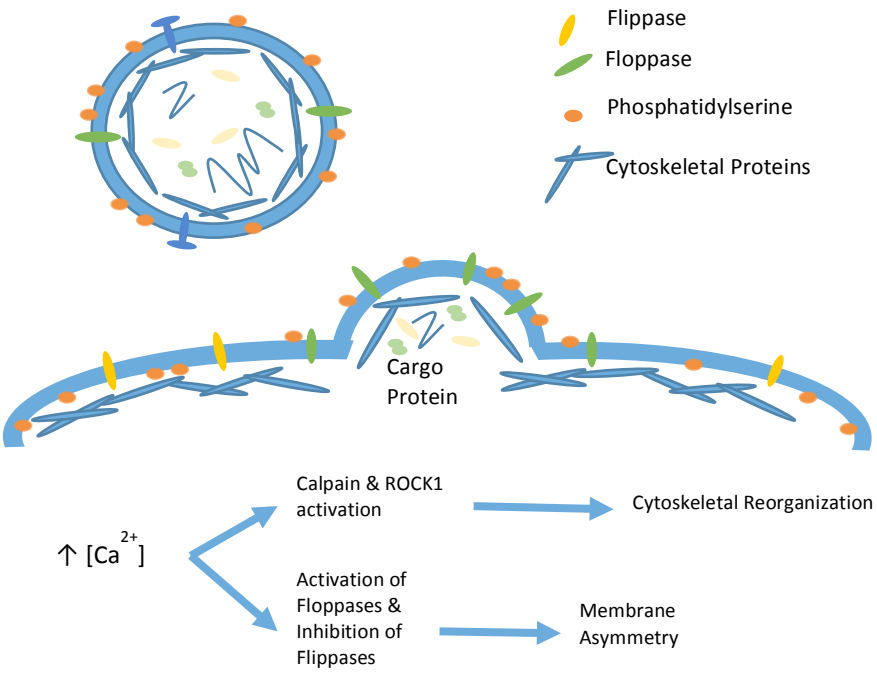

Figure 4: The molecular mechanism contributing to micropaticle formation.

In addition to PS, MPs are also composed of cell membrane and cytosolic proteins and RNA. Interestingly, their molecular cargo is a unique molecular fingerprint, specific to their origins[46,55,56]. Antibodies specific to PECAM (CD31), E-selectin (CD62E), VE Cadherin (CD144), Endoglin (CD105) and ICAM (CD54) are widely used to identify eMPs, while CD42a, CD42b, CD41, CD61 and P-selectin (CD62P) identify pMPs, CD14

to identify mMPs, CD45 for lMPs and CD235 for erMPs[45,46,57]. Not only can their cellular origins be identified from their protein composition, but also their biogenesis. A comparison of eMPs formed during activation versus apoptosis found that the former were enriched with ICAM, E-selectin and VCAM (CD106), while the latter were enriched with PECAM, Endoglin and VE-Cadherin[56]. Similarly, Peterson *et al.* identified marked changes in composition of eMPs derived from cells exposed to TNF-α versus PAI-1[58].

Initially, MPs were thought of as inert "platelet dust"[59,60]; however Barry et al[61] observed pMPs-mediated arachidonic acid transfer, and a subsequent increase in cyclooxygenase-2 and ICAM-1 expression among cultured ECs. Since these early findings, MPs have been identified as novel mediators of intracellular communication. Our lab and others have assessed their physiological effects *in vitro, ex vivo* and *in vivo* and concluded their ability to induce intracellular signalling responses leading to oxidative stress, inflammation, senescence, and apoptosis[46,55,62–64]. eMPs-induced oxidative stress has been attributed to both *de novo* ROS production and direct epidermal growth factor interactions (EGF-) receptor interactions[62,65,66]. Similarly, Sabatier *et al.* observed eMPs pro-inflammatory and pro-coagulant effects to be mediated by cell receptor-adhesion protein interactions[63]. In addition to direct receptor interactions, their pro-coagulant abilities have also been attributed to their anionic phospholipid (PS), TF and thrombin receptor containing membrane, which acts as the catalytic prothrombinase complex for the initiation of the coagulation cascade[46,51,55,67,68]. They have also been shown to amplify thrombus generation by recruiting, fusing and transferring their contents with activated platelets. In addition to these effects, eMPs are proposed as potent

modulators of vascular tone by impairing NO availability and inducing oxidative stress[62,66].

1.4.2. Microparticles in Pathology

Given that eMPs composition mirrors their origins and biogenesis, their utility as molecular biomarkers in vascular pathology is not surprising. Their levels, composition and biological activities have been quantified and assessed in response to different stimuli and in various diseases characterized by vascular damage and inflammation. eMPs levels are increased in response to both activation and apoptosis however both populations possess distinct molecular compositions, with the apoptosis-derived population being more procoagulant[56]. Extending on this, eMPs levels are elevated in vascular pathologies characterized by inflammation and oxidation stress, such as preeclampsia, hypertension, DM, end stage renal disease (ESRD), ischemic heart disease, hypertriglyceridemia, acute coronary artery disease and peripheral vascular disease[55,69,70]. Mallat *et al.* observed elevated pro-coagulant eMPs (expressing $CD146^+$ or $CD31^+$) in plasma collected from patients with acute coronary heart disease[71]. These eMPs reduced NO bioavailability and impaired vascular reactivity in isolated rat aortic rings when assessed through wire myography[71,72]. Similarly, Werner *et al.* report an increase in apoptosis derived eMPs in patients with acute coronary artery disease, which also impaired endothelial-dependent vascular reactivity via NO availability[73]. Extending on these eMPs-induced impairment in endothelial–dependent vascular reactivity, eMPs isolated from patients with metabolic syndrome showed a similar effect when injected in mice and measuring the response on a wire myograph[74]. Suggestive of a ubiquitous endothelial response following the exposure

of eMPs isolated from patients a disease characterized by inflammation and oxidative stress.

1.4.2.1. Microparticles in DM

In T1DM, Sabatier et al. observed an increase in cMPs, pMPs and eMPs levels, to which they correlated with HbA_{1C} levels[75]. Similarly, Feng et al. observed an increase in these MPs populations among patients with T2DM and report a positive correlation with HbA_{1C} levels[50]. More specifically, they report an increase in eMPs procoagulant ability and a negative correlation between eMPs levels and patient FMD scores, suggesting that as eMPs levels rise, the vessels responsiveness to shear stress-induced NO production decreases indicating an impairment in endothelial function[50]. Thus concluding the degree of eMPs elevation is proportional to the degree of endothelial damage. Extending on this, Sabatier et al. report a correlation between eMPs levels in patients with DM and future adverse cardiovascular complications, supporting the relationship between eMPs, endothelial damage and cardiovascular complications in DM[75,76].

1.4.2.2. Microparticles in High Glucose

Seeing as hyperglycemia is a major mediator and contributor to the development of endothelial dysfunction and eMPs levels are proportional to the degree of endothelial damage in DM, the exclusive effects of HG stress on eMPs biological activity and composition is attracting interest and being assessed. Jansen et al. observed an increase the induction of cellular ROS production, monocyte adhesion and downstream inflammatory signals in ECs treated with eMPs formed under HG stress ($eMPs^{HG}$) versus basal glucose conditions

(eMPs^{NG})[66]. Extending on this, they also observed (in response to eMPs^{HG}) an increase in atherosclerotic plaque formation and an impairment in endothelial dependent vascular reactivity, when using the Apolipoprotein E deficient mice (ApoE$^{-/-}$), a model to assess the development of atherosclerosis. Concluding that, eMPs^{HG} increase oxidative stress and promote inflammation, accelerating endothelial damage and atherosclerosis in underlying pathology[66].

In addition to the change in biological activity, evidence points to a change in eMPs^{HG} molecular composition. Zu et al. identify the presence of 30 Alzheimer's related proteins exclusively found in the eMPs^{HG} population[77]. Alzheimer's is a chronic neurodegenerative disorder with similar risk factors as insulin resistance and cardiovascular disease. Interestingly, patients with Alzheimer's have a higher risk of developing insulin resistance while DM patients have a higher risk of developing dementia. Zu et al. association between HG formed vesicles and their exclusive protein content being associated with Alzheimer's, provides an avenue to assess eMPs^{HG} utility as a biomarkers of cell stress and future cardiovascular events while also providing insight on active signalling processes occurring in the vasculature.

1.5. Rational, Hypothesis and Objectives

Literature indicates a compositional and functional change in eMPs in response to a hyperglycemic environment. Not only are they biologically more potent at impairing endothelial function through pro-inflammatory and pro-oxidative mechanisms; they are also biological vectors that convey information of their cellular origins and active signalling processes.

Accordingly, they may provide use as biomarkers of endothelial damage and dysfunction or markers for therapeutic targeting.

The purpose of this thesis was to assess the exclusive effects of HG on eMPs protein composition and biological activity to gain insight into the molecular events occurring in a hyperglycemic environment. As mentioned, MPs levels are routinely used as biomarkers for pathology and cell damage, in addition, $eMPs^{HG}$ possess a distinct protein composition associated with Alzheimer's disease. However, Zu et al. employ a non-selective method of vesicle isolation and therefore have probable EXOs contamination. In light of this, w*e hypothesize that* $eMPs^{HG}$ *(selectively isolated for 100-1000nm vesicles) protein composition are reflective of active cell signalling processes that mirror the clinical effects of hyperglycemia*. In addition, *we hypothesize HG alters eMPs bioactivity, making them more potent inducers of oxidative stress, thrombosis and endothelial dysfunction in the absence of underlying pathology.* Insight into the exact molecular signature of $eMPs^{HG}$ could assist with developing a simple and minimally invasive blood-based biomarker to help clinicians identify endothelial damage and vascular injury in DM and at risk populations as well as predict the prognosis of DM and future adverse cardiovascular complications.

2.0. Materials and Methods

2.1. Chemicals and Reagents

Information on all chemicals and reagents can be found in Table 1.

2.2. Buffers and Solutions

Buffers and solutions used were phosphate buffered saline (PBS, 1x and 0.05x), radioimmunoprecipitation assay (RIPA) buffer, transmission electron micrograph (TEM) fixative and buffer, tris glycine (10x), tris running buffer, physiological saline solution (PSS, 25x and 1x), potassium- physiological saline solution (KPSS, 10x and 1x) and Hanks buffer and high performance liquid chromatography (HPLC) solution A and B. All buffers and solution recipes can be found on Table 2.

2.3. Animal Handling

This study was approved by the animal ethics committee of the University of Ottawa and performed according to the recommendations of the Canadian Council for Animal Care. All mice were housed at the University of Ottawa animal care facility in a ventilated rack system with free access to food and water on a 12-hour day-night cycle. Endothelial dependent vessel reactivity was assessed on a wire myograph according to section 2.13 using mesenteric arteries isolated from male C57BL/6 mice, purchased from The Jackson Laboratory.

2.4. Culture of Endothelial Cells

Human umbilical vein endothelial cells (HUVECs) are a robust and widely used cell type when assessing ECs activities. Although venous in origins, HUVECs responses mirror other ECs in culture, with respect to NO production, and the expression of cell adhesion molecules[62,78,79]. In addition, they maintain their phenotype over large scale passaging, making them ideally suited

for the volume necessary to generate large quantities of MPs. Therefore, we elected to assess the effects of HG on eMPs with HUVECs origins.

HUVECs were purchased from American Type Culture Collection and cultured in a humidified incubator at 37°C and 5% CO_2. Cells were cultured on attachment factor coated flasks in EndoMAX Medium supplemented with EMS-18, 100 U/ml penicillin/streptomycin and 10% heat-inactivated-exosome-free fetal bovine serum (FBS). FBS was heated to 56°C for 30 minutes to inactivate the bovine-specific complement proteins and centrifuged at 100,000 x g (90 minutes, 4°C) to eliminate artificial and bovine-specific vesicles and RNA [43,44]. Resultant supernatant was defined as heat-inactivated-exosome-free FBS and used to supplement culture media as indicated above. Media was changed every two days, collected from cells at 75% confluence and stored at -80 °C for future processing.

2.5. Glucose Treatments and Cell Lysis

HUVECs were treated at 85% confluence with media containing 1) basal glucose (5.6mM D-glucose; $eMPs^{NG}$), 2) high glucose (25mM: basal glucose [5.6mM] + 19.4mM D-Glucose; $eMPs^{HG}$) or 3) high L glucose (basal glucose [5.6mM] + 19.4mM L-Glucose; $eMPs^{LG}$) for 24 hours. High L-glucose was used to control for osmotic stress and was chosen over mannitol because it is an enantiomer of D-glucose and taken up by the cell in a similar fashion. The 24hour treatment time and 25mM glucose dose was chosen to model acute uncontrolled hyperglycemia, shown to induce minimal apoptosis and allow for transcriptional responses to occur in an acute setting (Burger, unpublished work). Culture media was collected and centrifuged at 2500 xg to sediment apoptotic bodies. Residual supernatant was collected and stored at -80 °C for future processing. Zhou et al. report stable vesicle numbers following 7-month storage at -80°C versus -20°C; similarly, Yuana et al report stable numbers and size of

plasma EVs following 1-year storage[80,81]. Accordingly, we froze our samples at -80°C (as oppose to -20°C or 4°C) to reduce variability. Following vesicle isolation and prior to the initial freeze, samples were aliquot to smaller (single use) quantities to minimize multiple thaw cycles. To reduce the effects from freeze-thaw cycles untreated and treated samples remained in the same conditions. Trummer et al. report reduced MPs counts when samples thaw over ice versus at room temperature or at 37°C in a water bath, therefore we elected to thaw our samples at room temperature[82].

Treated cells were used to normalize vesicle numbers to cell protein and therefore washed twice with 1xPBS (at 4°C), scrapped in RIPA buffer (4°C, on ice), sonicated for 20 seconds to permebalize the membranes and centrifuged at 1,200 xg for 5 minutes (4°C). The supernatant was collected and cell protein concentration was measured according to section 2.7.

2.6. Extracellular Vesicle Isolation

Vesicle populations were isolated from collected culture media via differential centrifugation. Centrifugation fractions vesicles within a sample based on size and density. Initially, we deplete the media of larger particles, such as ABs and cell debris with a low speed spin (2500 xg for 10 minutes). The supernatant was then collected and centrifuged at 20,000 x g (20 minutes, 4°C) to separate MPs and EXOs and obtain a MPs-rich pellet. Finally, we isolate EXOs from the media with ultra-centrifugation at 100,000 x g (90 minutes, 4°C)[44,83]. Vesicle isolates were washed with 1xPBS via centrifugation at their respective protocols to reduce impurities and eliminate the contamination with different vesicle populations, extra-vesicular proteins, lipoprotein particles and aggregated vesicles, which are all common occurrences during vesicle isolation [43,44]. Lastly, vesicle isolates were stored at -80°C in 1xPBS for quantification,

sizing, TEM and biological activity assays, or RIPA buffer for liquid chromatography-tandem mass spectrometry (LC-MS/MS) analysis.

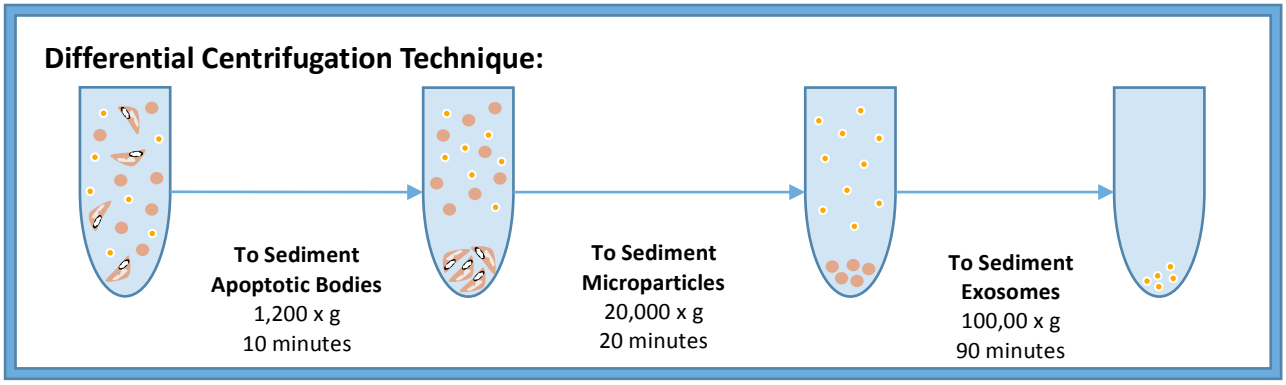

Figure 5: The centrifugation protocol to isolate extracellular vesicles.

2.7. Measurement of Protein Concentration

Vesicle and cell lysate protein concentration was measured using the Bio-Rad Detergent Compatible (DC) protein assay, according to manufacturer's instructions. The Bio-Rad protein kit is a colorimetric assay, whereby protein reacts with an alkaline copper tartrate solution (Reagent A) and is subsequently reduced by the folin reagent (Reagent B) to a product with a measurable absorbance.

Bovine serum albumin (BSA) was used as a reference standard and a stock solution (10.24g/ml) was prepped in RIPA buffer. The stock BSA was serially diluted in RIPA buffer (units = g/mL; 5.12, 2.56, 1.28, 0.64, 0.32, 0.16, 0.08, 0) and stored at -20^{o}C for future use. Samples in 1xPBS were diluted with RIPA buffer (1:1), while samples in RIPA buffer remained as is. Five microliters of both protein standards and samples (in duplicate) were added to the wells of a clear 96-well plate. Twenty microliters of the working reagent, 50:1 of the copper tartrate solution (Reagent A) and Reagent S, was added to each well, followed by 200µl of the folin solution (Reagent B). Absorbance was measured on the ELx808 Biotek's Absorbance reader (Biotek Instruments, Winooski VT, USA) at 750nm.

2.8. Extracellular Vesicle Characterization

Vesicle populations can be distinguished based on their size, morphology, and protein expression. The journal of extracellular vesicles (JEV) suggests at least 2 different techniques, showing vesicle size, morphology or protein expression, be used to confirm the existence of a vesicle population [43]. To confirm the sizing of vesicle isolates, NTA was employed (section 2.8.1) while membrane morphology was confirmed with TEM (section 2.8.2).

2.8.1. Nanoparticle Tracking Analysis of eMPs

NTA is a technique employed by the Zetaview PMX110 Multiple Parameter Particle Tracking Analyzer (Particle Metrix, Meerbusch Germany) to quantify and size particles in solution[84]. It utilizes a laser-scattering microscope to illuminate the suspended particles and a video camera to record the particle's Brownian motion (Figure 6). Brownian motion is the random movement of microscopic particles in suspension, due to collisions and interactions with surrounding particles. This particle displacement (per time interval, Dt) can be determined from point 1 to 2 using the x and y planes and calculated using Equation 1. The calculated particle displacement can be used with the Stokes-Einstein equation to infer physical characteristics (radius) of the particle (Equation 2). The zetaview calculates sizes for all particles in the recording to determine the average particle size and compute a size distribution chart.

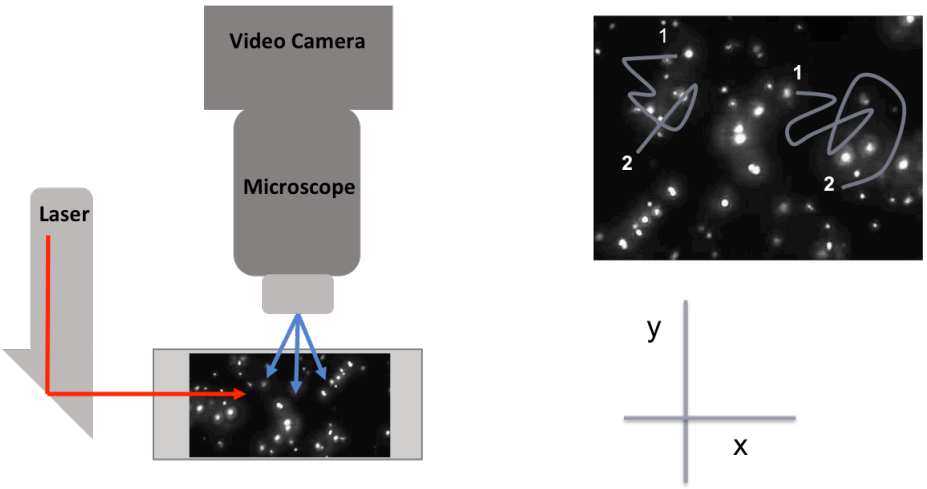

Figure 6: The theory behind the ParticleMetrix Zetaview and nanoparticle tracking analysis.

Equation 1: Average mean square displacement (1 → 2) per time interval.

$$Dt = \frac{< \overline{x,y}^2 >}{4}$$

Equation 2: Stokes-Einstein equation.

$$Dt = \frac{k_B T}{6\pi\eta r}$$

Dt = Particle Displacement/Time Interval
$< \overline{x,y}^2 >$= Mean Square Displacement
k_B = Boltzmann's Constant
T = Absolute Temperature
η = Viscosity of the Liquid
r = Radius of the Particle

2.8.1.1. Population Size Confirmation.

Culture media was collected from HUVECs at 90% confluence, centrifuged according to section 2.6 and figure 5 and vesicles were diluted to the working range of the system (~10^7 particles/ml) in 1xPBS. The Zetaview was programmed to capture 2-second videos, at 11 camera positions, with a camera frame rate of 15 fps (frames per second) (MPs) or 30 fps (EXOs) while in size mode. Videos were analyzed and with the

help of the particle tracking software (version 8.02.28), particle size was calculated as above, using Equations 1 and 2. The distribution of particle size was plotted and presented with the median size, mean size and the percentage of vesicles less than and greater than 105nm for the EXOs and MPs populations, respectively.

2.8.1.2. Quantification of eMPs Following HG Treatment.

The Zetaview was also used to assess the effects of 24 hours HG exposure on eMPs levels and size. HUVECs were treated according to section 2.5, media was collected, vesicles were isolated according to section 2.6 and suspended in 1xPBS (Figure 8 for schematic representation of treatment protocol and subsequent experiments). Samples were diluted with 1xPBS to the working range of the system and analyzed according to the MPs parameters above. Treated cells were harvested according to section 2.5 and protein concentration was measured according to section 2.7 to normalize eMPs concentrations to cell protein content.

2.8.1.3. Assessment of Zeta Potential Following HG Treatment.

In addition to size mode, the Zetaview features a zeta potential mode and is able to assess a particles zeta potential. "Zeta potential is a measure of surface charge of a particle and is dependent on its protein/phospholipid composition"[79] . It is an indicator of a particle's stability in solution and indirectly measured via a particles electrophoretic mobility. As depicted with figure 7, an electric field is applied to the fluid cell and the particles migration, is assessed at 2 stationary layers of the cell and the electrophoretic mobility is calculated using equation 3. From that, zeta potential is calculated using the Smoluchowski equation, equation 4.

To assess the effects of HG on eMPs zeta potential the treatment protocol depicted in Figure 8 was employed. Vesicles isolates were suspended in 0.05x PBS (to adjust the solutions conductivity to ~500μS/cm) and electrophoretic mobilities were measured in zeta potential mode.

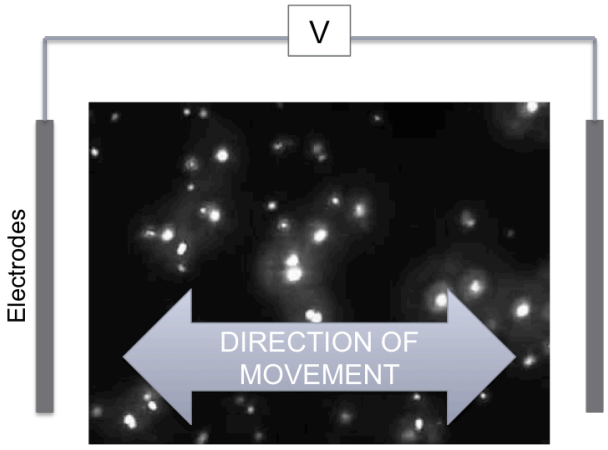

Figure 7: The theory of the Zetaview in zeta potential mode.

Equation 3: Electrophoretic Mobility Calculation.

$$\mu_e = \frac{v}{E}$$

μ_e = Electrophoretic Mobility
v = Velocity of Particle in Electric Field
E = Electrical Field

Equation 4: Smoluchowski Equation to Determine Zeta Potential.

$$\zeta = \frac{4\pi\eta}{\varepsilon} f(\kappa a) \cdot \mu_e$$

ζ = Zeta Potential
μ_e = Electrophoretic Mobility
f(κa) = Debye Function
η =Viscosity of Medium
ε = Dielectric Constant

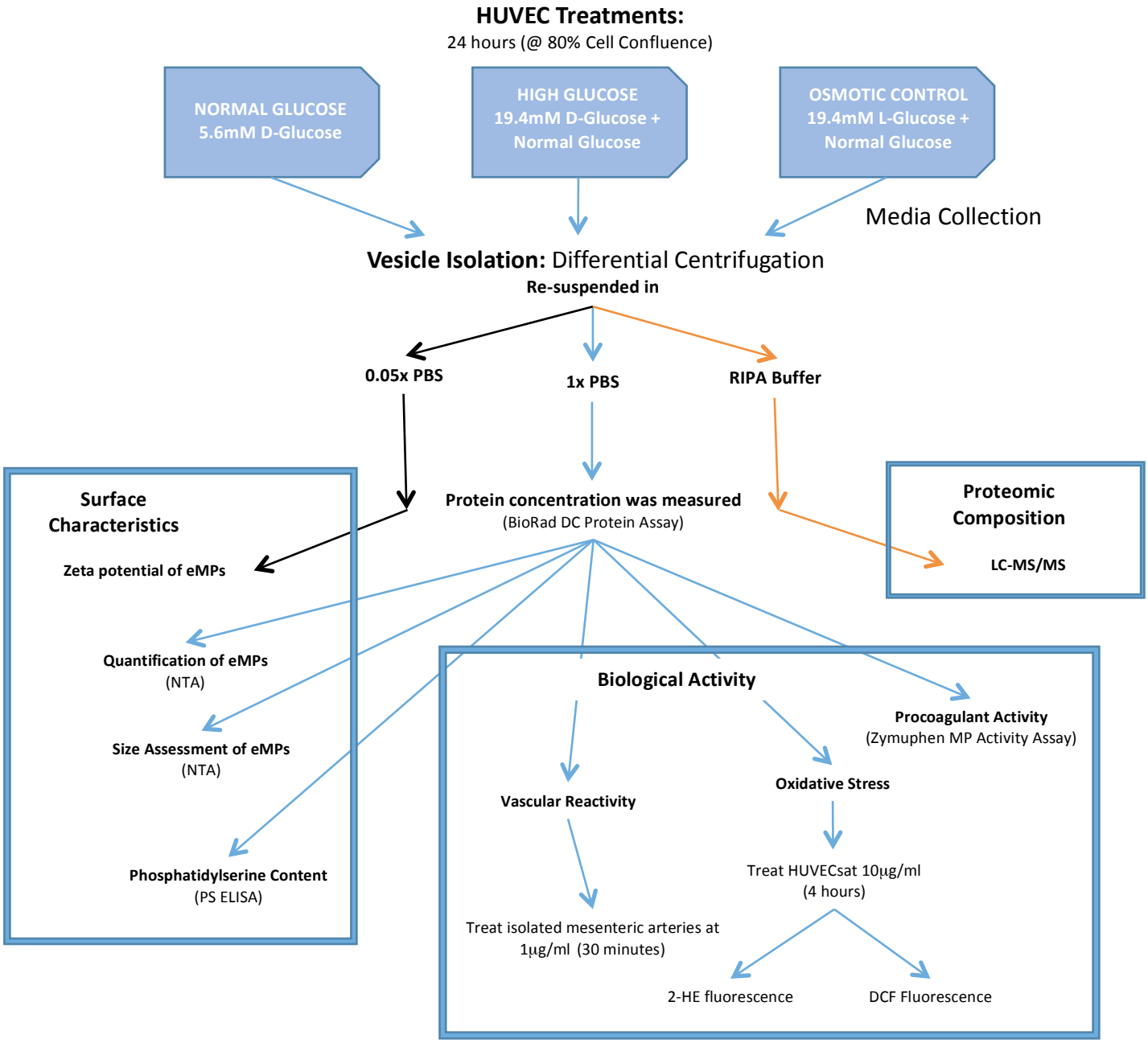

Figure 8: Thesis schematic of microparticle preparations and downstream applications.

2.8.2. Transmission Electron Microscopy of eMPs

TEM is an imaging technique like optical microscopy; however the generated image is based off the interaction between a beam of electrons and the samples atoms, as opposed to a beam of photons. Electrons have a smaller wavelength than photons, therefore TEM imaging can be done at a higher magnification, resulting in more detailed images[85].

TEM was conducted by Arkadiy Reunov as previously described, with slight modifications[86]. MPs and EXOs were isolated from media according to section 2.6 however remained in pellet form following the final wash step. Vesicle isolates were fixed overnight (4 ^{o}C) in TEM fixation buffer and washed the next day with 1M sodium cacodilate buffer, post-fixed in 2% OsO_4, and dehydrated in graded ethanol series and embedded in LF White Resin. Thin 60nm sections were cut, placed on cooper grids, covered by formvar film, dried and stained with 5% uranyl acetate in ethanol and Reynold's lead citrate. Vesicles were visualized on a JEM-1230 electron microscope (JEOL, Japan) and MPs were identified as small (0.1–1.0 μm), membrane enclosed, rounded objects.

2.9. eMPs Phosphatidylserine Content

We examined the effects of HG on the externalization of PS in eMPs with a human PS enzyme-linked immunosorbent assay (ELISA) kit (Elabscience, Beijing, China). Test samples were obtained and prepared according to the treatment protocol (Figure 8). Pilot experiments were conducted to optimize the working range of the assay and 1μg of eMPs protein was selected for subsequent experiments. The experiment was performed according to the manufacturer instructions with minor modifications; 1μg of sample protein was diluted with

sample diluent, added to the anti-PS pre-coated micro ELISA plate and incubated for 90 minutes (37^{o}C). Next, a biotinylated PS-specific antibody was added and incubated for 1 hour (37^{o}C), the wells were washed three times, and incubated with a horse radish peroxidase (HRP) conjugated secondary antibody for 30 minutes (37^{o}C), washed five times and incubated with the substrate reagent (TMB, 3,3',5,5'-tetramethylbenzidine) for 15 minutes to allow the reaction to occur and colour development. In the presence of HRP, TMB elicits a blue colour. With the addition of the stopping solution, sulphuric acid, the colour changes to yellow and the absorbance can be read at 450nm. We used the ELx808 Absorbance reader and expressed the results PS (ng/ml).

2.10. eMPs Protein Composition

We assessed the effects of HG on protein composition of eMPs via label-free LC-MS/MS and functionally analyzed the exclusive proteins for insights into distinct molecular signatures associated with a 24 hour HG exposure. Test samples was obtained and prepped according to the treatment protocol (Figure 8). Equivalent eMPs isolates (n = 3/eMPs treatment condition) were prepared in RIPA buffer plus 4x laemmli dye and separated by gel electrophoresis on a 4-15% Mini PROTEAN TGX Gel. Separated proteins were excised using a gel excision tool (The Gel Company, San Francisco CA, USA), placed in 1% acetic acid and sent to Lawrence Puente and the OHRI proteomics Core Facility. The in gel proteins were digested with trypsin, purified by ZipTip, concentrated in an Eppendorf vacufuge (ThermoFisher Scientific) and re-suspended in 0.1% formic acid.

2.10.1. Liquid Chromatography-Tandem Mass Spectrometry

Digested peptides were analyzed by label-free LC-MS/MS, with a system consisting of an UltiMate 3000 RSLC nano HPLC, LTQ Orbitrap XL hybrid mass

spectrometer, the XCalibur software (version 2.0.7) and a nanospray ionization source. An auto-sampler loaded the peptides into the trap column, in a 3% acetonitrile and 0.1% formic acid solution, (Acclaim PepMAP C18, ThermoFisher Scientific) at a flow rate of 15μL/minute for 5 minutes. Peptides were eluted over a 60 minute gradient of 3% - 45% acetonitrile at a flow rate of 300nL/minute through a 10-cm long column with integrated emitter tip (Picofrit PF360-75-15-N-5 from New Objective packed with Zorbax SB-C18, 5 micron from Agilent, Santa Clara, CA), and nano-sprayed into the MS. MS scans were acquired in FTMS mode at a resolution setting of 60,000. MS^2 scans were acquired in ion trap CID mode using data-dependent acquisition of the top 5 ions from each MS scan. The MASCOT software (Matrix Science, Boston MA, USA, version 2.5.1) was used to infer peptides and proteins from the observed MS/MS spectra and matched against human sequences from SwissProt (version 2014-08). Mass tolerance parameters were MS ±10 ppm and MS/MS ±0.6 Da. Enzyme specificities were set to 'Trypsin' with <=2 miscuts, variable modifications was set to oxidation of methionine, protein N-terminal acetylation, pyrocarbamidomethlyation of N-terminal cysteine, and conversion of glutamine to pyroglutamate and fixed modifications was set to Carbamidomethylation of cysteine.

2.10.2. Bioinformatics and Functional Analysis

"Identified MASCOT peptides and proteins were validated using Scaffold (Proteome Software Inc. Portland OR, USA version Scaffold_4.7.3, Proteome Software Inc., Portland OR, USA)" [79] . The scaffold local FDR algorithm accepted peptides with a greater than 95% probability and proteins were accepted if they contained at least 2 identified peptides and had a greater than 99% probability. Proteins with a minimum of 2

spectral counts in all three treatment samples were included in the ClueGO functional analysis. Cytoscape (3.4.0, java version: 1.8.0_121), a software platform to create, integrate and visualize complex networks, was used with the ClueGO and CluePedia plug-ins (v2.3.3 and v1.3.3)[87,88]. "Proteins exclusive to the eMPs^{HG} population were analyzed for functional enrichment in gene ontology biological processes (updated February 23, 2017) and Reactome pathways (updated March 1, 2017)" [79]. ClueGO recognized analyzed and clustered 67 out of the 68 uploaded proteins into functional groupings. Analysis parameters were set to perform a one sided hypergeometric tests for functional enrichments with a Benjamin-Hochberg correction, GO term fusion and a kappa score threshold of 0.4.

2.11. eMPs Procoagulant Activity

We assessed eMPs coagulant activity using the Zymuphen^{TM} MP Activity assay (Aniara, West Chester, OH, USA). PS is a procoagulant phospholipid that works with other thrombotic membrane proteins on the surface of eMPs, catalyzing the prothrombin to thrombin reaction in the coagulation cascade. In this assay, thrombin generation is quantified by the addition of a thrombin specific chromogenic substrate, which gets cleaved in the presence of thrombin and releases the p-nitroaniline (pNA) chromophore. This chromophore emits a yellow colour and the absorbance can measured at 405nm.

Test samples was obtained and prepped according to the treatment protocol (Figure 8**Error! Reference source not found.**). Pilot experiments were conducted to determine the working range of the assay, with 0.1 μg of eMPs protein as the optimal quantity of eMPs isolates (unpublished). Calibrators, controls and eMPs were loaded into an annexin V coated micro ELISA plate and incubated (1 hour at 37 ^{o}C) to allow PS-annexin V binding. Following several

washes, Reagent 1 (bovine FXa-FVa + Calcium) and Reagent 2 (human prothrombin) are added to the microplate and incubated (10 minutes at 37 ^{o}C). Reagent 3, the thrombin specific chromogenic reagent was introduced to the microplate wells, row by row (at precise time intervals) and the reaction was left to develop for ~3 minutes at 37 ^{o}C. Following the same time intervals, the reaction was stopped with 2% citric acid and left to stabilize for 10 minutes. eMPs pro-coagulant capacity was inferred from the absolute absorbance value measured at 405nm on the ELx808 Absorbance reader (blank subtracted).

2.12. eMPs-Induced Oxidative Stress

We assessed eMPs-induced oxidative stress on cultured HUVECs via dihydroethidium-high performance liquid chromatography (DHE-HPLC) and 7′-dichlorofluorescein diacetate fluorescence (DCFDA). For both techniques, HUVECs were treated with 10μg/mL of eMPs (obtained and prepped according to the treatment protocol Figure 8) or equivalent volumes of PBS for 4 hours; a dose and time point previously identified to induce oxidative stress in cultured mouse aortic endothelial cells (MAEC)[62].

2.12.1. DHE-HPLC

DHE is a non-fluorescent dye permeable to the plasma membrane, upon entry it specifically gets oxidized by O_2^- to form 2-hydroxyethidium and non-specifically by other intracellular ROS to form ethidium (Eth)[89]. Following cell harvest and acetonitrile extraction the reaction products can be separated via HPLC and quantified by fluorescence.

DHE-HPLC studies were conducted according to Fernandes et al with minor modifications[65,89–91]. Treatment eMPs were obtained and prepped according to the treatment protocol Figure 8 and the three-glucose eMPs populations were used to treat

healthy HUVECs for 4 hours at 10μg of eMPs protein/mL. Following treatments, cells were washed once with Hanks buffer + 100μM diethylenetriaminepentaacetic acid (DTPA) and incubated for 30 minutes (37ºC) with Hanks buffer + 100μM DTPA + 50μM DHE. DTPA has high affinity for metal cations and therefore used in our experiment to prevent artificial secondary oxidizing reactions[89,90]. Following the incubation, cells were washed twice with Hanks + 100μM DTPA, harvested in acetonitrile for DHE-product and DNA extraction, centrifuged at 12,000 x g (10 minutes, 4 °C) and the resultant supernatant was dried under vaccufuge (low setting, no heat, no light). HPLC solution A (Table 2) was used to re-suspend the extracted products, which were then injected into the HPLC system. The separation of DHE, 2-HE and Eth was conducted across an Agilent Zorbax C18 (pore size of 80 Å, surface area of 180 m^2/g) column, at a temperature of 26°C and a flow rate of 0.4ml/min. The flow began as 100:0 (Solution A: Solution B (Table 2)), decreased to 50:50 (Solution A: Solution B) in a step wise fashion over 10 minutes, remained for 10 minutes, then decreased to 0:100 (solution A: Solution B) in a step-wise fashion over 5 minutes. Between samples, the column was washed and equilibrated for 10 minutes with 100% solution A.

2-HE fluorescence was detected using an excitation of 510nm and emission of 595nm, while DHE was detected by ultraviolet absorption at 245nm and used as an internal control. Results were expressed as a ratio of 2-HE generated per DHE consumed (initial DHE concentration minus remaining)

2.12.2. DCFDA-Fluorescence

The second technique used to assess eMPs-induced oxidative stress, was quantifying the fluorescence of 2',7'-dichlorofluorescein (DCF). DCFDA is non-

fluorescent and diffuses into a cell, becomes de-acetylated by cellular esterases and subsequently oxidized by ROS into DCF. DCF is a quantifiable fluorescent compound with an excitation of 485nm and emission of 520nm[62,65,86]. Following the eMPs treatments (10 μg/ml, 4h, determined as above), HUVECs were washed with 1x assay buffer, incubated with 5 μM DCFDA for 30 minutes and washed twice with 1x assay buffer. Fluorescence was measured on the Fluostar Galaxy microplate reader (BMG Labtechnologies, Ortenbberg, Germany) with an excitation of 485 nm and emission of 520 nm.

2.13. Vascular Reactivity

Wire myography measures vascular reactivity, *ex vivo,* in isolated vessels mounted into a myograph chamber[91,92]. We assessed the effects of HG on eMPs-mediated damage of endothelial-dependent vascular reactivity. Male C57BL/6 mice (aged 3 – 4 months, 20-30g) were euthanized with CO_2 asphyxiation, third order mesenteric artery branches were dissected and cleaned of adhering fat. Vessels were cut to a length of 1.5-2mm using a light microscope, mounted on 2 tungsten wires (25 μm diameter, fed through the lumen), placed in the myograph chamber (Tissue Bath System – 720MO, DMT, Danish Myo Technology, Ann Arbor, MI, USA) and equilibrated in PSS (Table 2) for 10 minutes (37ºC, bubbled continuously with 95% O_2 and 5% CO_2). One wire is attached to a micrometer to measure the vessel circumference, while the other is attached to a force transducer to measure changes in wall tension.

Mounted vessels are normalized using the DMT normalization module in the LabChart 7 Pro software (ADInstruments, Dunedin, NewZealand, version 8.1.1). The normalization step is performed to standardize vessel studies to a consistent, baseline, physiologically relevant transmural pressure of 100mm Hg or 13.3kPa (kPa = mN/mm^2). Transmural pressure is the

difference in pressure between the inner and outer vessel wall. In a stepwise fashion, the internal circumference is manually increased and the force transducer computes the force exerted on the vessel wall. From that, the effective pressure (Pi/Transmural pressure) can be calculated using the Law of La Place equation (Equation 5)[93]. Once the baseline stretch has been determined, the vessel diameter remains constant to ensure isometric conditions[93].

Equation 5: Normalization Equation (Law of La Place):

$$Pi = \frac{T}{\frac{IC}{(2\pi)}}$$

Pi = Effective Pressure/Transmural Pressure (kPa =mN/mm^2)
T = Wall tension (force exhibited by vessel wall/unit of vessel lenght, mN/mm)
IC = Internal circumference (mm)

To assess vessel viability, vessels were maximally contracted with KPSS (Table 2) + 10^{-5} M of phenylephrine, a potent vaso-constrictor through its agonistic actions on α_1-adrenergic receptors, testing the vessels maximal relaxation, using acetylcholine (10^{-5} M), a vasodilator that exerts its effects on muscarinic receptors on the endothelium. Vessels failing to relax at least 70% of their maximal contraction were excluded, while included vessels were washed with fresh PSS, equilibrated for 20 minutes, and then randomly assigned to eMPs- or PBS-treated groups. Treatment eMPs were obtained and prepped according to the treatment protocol (Figure 8). Vessels were treated with either $eMPs^{NG}$, $eMPs^{HG}$ (10^4 eMPs/ml) or an equivalent volume of PBS and incubated for 30 minutes. Vessels were pre-constricted with phenylephrine at a concentration that caused approximately 80% of the previously determined maximal contraction and endothelial dependent relaxation was assessed in response to 10^{-9}-10^{-5}M serial doses of

acetylcholine. Maximal relaxation was considered when vessels relaxed either 1) 100% of its own pre-constriction, 2) began VSMCs-mediated contraction, an acetylcholine induced response when in excess, or 3) after the 10^{-5} M acetylcholine dose. Analysis was performed using LabChart 7 Pro software. Vascular reactivity was expressed as a percentage of acetylcholine induced relaxation and graphed on a logarithmic scale while acetylcholine potency was expressed as the pD_2 =-log(EC_{50}), otherwise known as the pEC_{50}. Briefly, EC_{50} is the acetylcholine dose that results in 50% of maximal effects. Keeping in mind our concentration response curve is on a logarithmic scale, the pD_2 makes for a visually simple graphical representation of the logEC_{50}.

2.14. Statistical Analysis

Unless otherwise noted comparisons were performed using an unpaired t-test (2 tailed) or one way ANOVA followed by a Bonferroni multiple comparison test, were appropriate. A value of $P<0.05$ was considered statistically significant and results are presented as means ± SEM.

3.0. Results

3.1. Confirmation of membranous vesicles ranging from 100-1000nm.

To confirm the presence of membrane-derived vesicles between 100-1000nm (MP characteristics) in the vesicle population isolated with a 20,000 xg, we assessed vesicle size via NTA and morphology via TEM. Figure 9 shows the distinct size distributions between the vesicle populations obtained from our centrifugation protocol. With 80% of the vesicles above 105nm and 20% below 105nm, which we conclude as debris (seeing as the Zetaview is an open system). With that in mind and the results from the electron micrographs showing membranous vesicles above 100nm (Figure 10), we conclude our 20,000 xg centrifugation protocol is capable of isolating a vesicle population with a size consistent with previous MPs literature[46,94].

3.2. High glucose alters eMPs levels and surface characteristics.

While eMPs are markers of vascular pathology and in DM levels have been correlated with HbA_{1c} levels, the exclusive effects of HG on eMPs properties are not fully understood[28,29,95]. Thus, we assessed 24 hour HG exposure on eMPs levels and size via NTA. As seen in Figure 11 and Figure 12, eMPs levels and size significantly increase with HG exposure compared to the NG and LG control conditions. Next, we assessed the vesicle's surface charge, by measuring their electrophoretic mobilities and observed an increase in their absolute electronegativity following HG exposure (Figure 13). A particle`s surface charge can be attributed to its surface protein and phospholipid composition, thus we quantified PS following HG treatment and observed a significant increase (Figure 14). These morphology changes are indicative of a HG-induced molecular signature of eMPs.

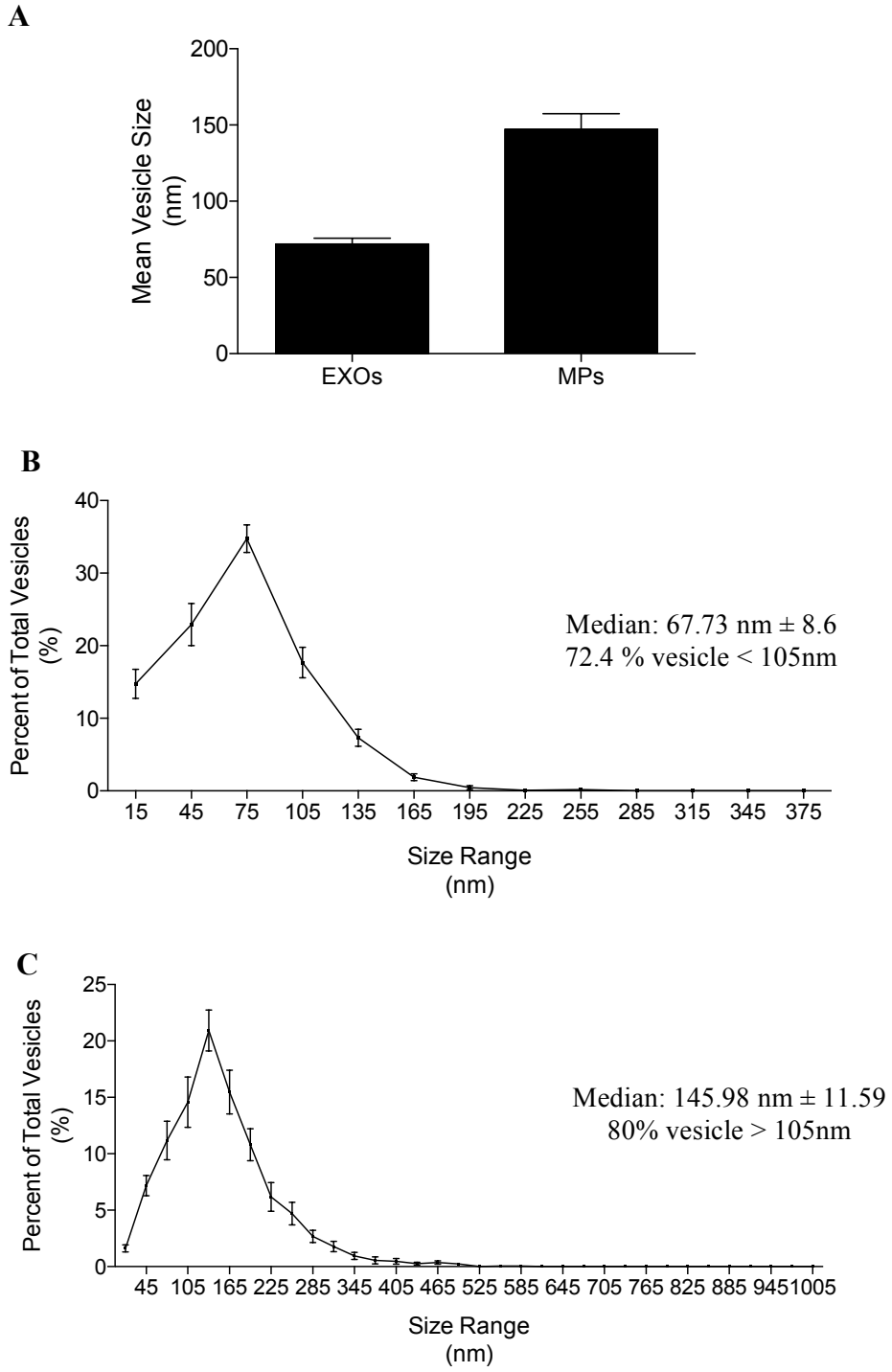

Figure 9: Size confirmation of vesicle isolates.

A: Mean Particle size of MPs and Exosomes isolates, assessed via NTA. B: Size distribution of the vesicle population obtained from the 100,000xg centrifugation, that we conclude as Exosomes. C: Size distribution of the vesicle population obtained from the 20,000xg centrifugation; that we conclude as Microparticles.

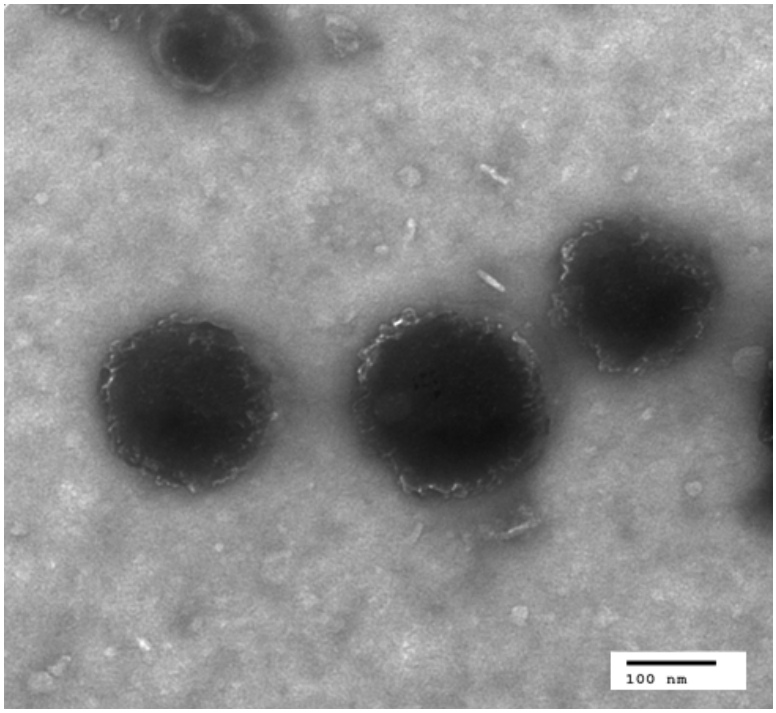

Figure 10: Confirmation of membranous vesicles sized 100-1000nm.

TEM images of vesicle isolates obtained via the 20,000xg centrifugation spin. Magnification: 25000x.

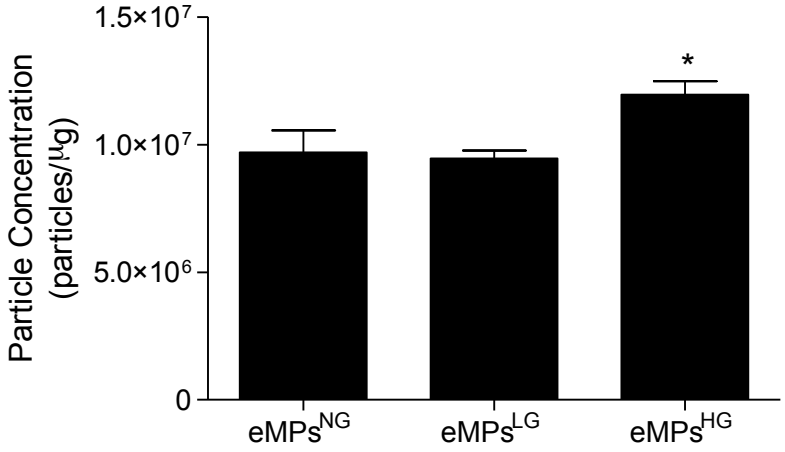

Figure 11: The effects of HG exposure on eMPs formation.

eMPs were collected and prepped as described in Figure 8 to quantify levels via NTA. Treated cells were harvested and protein was quantified and used to normalize results. *P<0.05 vs. $eMPs^{NG}$ & $eMPs^{LG}$. n: $eMPs^{NG}$ = 5, $eMPs^{LG}$ & $eMPs^{HG}$ = 6. Results are presented as means ± SEM.

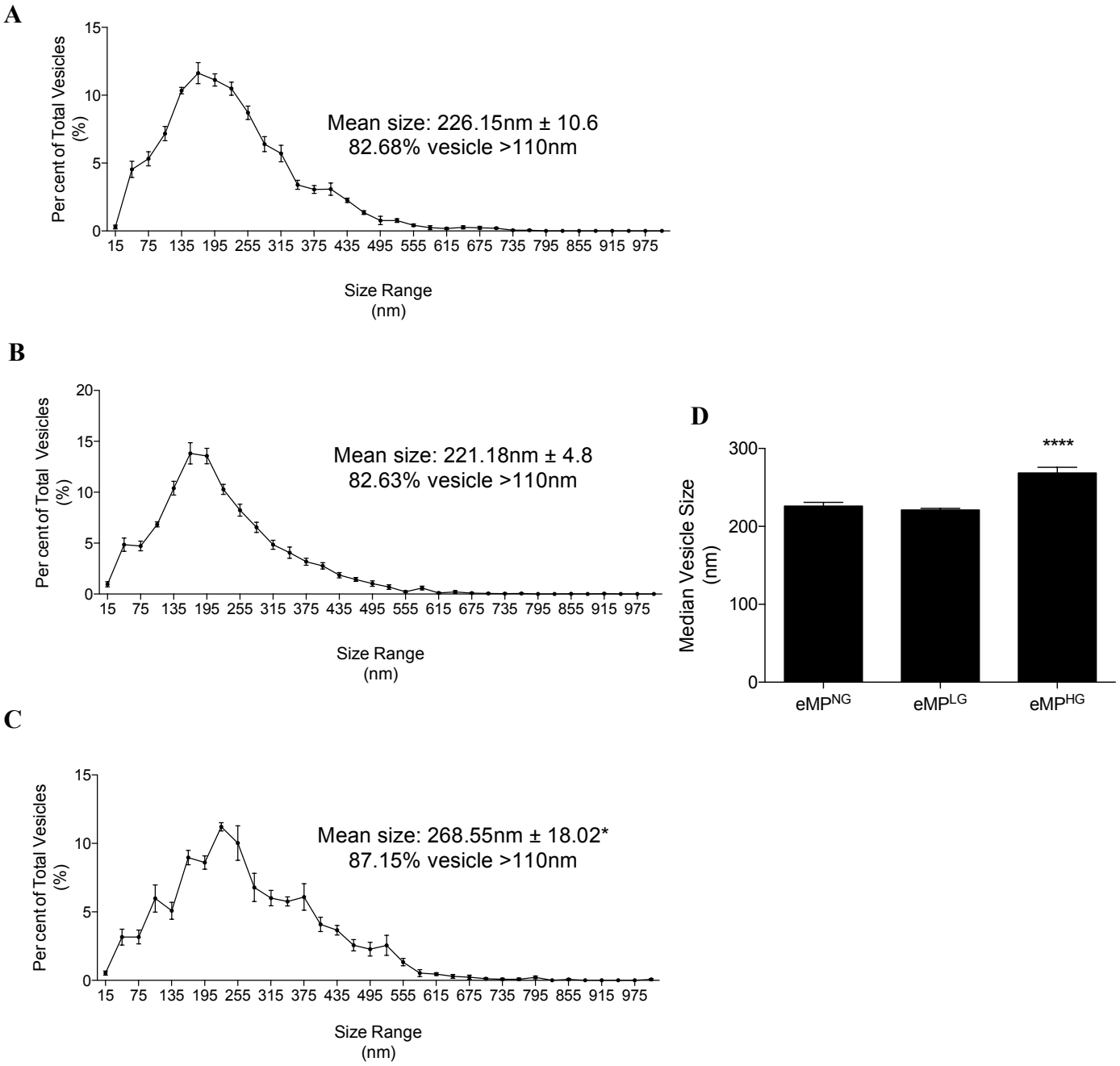

Figure 12: The effects of HG exposure on eMPs size.

eMPs were collected and prepped as described in Figure 8 to assess vesicle size via NTA. A-C: Percent size distribution of eMPs treatments, A: $eMPs^{NG}$. B: $eMPs^{LG}$. C: $eMPs^{HG}$. D: Median size of eMPs treatments. *P<0.05 vs. $eMPs^{NG}$ & $eMPs^{LG}$. ****P<0.0001 vs $eMPs^{NG}$ & $eMPs^{LG}$. n: $eMPs^{NG}$ = 5, $eMPs^{LG}$ & $eMPs^{HG}$ = 6. Results are presented as means ± SEM.

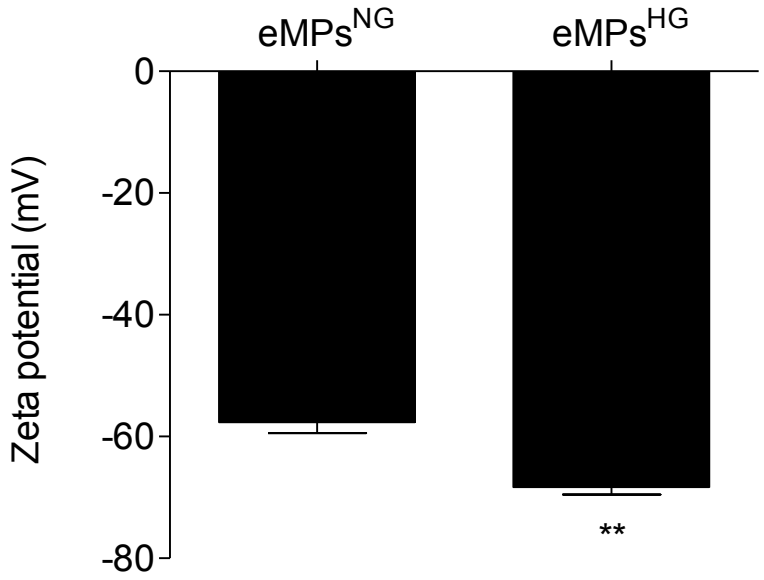

Figure 13: The effects of HG exposure on eMPs zeta potential.

eMPs were collected and prepped as described in Figure 8 and their electrophoretic mobilities were assessed using the Zetaview in zeta potential mode. **P<0.01 vs. $eMPs^{NG}$. n = 5. Results are presented as means ± SEM.

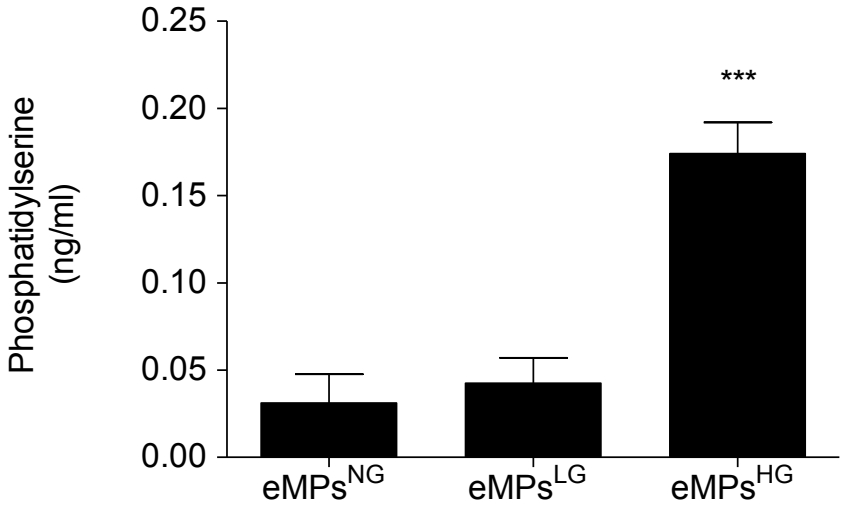

Figure 14: The effects of HG exposure on eMPs phosphatidylserine content.

eMPs were collected and prepped as described in Figure 8 to assess their PS content via ELISA. ***P<0.001 vs. $eMPs^{NG}$ & $eMPs^{LG}$. n = 4. Results are presented as means ± SEM.

3.3. High glucose changes the protein composition of eMPs.

Since the changes in membranous lipid content, size and surface charge observed above are indicative of HG-induced morphological changes; we employed label free LC-MS/MS to investigate any potential HG-induced protein changes among the eMPs populations. "Of the 1,212 proteins identified, 724 were common to all treatment groups while 68 were unique to the $eMPs^{HG}$, 111 were unique to the $eMPs^{LG}$ population and 18 were unique to the $eMPs^{NG}$ (Figure 15 and Table 3)"[79]. The Cytoscape ClueGO and CluePedia plugin was used to identify potential functional signatures exclusive to HG exposure. Figure 16 and Table 4 shows the eMPs-exclusive enriched functional processes, which involve hemostasis, metabolic processes, oxidation-reduction processes and cell surface interactions at the vascular wall.

3.4. High glucose increases the pro-coagulant activity of eMPs.

Sabatier et al. correlated cMPs and their increased pro-coagulative activity in individuals with DM to HbA_{1c} levels[63]. Interestingly, our functional assessment of eMPs identified an enrichment of proteins associated with hemostasis and blood coagulation in the HG population. Extending from this, we examined the effect of HG on eMPs procoagulant capacity with the Zymuphen MP Activity assay and observed an increase in $eMPs^{HG}$ activity (Figure 17).

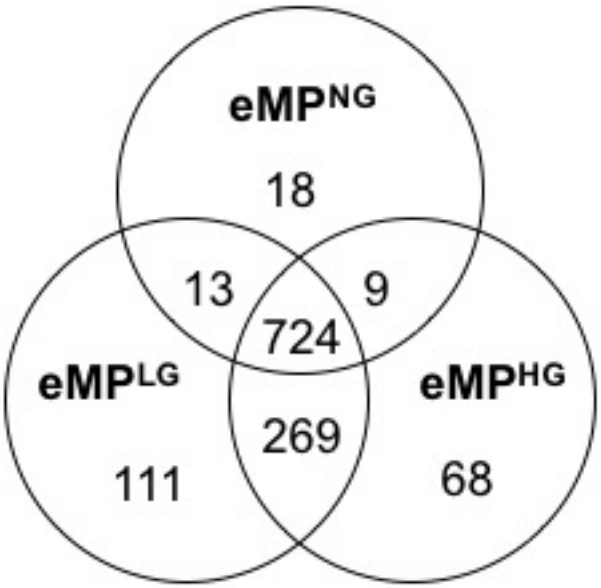

Figure 15: The effects of HG exposure on eMPs protein content.

eMPs were collected and prepped as described in Figure 8 to assess protein composition via label-free LC-MS/MS. A) Venn diagram depicting the protein differences across eMPs population. Proteins were considered true to a condition if they had at least 2 spectral counts per sample.

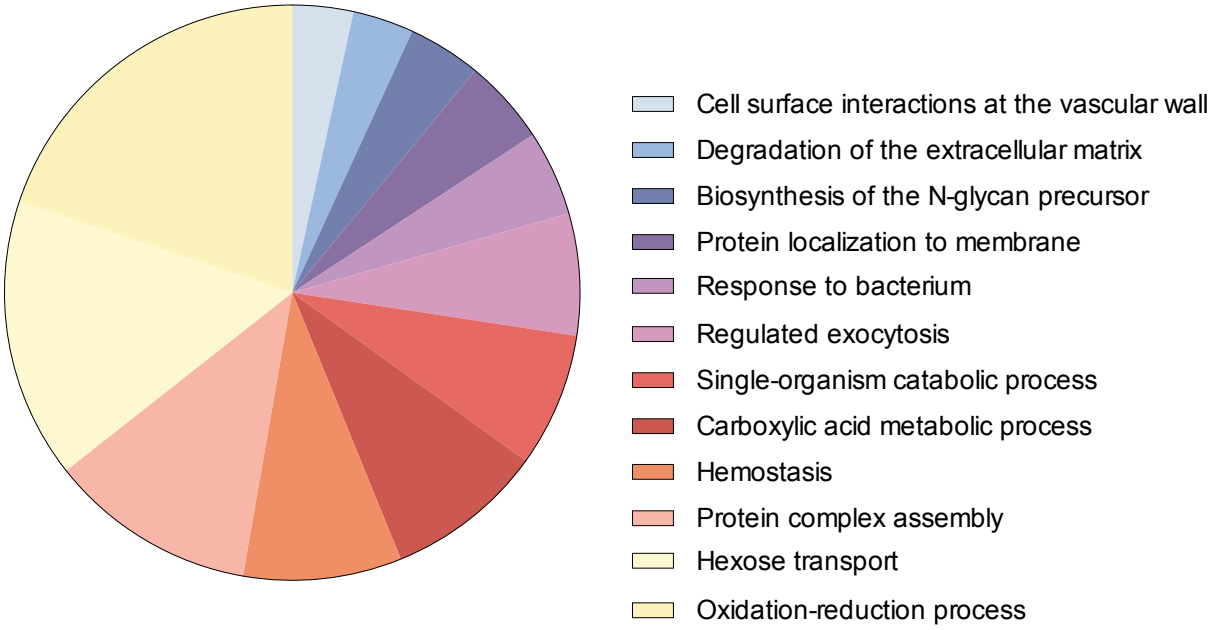

Figure 16: ClueGO predicted enriched biological processes associated with eMPs^{HG}-exclusive proteins.

eMPs were collected and prepped as described in Figure 8 to assess protein composition via label-free LC-MS/MS. Proteins exclusive to the eMPs^{HG} condition were analyzed for functional enrichments using ClueGO, a Cytoscape plugin.

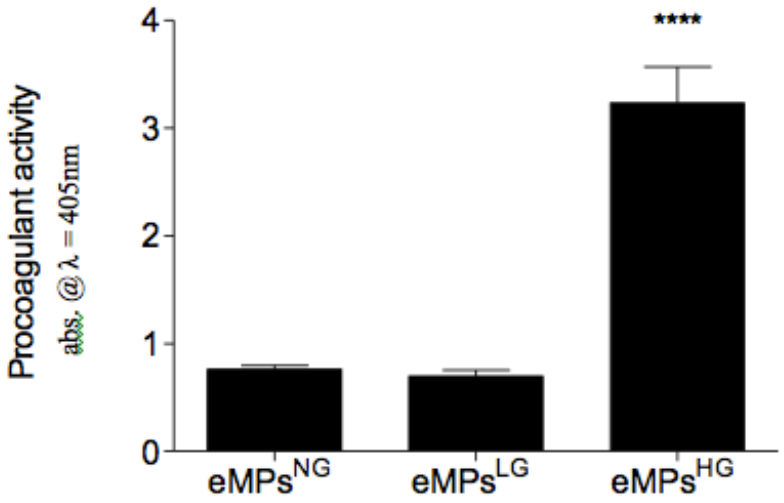

Figure 17: The effects of HG exposure on eMPs procoagulant activity.
eMPs were collected and prepped as described in Figure 8 to assess eMPs procoagulant activity via the Zymuphen MPs Activity Assay. ***P<0.001 vs. $eMPs^{NG}$ & $eMPs^{LG}$. n = 4. Results are presented as means ± SEM.

3.5. High glucose increases eMPs-induced oxidative stress on cultured HUVECs.

Our functional assessment of the HG exclusive proteins identified an enrichment in oxidation-reduction processes. Therefore, we assessed HG effects on eMPs-mediated oxidative stress using DHE-HPLC and DCF-fluorescence. Figure 18 shows the induction of intracellular ROS formation in response to all vesicle populations; however, when cells were treated with MPs formed under HG stress, this induction of intracellular ROS production was intensified and accompanied by O_2^- production (Figure 19).

3.6. High glucose increases the capacity of eMPs to impair endothelial dependent vascular relaxation *ex vivo*.

Impairments in endothelial-dependent vascular reactivity are associated with increased risk of cardiovascular complications in DM[29,27,96]. Interestingly, an enrichment in proteins associated with cellular interactions at the vascular wall appeared in our proteomic functional analysis of the $eMPs^{HG}$. Therefore, we assessed the effects of HG on eMPs-mediated impairment of vascular reactivity in isolated C57BL/6 mesenteric arteries. Figure 20 suggests a deleterious effect of $eMPs^{NG}$ on endothelial dependent vascular relaxations; however, with HG exposure, such effect was intensified, indicated by a rightward shift in relaxation curve, reduced maximal relaxation and increased sensitivity to acetylcholine ($pD_2 = -\log(EC_{50})$).

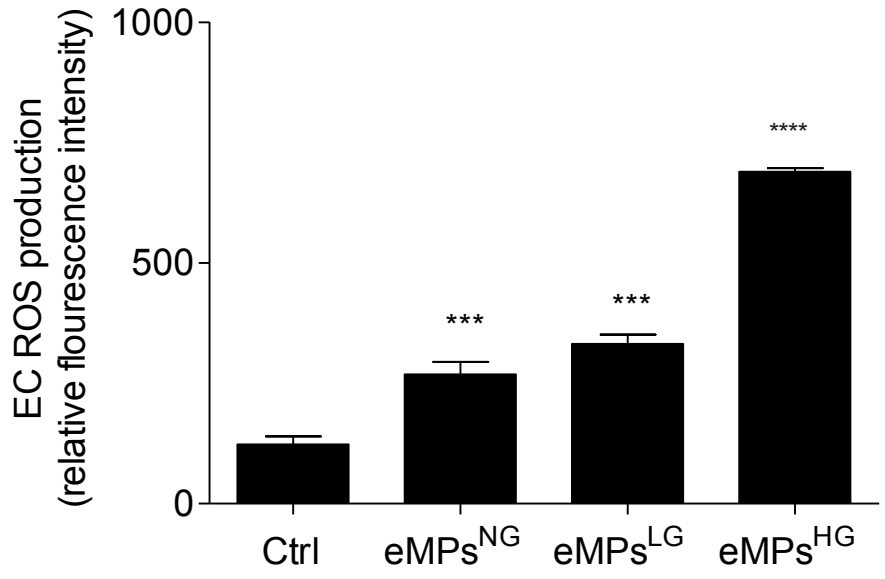

Figure 18: The effects of HG exposure on eMPs-induced intracellular ROS production.

eMPs were collected and prepped as described in Figure 8 to treat HUVECs (4hours, 10μg/ml) and eMPs-induced ROS production was assessed via DCF fluorescence. ***P<0.001 vs. PBS-treated control, ****P<0.0001 vs eMPs^{NG} & eMPs^{LG}. n = 3. Results are presented as means ± SEM.

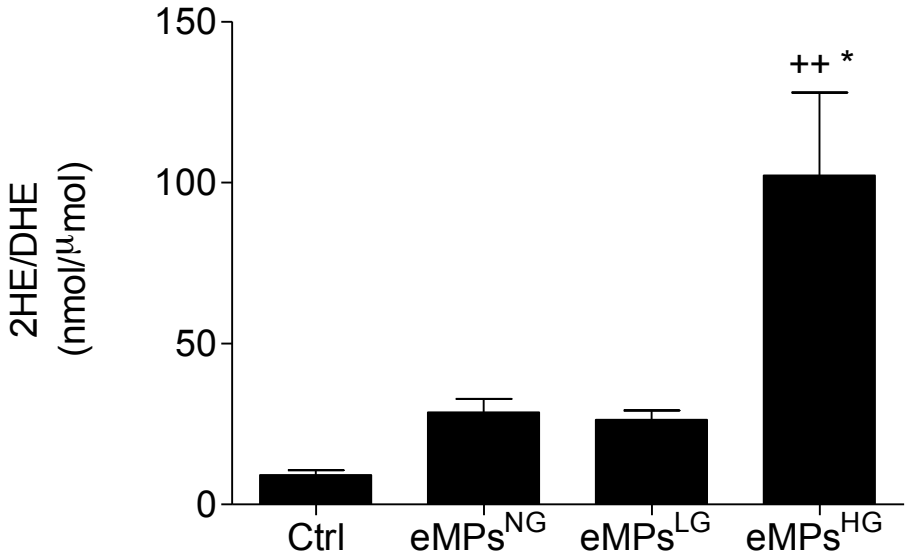

Figure 19: The effects of HG exposure on eMPs-induced cellular superoxide production.

eMPs were collected and prepped as described in Figure 8 to treat HUVECs (4 hours, 10μg/ml) and eMPs-induced superoxide production was assessed via DHE-HPLC. ++P<0.01 vs. PBS-treated control, *P<0.05 vs $eMPs^{NG}$ & $eMPs^{LG}$. n = 3. Results are presented as means ± SEM.

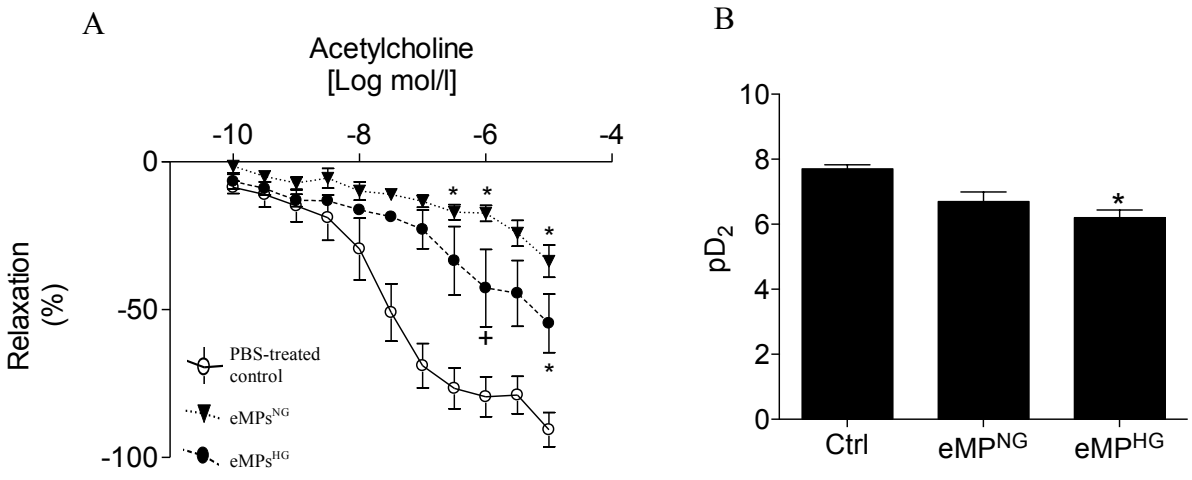

Figure 20: The effects of HG on eMPs-mediated impairment of endothelial dependent vascular reactivity.

eMPs were collected and prepped as described in Figure 8 to treat isolated mesenteric arteries (for 30 minutes at 1μg of eMPs proteins/ml). A: Concentration-response curve to acetylcholine for the PS-treated control vessel, $eMPs^{NG}$-treated and $eMPs^{HG}$-treated. B: Vessel sensitivity to acetylcholine treatment, expressed as the $pD_2 = [-\log(EC_{50})]$. +P<0.05 vs $eMPs^{HG}$-treated. *P<0.05 vs PBS-treated control vessel. n: PBS-treated control vessels – 8, $eMPs^{NG}$ – 6. $eMPs^{HG}$ – 5. Results are presented as means ± SEM.

4.0. Discussion

The purpose of this thesis was to assess the exclusive effects of HG on eMPs protein composition and biological activity, to gain insight into the molecular events occurring in a hyperglycemic environment. *We hypothesized that eMPs exposed to HG have a protein composition reflective of active signalling processes and the cells response to hyperglycemia.* In addition, *we hypothesize that HG alters eMPs bioactivity, making them more potent inducers of oxidative stress, thrombosis and endothelial dysfunction in the absence of underlying pathology.*

Novel findings from this work include the observation that HUVECs exposed to 25mM HG produce more eMPs that are distinct from control conditions in size, surface charge and PS content. We report that $eMPs^{HG}$ also possess a distinct molecular composition with an enrichement in proteins associated with metabolic processes, hemostasis, cell surface interactions at the vascular wall, and oxidation-reduction reactions. Similarly, our functional assessments of biological activity (pro-coagulant ability, pro-oxidative ability and endothelial dependent vascular reactivity) align with the predicted biological processes. Together, these results suggest a central role for HG at altering the molecular composition and bioactivity of eMPs, compounding endothelial damage and dysfunction in DM.

Elevations in eMPs have been reported in both insulin resistant and insulin deficient DM, more specifically these levels are correlated with the degree of HbA_{1C} levels[50,75], suggestive of a role for glucose in eMPs formation. We report an increase in the formation and size of eMPs following 24-hour HG exposure. Similarly, we've observed these effects in MPs derived from arterial, non-fetal ECs (human microvascular endothelial cells - HMECs) following 24-hour 25mM HG exposure[79]. Most notably, these HG-mediated increases in formation are conserved across other MPs populations, such as mesangial MPs and podocyte MPs[41,97]. "Given the variety of cells that release MPs in response to HG, it is possible that increased MPs formation

represents a ubiquitous response to glucose-induced cell stress"[79] and provides a possible explanation for the observations of Njock *et al.*[98] who observed an increase in size and formation of cMPs isolated from a mouse and rat model of T2DM (exact models were unspecified).

Next we report an increase in eMPs absolute surface charge. Although novel to a hyperglycemic environment, changes in size and accompanying surface charge, have been reported in other pathologies characterized by chronic oxidative stress and low-grade inflammation, a characteristic of a hyperglycemic environment. Redman *et al.* observed an increase in eMPs size and formation in plasma collected from women with pre-eclampsia[99,100] while Baran *et al.* report an increase in formation, size and absolute surface charge in cMPs with tumor origins in plasma from patients with gastric cancer[101]. As previously mentioned, zeta potential is influenced by surface proteins and lipids holding a negative electric charge. PS, a negatively charged phospholipid, as well as glycoproteins and glycolipids carrying sialic acid (which holds a negative charge at physiological pH) contribute to a particles surface charge and stability[102]. Akagi et al. report larger and more negatively charged circulating EXOs (cEXOs) correlated with the quantity of sialic acid containing glycoproteins and glycolipids on cEXOs in patients with prostate cancer[103]. Interestingly, our $eMPs^{HG}$ population contained sialic acid synthase, an enzyme involved in sialic acid synthesis; possibly indicating increased cellular expression in response to the HG environment. In addition, we report an increase in PS content, a possible contributor to the increase in surface negativity.

In light of these findings, we propose that a pathophysiological microenvironment characterized by chronic inflammation and oxidative stress induces the production of larger, more negatively charged vesicles, as a mechanism to cleanse the cell of various contents and inform the surrounding environment of the cells state. However, as evident in our protein

composition and biological activity assessments, such effects may have repercussions and contribute to the macro- and micro- vascular damages associated with hyperglycemia and DM.

4.2. HG exposure results in a distinct molecular signature among eMPs populations.

Vesicles formed under various stimuli possess a distinct molecular signature. In support of this, our proteomic analysis identified 68 proteins exclusive to $eMPs^{HG}$, 18 proteins exclusive to $eMPs^{NG}$ and 111 proteins exclusive to $eMPs^{LG}$. Due to the nature of our experimental approach and the inaccuracy of label-free LC-MS/MS, we avoided interpretation of relative protein quantities. As such we assessed the associated biological processes of the 68 proteins exclusive to the HG condition.

As mentioned, glycolytic processes are stalled in response to HG, leading to the build-up of metabolites that are shunted down glycolysis side pathways resulting in AGE formation, ROS production and protein glycosylation. Not surprisingly, our $eMPs^{HG}$ contain various proteins involved in protein glycosylation and glucose transport, metabolism and storage (Table 3, ie. MGAT1, DPM3 GLGB, ADPGK, GALK1, GNA1, NDUBB, NDUS8). The fact that we observed an enrichment in proteins associated with hexose transport, carbohydrate metabolic processes, oxidation reduction processes and the generation of precursor metabolites and energy are enriched in our $eMPs^{HG}$ population (Table 4), suggests that eMPs are reflective of their cell of origin's ongoing response to metabolic stress. This eMPs trait may facilitate intercellular communications, notifying cells of the ongoing metabolic stress and may provide use as a biomarker subclinical glucose damage.

Our $eMPs^{HG}$ were also enriched in proteins associated with hemostasis and coagulation, oxidative-reduction processes, extracellular matrix (ECM) organization and degradation, and cell surface interactions at the vascular wall. Interestingly, our functional assessment of MPs

biological activities mirrors this shift in protein phenotype, suggestive of a link between eMPs protein content and biological activities and may provide further insight into the pathophysiological status of a cells environment.

MPs procoagulant activity has previously been attributed to its role in the prothrombinase complex, its quantity of externalized PS and TF; however our results suggest pro-coagulant proteins may also contribute to these activities, as indicated in the functional assessment of our $eMPs^{HG}$ exclusive proteins.

Activated platelets and coagulation factors (FXa, FV and prothrombin) assemble at the negatively charged phospholipid-containing surface (PS-rich membrane), creating the prothrombinase complex which amplifies coagulation and thrombus formation[24,25,54,68]. Its proposed that a more negatively charged particle is more adherent to surrounding particles and cell surfaces, contributing to thrombus formation endothelial damage and atherosclerosis[101,104]. Not surprisingly, accompanying the increase in PS content, surface negativity and enrichment in thrombotic proteins, we observe a functional increase in procoagulant activity. These observations are indicative of a pro-thrombotic eMPs phenotype in response to HG exposure. Although eMPs account for only 5-15% of cMPs[46] in plasma; the enrichment in proteins associated with hemostasis and the altered PS phenotype provides an explanation for the observations of Sabatier *et al.* who correlate eMPs pro-coagulant capacity and HbA_{1c} levels in DM[75].

In DM, eMPs levels are inversely correlated with FMD scores[75], procoagulant phenotype and HbA_{1C} levels[50]. Previously, we report 10µg eMPs proteins/mL of $eMPs^{NG}$ have the capacity to impair endothelial dependent vascular reactivity; however here, we report that a lesser, more physiological dose[65] (1µg eMPs proteins/mL) of $eMPs^{NG}$ are able to impair endothelial dependent vascular reactivity. More importantly, we report an increase in $eMPs^{HG}$ ability to

impair endothelial-dependent relaxation and the vessel's sensitivity to acetylcholine in the absence of underlying pathology at this lower dose. Jansen *et al.* report that $eMPs^{HG}$ impair vascular reactivity, however their $eMPs^{NG}$ population had no effect[66]. Their myograph assessments were conducted on aortas isolated from $ApoE^{-/-}$ mice, a model to assess atherosclerosis, a condition that is preceded by endothelial dysfunction. Prior to assessments, these mice showed increased atherosclerotic plaque build-up than the wildtype controls, displaying underlying tissue injury, potentially masking any small $eMPs^{NG}$ effects. In addition, they injected the vesicles into the mice prior to euthanasia and vessel isolation, potentially activating an immune response, indirectly affecting vascular reactivity. Our myograph assessments were conducted on healthy mesenteric arteries from male C57BL/6 mice that were treated with eMPs for 30 minutes *ex vivo*. Small arteries, such as the mesenteric arteries constitute the primary source of vascular resistance and are therefore a preferred model to assess endothelial function compared with large vessels like the aorta, which have limited surface area and are not major determinants of blood pressure. More importantly, we treat our vessels ex vivo, therefore avoiding any potential immune-mediated indirect effects on vascular function. Our results show a direct impairment of healthy vessels by eMPs, which is enhanced in response to $eMPs^{HG}$.

Jansen *et al.* attribute the detrimental effects of $eMPs^{HG}$ on endothelial function to the increased induction of ROS production and oxidative stress, which induces the expression of adhesion proteins and downstream inflammatory signals[66]. These effects were assessed in human coronary artery endothelial cells (HCAECs) treated for 30 minutes with HCAECs derived eMPs. Similarly, we observe an increase in the induction of HUVECs intracellular ROS production and superoxide specific oxidative stress in response to $eMPs^{HG}$ 4-hour treatments. Extending on this, there were enrichments in proteins associated with ECM reorganization and degradation and cell

surface interactions at the vascular wall (clustering with cell death and death receptor signalling) among the eMPs^{HG} population (Table 4). Our eMPs^{HG} are enriched in proteins associated with TP53 regulation of cell death genes, receptors and ligand transcription. This pro-death profile indicating a change ECs gene expression could provide use as a diagnostic biomarker, identidying endothelial damage before overt clinical signs such as increased blood pressure. With ECs damage, ECM reorganization and degreadation occur, cells die and detach, exposing the basement membrane to circulating blood. The basement membrane becomes an ideal surface for platelets to adhere and aggregate accelerating endothelial damage and atherosclerosis. Even though we did not directly assess whether ROS or adhesion proteins were the main agonists impairing endothelial function, our data supports the pro-adhesion and pro-oxidative mechanism of eMPs^{HG} action on endothelial dysfunction[66].

Our proteomic observations differ slightly from Zu *et al.*, who also conducted label-free LC-MS/MS on endothelial extracellular vesicles (eEVs) following HG exposure[77]. Of the 30 Alzheimer's related proteins exclusively found in their HG EVs, 11 were also identified in our screen, although none exclusive to our eMPs^{HG}. It is notable that Zu *et al.* treated for 4 hours prior to vesicle isolation, while we assessed changes after 24 hours. The extended exposure in our study may allow for more transcriptional-related protein changes to occur and may be reflected in eMPs content. In addition to this, Zu *et al.* employed a non-selective centrifugation protocol, where collected culture medium was initially centrifuged at 800g to sediment cell debris, with the remaining supernatant centrifuged at 100,000xg for one hour for vesicle collection. There isolation is likely to contain all three-vesicle populations, ABs, EXOs and MPs. We employ a protocol that consists of a low speed centrifugation to eliminate ABs, followed by a 20,000 xg centrifugation for 20 minutes to isolate the MPs from EXOs. Following that, we wash the MPs isolates to purify our samples and eliminate contamination with different vesicle

populations, extra-vesicular proteins, lipoprotein particles and aggregated vesicles. While there is no centrifugation-based technique that will completely isolate individual vesicle populations, our technique is capable of isolating a relatively pure population of membranous vesicles with a size consistent with our definition of MPs.

4.3. Study Limitations

Our observations provide initial evidence of HG-induced changes in eMPs protein composition and biological activity. Cultured HUVECs exposed to 25mM of HG for 24 hours increases the formation of eMPs that are more potent inducers of endothelial and vascular damage mirrored in their protein content. Nevertheless there are a number of study limitations that must be acknowledged.

As outlined in our methods, we elected to use HUVECs as a model system. Although widely used to assess endothelial activities and ideal for large scale culturing (a necessity for studying EVs), they are venous in origin and do not contribute to blood pressure regulation. Nevertheless, we observed a similar increase in eMPs levels from cells derived from resistance arteries, HMECs[79] and our biological effects mirror the effects of MPs derived from mouse aortic endothelial cells[62] and HCAECs[66]. In addition, our biological procoagulant effect, size and formation extend to eMPs isolated from human, mouse and rat DM plasma[50,75,76]. Thus the effects on MPs appear to be conserved across ECs of multiple lineages both in vivo and in vitro.

In addition, we assessed 25mM D-Glucose over 24 hours, which would most closely approximate acute uncontrolled hyperglycemia in vivo. Practically, ECs cultures are limited to short term studies and, as such, is a poor model system to recapitulate the long-term effects of small changes in glucose seen in DM. Accordingly, higher disease of glucose are often necessary to recapitulate chronic responses to human DM in the acute setting. The dosing and time of

exposure in our studies were chosen based on prior studies to ensure transcriptional and translational molecular events could occur, while limiting EC apoptosis. We acknowledge that HG effects may be time and dose sensitive and ultimately it will be necessary to recapitulate our observations in the in vivo setting.

A final limitation of our study is the semi-quantitative nature of label-free LC-MS/MS. Due to this, we elected not to quantify protein spectral counts or look at specific enrichments in proteins between treatment groups. Had we chosen a labelling technique more amenable to quantification, such as isobaric tags for relative and absolute quantification (ITRAQ), isobaric labeling (tandem mass tag, TMT) or stable isotope labeling with amino acids in cell culture (SILAC), then quantitation would have been possible. Given that our $eMPs^{NG}$ induced a small biological effect on ECs function insight into protein enrichments and depletions between the $eMPs^{NG}$ and $eMPs^{HG}$ populations may provide insight into eMPs signalling. For example, thrombospondin-1 (TSP-1) a secreted glycoprotein with anti-angiogenic properties is proposed to mediate eMPs signalling and induce platelet adhesion and thrombosis in mice. Interestingly, our semi-quantitative assessment of spectral counts showed a 2-fold increase in TSP-1 in our $eMPs^{HG}$ population[105,106].

4.4. Future Directions

To account for some of these limitations and to increase the strength of our findings, future assessments should examine: 1) Verifying our HG-induced protein signature in another eMPs ECs population, such as HMECs. 2) Assessing and comparing the protein composition in the ECs of origins to confirm eMPs utility as biomarkers. 3) Assessing the miRNA content of $eMPs^{HG}$. MiRNA mediate both EXOs and MPs signalling and therefore a complete profile of both protein and miRNA profiles may provide more insight into the molecular signalling and

pathophysiology of the hyperglycemic microenvironment. 4) Also confirming this phenotype *in vivo*, therefore assessing the molecular composition and biological activities of cMPs and selectively isolating eMPs from plasma that has been collected from hyperglycemic mice or DM patient. Future directions could extend on this and compare the mouse cMPs and eMPs with a direct biopsy from the mouse microvasculature. These proposed experiments would strength these findings and allow for stronger conclusions to be made about eMPs utility as a biomarker for endothelial damage and dysfunction in response to HG stress and hyperglycemia.

4.4. Clinical Relevance and Conclusions

Traditionally, tests assessing endothelial function lack reproducibility, reliability and are extremely patient and operator dependent[96]. eMPs levels are emerging as an early minimally-invasive biomarker of tissue damage and vascular injury[53,57,107,108]. Their increase in levels have also been shown to predict future cardiovascular complications in patients with coronary artery disease and DM[109,76]. However, eMPs may also provide, in detail, insights into the pathophysiological status of a cells microenvironment. Biopsies are routinely performed to diagnose cancer and to gain insight into the cancer type and dysregulated pathways. Therefore, the information obtained from a tumor biopsy allows for individualized treatment regimes. Unfortunately, ECs biopsies are not routinely conducted and therefore treatment of vascular disease is limited and generalized. We report that $eMPs^{HG}$ possess a distinct molecular signature in both protein profile and biological activity in response to HG stress.

Given the close association between the predicted biological processes associated with our $eMPs^{HG}$ proteins and our observed biological activities, assessment of eMPs protein content could provide use as a minimally invasive blood-based biomarker of HG-induced endothelial damage and used clinically to identify dysregulated pathways for therapeutic targeting.

5.0. Tables

Table 1: List of Chemicals and Reagents.

Company	Product
ATCC (Manassas, VA, USA)	Fetal Bovine Serum Human Umbilical Vein Endothelial Cells
Bio-Rad Laboratories (Hercules CA, USA)	4X Laemmli Dye 4-15% Mini PROTEAN TGX Gel DC Protein Assay Reagents (A, B and S)
Canemco Marivac (Lakefield, QC, Canada)	Sodium Cacodilate Copper Grids
EMD Millipore (Billerica, MA, USA)	EDTA $CaCl_2$ KCl $MgSO_4$ -$7H_2O$ Triton X-100
Sigma-Aldrich (St. Louis, Missouri USA)	Acetylcholine Bovine Serum Albumin diethylenetriaminepentaacetic acid EGTA L-Glucose $NaHCO_3$ NP40 Phenylephrine Protease Inhibitor Cocktail Sodium Deoxycholate Sodium dodecyl sulfate
Ted Pella Inc. (Redding CA, USA)	LR White Resin (medium grade)
ThermoFisher Scientific (Waltham MA, USA)	7′-Dichlorofluorescein Diacetate Acetonitrile Attachment Factor D-Glucose Dihydroethidium Glutaraldehyde Glycine KH_2PO_4 Lead Nitrate Methanol NaCl Na_2HPO_4 Osmium Tetroxide Paraformaldehyde Sodium Citrate Trifluoracetic Acid

	Tris Base Tween20 Uranyl Acetate
Wisent Bioproducts (Saint Jean-Baptiste, QC, Canada)	Endomax Medium EMS-18 Penicillin/Streptomycin

Table 2: List of Buffers and Solutions.

	Solutions	Recipe
	Phosphate Buffered Saline (PBS) Solution (1x)	137mM NaCl 2.7mM KCl 10mM Na_2HPO_4 1.76mM KH_2PO_4
	Radioimmunoprecipitation Assay (RIPA) Buffer + 1:100 Protease Inhibitor Cocktail	50mM Tris Base 150mM NaCl 0.1% SDS 0.5% Sodium Deoxycholate 1% Triton X-100 1:100 dilution of Protease Inhibitor Cocktail
Transmission Electron Micrograph (TEM)	TEM Fixative	16% paraformaldehyde 25% glutaraldehyde
	Reynold's Lead Citrate	Lead Nitrate Sodium Citrate
Liquid Chromatography-Tandem Mass Spectrometry (LC-MS/MS)	10x Tris Glycine Buffer	247.6mM Tris Base 2.5M Glycine Water
	Tris Running Buffer	10x Tris Glycine Buffer Water 10% SDS
Wire Myography	25x PSS	3250 mM NaCl 117.5 mM KCl 29.5 mM KH_2PO_4 29.25 mM $MgSO_4$
	PSS	Dilute 25x PSS with water 15 mM $NaHCO_3$ 5.5 mM Glucose 0.005mM EDTA 1.6mM$CaCl_2$
	10x KPSS	747mM NaCl 600mM KCl 11.8mM KH_2PO_4 11.7mM $MgSO_4$ -$7H_2O$
	KPSS	Dilute 10x KPSS with water 15 mM $NaHCO_3$ 5.5 mM Glucose 0.005mM EDTA 1.6mM $CaCl_2$

HPLC	Hanks + DTPA	1.3mM $CaCl_2$ 0.8mM $MgSO_4$ 5.4mM KCl 0.4mM KH_2PO_4 4.3mM $NaHCO_3$ 137mM NaCl 0.3mM Na_2HPO_4 5.6mM Glucose pH: 7.4 100μM DTPA
	Solution A	20% Methanol 0.1% Trifluoroacetic acid In water
	Solution B	100% Methanol (HPLC Grade)

Table 3: List of eMPs Associated Proteins.

Accession Number	Identified Proteins	eMP^{HG}	eMP^{LG}	eMP^{NG}
CH10_HUMAN	10 kDa heat shock protein, mitochondrial	X	X	X
1433B_HUMAN	14-3-3 protein beta/alpha	X	X	X
1433E_HUMAN	14-3-3 protein epsilon	X	X	X
1433F_HUMAN	14-3-3 protein eta	X	X	X
1433G_HUMAN	14-3-3 protein gamma	X	X	X
1433T_HUMAN	14-3-3 protein theta	X	X	X
1433Z_HUMAN	14-3-3 protein zeta/delta	X	X	X
ODO1_HUMAN	2-oxoglutarate dehydrogenase, mitochondrial	X	X	X
PRS10_HUMAN	26S protease regulatory subunit 10B	X	X	X
PRS6A_HUMAN	26S protease regulatory subunit 6A	X	X	X
PRS8_HUMAN	26S protease regulatory subunit 8	X	X	X
PSMD1_HUMAN	26S proteasome non-ATPase regulatory subunit 1	X	X	X
PSD11_HUMAN	26S proteasome non-ATPase regulatory subunit 11	X	X	X
PSD13_HUMAN	26S proteasome non-ATPase regulatory subunit 13	X	X	X
PSDE_HUMAN	26S proteasome non-ATPase regulatory subunit 14	X	X	X
PSMD2_HUMAN	26S proteasome non-ATPase regulatory subunit 2	X	X	X
PSMD3_HUMAN	26S proteasome non-ATPase regulatory subunit 3	X	X	X
PSMD7_HUMAN	26S proteasome non-ATPase regulatory subunit 7	X	X	X
RT36_HUMAN	28S ribosomal protein S36, mitochondrial	X	X	X
THIM_HUMAN	3-ketoacyl-CoA thiolase, mitochondrial	X	X	X
THIK_HUMAN	3-ketoacyl-CoA thiolase, peroxisomal	X	X	X
RS10_HUMAN	40S ribosomal protein S10	X	X	X
RS11_HUMAN	40S ribosomal protein S11	X	X	X
RS12_HUMAN	40S ribosomal protein S12	X	X	X
RS13_HUMAN	40S ribosomal protein S13	X	X	X

RS14_HUMAN	40S ribosomal protein S14	X	X	X
RS15A_HUMAN	40S ribosomal protein S15a	X	X	X
RS16_HUMAN	40S ribosomal protein S16	X	X	X
RS17_HUMAN	40S ribosomal protein S17	X	X	X
RS18_HUMAN	40S ribosomal protein S18	X	X	X
RS19_HUMAN	40S ribosomal protein S19	X	X	X
RS2_HUMAN	40S ribosomal protein S2	X	X	X
RS20_HUMAN	40S ribosomal protein S20	X	X	X
RS21_HUMAN	40S ribosomal protein S21	X	X	X
RS24_HUMAN	40S ribosomal protein S24	X	X	X
RS25_HUMAN	40S ribosomal protein S25	X	X	X
RS26_HUMAN	40S ribosomal protein S26	X	X	X
RS27L_HUMAN	40S ribosomal protein S27-like	X	X	X
RS29_HUMAN	40S ribosomal protein S29	X	X	X
RS3_HUMAN	40S ribosomal protein S3	X	X	X
RS3A_HUMAN	40S ribosomal protein S3a	X	X	X
RS4X_HUMAN	40S ribosomal protein S4, X isoform	X	X	X
RS4Y1_HUMAN	40S ribosomal protein S4, Y isoform 1	X	X	X
RS5_HUMAN	40S ribosomal protein S5	X	X	X
RS6_HUMAN	40S ribosomal protein S6	X	X	X
RS7_HUMAN	40S ribosomal protein S7	X	X	X
RS8_HUMAN	40S ribosomal protein S8	X	X	X
RS9_HUMAN	40S ribosomal protein S9	X	X	X
RSSA_HUMAN	40S ribosomal protein SA	X	X	X
4F2_HUMAN	4F2 cell-surface antigen heavy chain	X	X	X
5NTD_HUMAN	5'-nucleotidase	X	X	X
CH60_HUMAN	60 kDa heat shock protein, mitochondrial	X	X	X
RLA0_HUMAN	60S acidic ribosomal protein P0	X	X	X

RLA1_HUMAN	60S acidic ribosomal protein P1	X	X	X
RLA2_HUMAN	60S acidic ribosomal protein P2	X	X	X
RL10_HUMAN	60S ribosomal protein L10	X	X	X
RL11_HUMAN	60S ribosomal protein L11	X	X	X
RL12_HUMAN	60S ribosomal protein L12	X	X	X
RL13A_HUMAN	60S ribosomal protein L13a	X	X	X
RL14_HUMAN	60S ribosomal protein L14	X	X	X
RL15_HUMAN	60S ribosomal protein L15	X	X	X
RL17_HUMAN	60S ribosomal protein L17	X	X	X
RL18_HUMAN	60S ribosomal protein L18	X	X	X
RL18A_HUMAN	60S ribosomal protein L18a	X	X	X
RL22_HUMAN	60S ribosomal protein L22	X	X	X
RL23_HUMAN	60S ribosomal protein L23	X	X	X
RL23A_HUMAN	60S ribosomal protein L23a	X	X	X
RL24_HUMAN	60S ribosomal protein L24	X	X	X
RL27A_HUMAN	60S ribosomal protein L27a	X	X	X
RL3_HUMAN	60S ribosomal protein L3	X	X	X
RL30_HUMAN	60S ribosomal protein L30	X	X	X
RL31_HUMAN	60S ribosomal protein L31	X	X	X
RL35A_HUMAN	60S ribosomal protein L35a	X	X	X
RL38_HUMAN	60S ribosomal protein L38	X	X	X
RL4_HUMAN	60S ribosomal protein L4	X	X	X
RL6_HUMAN	60S ribosomal protein L6	X	X	X
RL7_HUMAN	60S ribosomal protein L7	X	X	X
RL7A_HUMAN	60S ribosomal protein L7a	X	X	X
GRP78_HUMAN	78 kDa glucose-regulated protein	X	X	X
THIL_HUMAN	Acetyl-CoA acetyltransferase, mitochondrial	X	X	X
ARP2_HUMAN	Actin-related protein 2	X	X	X

ARPC3_HUMAN	Actin-related protein 2/3 complex subunit 3	X	X	X
ARPC4_HUMAN	Actin-related protein 2/3 complex subunit 4	X	X	X
ARPC5_HUMAN	Actin-related protein 2/3 complex subunit 5	X	X	X
ARP3_HUMAN	Actin-related protein 3	X	X	X
ACTC_HUMAN	Actin, alpha cardiac muscle 1	X	X	X
ACTG_HUMAN	Actin, cytoplasmic 2	X	X	X
ACOT9_HUMAN	Acyl-coenzyme A thioesterase 9, mitochondrial	X	X	X
APT_HUMAN	Adenine phosphoribosyltransferase	X	X	X
KAD1_HUMAN	Adenylate kinase isoenzyme 1	X	X	X
CAP1_HUMAN	Adenylyl cyclase-associated protein 1	X	X	X
APMAP_HUMAN	Adipocyte plasma membrane-associated protein	X	X	X
ARF1_HUMAN	ADP-ribosylation factor 1	X	X	X
ARF4_HUMAN	ADP-ribosylation factor 4	X	X	X
ARL2_HUMAN	ADP-ribosylation factor-like protein 2	X	X	X
AR6P1_HUMAN	ADP-ribosylation factor-like protein 6-interacting protein 1	X	X	X
ADT1_HUMAN	ADP/ATP translocase 1	X	X	X
ADT2_HUMAN	ADP/ATP translocase 2	X	X	X
ADT3_HUMAN	ADP/ATP translocase 3	X	X	X
SYAC_HUMAN	Alanine--tRNA ligase, cytoplasmic	X	X	X
AL1B1_HUMAN	Aldehyde dehydrogenase X, mitochondrial	X	X	X
ALDH2_HUMAN	Aldehyde dehydrogenase, mitochondrial	X	X	X
ACTN1_HUMAN	Alpha-actinin-1	X	X	X
ACTN2_HUMAN	Alpha-actinin-2	X	X	X
ACTN3_HUMAN	Alpha-actinin-3	X	X	X
ACTN4_HUMAN	Alpha-actinin-4	X	X	X
ACTZ_HUMAN	Alpha-centractin	X	X	X
CRYAB_HUMAN	Alpha-crystallin B chain	X	X	X
ENOA_HUMAN	Alpha-enolase	X	X	X

PARVA_HUMAN	Alpha-parvin	X	X	X
SNAA_HUMAN	Alpha-soluble NSF attachment protein	X	X	X
AIMP2_HUMAN	Aminoacyl tRNA synthase complex-interacting multifunctional protein 2	X	X	X
AMPN_HUMAN	Aminopeptidase N	X	X	X
TIE2_HUMAN	Angiopoietin-1 receptor	X	X	X
ANXA1_HUMAN	Annexin A1	X	X	X
ANX11_HUMAN	Annexin A11	X	X	X
ANXA2_HUMAN	Annexin A2	X	X	X
ANXA3_HUMAN	Annexin A3	X	X	X
ANXA4_HUMAN	Annexin A4	X	X	X
ANXA5_HUMAN	Annexin A5	X	X	X
ANXA6_HUMAN	Annexin A6	X	X	X
AP2A1_HUMAN	AP-2 complex subunit alpha-1	X	X	X
AP2A2_HUMAN	AP-2 complex subunit alpha-2	X	X	X
APOA4_HUMAN	Apolipoprotein A-IV	X	X	X
APOB_HUMAN	Apolipoprotein B-100	X	X	X
APOC3_HUMAN	Apolipoprotein C-III	X	X	X
BAX_HUMAN	Apoptosis regulator BAX	X	X	X
SYRC_HUMAN	Arginine--tRNA ligase, cytoplasmic	X	X	X
AATM_HUMAN	Aspartate aminotransferase, mitochondrial	X	X	X
SYDC_HUMAN	Aspartate--tRNA ligase, cytoplasmic	X	X	X
ASPH_HUMAN	Aspartyl/asparaginyl beta-hydroxylase	X	X	X
ATLA3_HUMAN	Atlastin-3	X	X	X
AT5F1_HUMAN	ATP synthase F(0) complex subunit B1, mitochondrial	X	X	X
ATP8_HUMAN	ATP synthase protein 8	X	X	X
ATPA_HUMAN	ATP synthase subunit alpha, mitochondrial	X	X	X
ATPB_HUMAN	ATP synthase subunit beta, mitochondrial	X	X	X

ATPD_HUMAN	ATP synthase subunit delta, mitochondrial	X	X	X
ATP5I_HUMAN	ATP synthase subunit e, mitochondrial	X	X	X
AT5EL_HUMAN	ATP synthase subunit epsilon-like protein, mitochondrial	X	X	X
ATPK_HUMAN	ATP synthase subunit f, mitochondrial	X	X	X
ATP5L_HUMAN	ATP synthase subunit g, mitochondrial	X	X	X
ATPG_HUMAN	ATP synthase subunit gamma, mitochondrial	X	X	X
ATPO_HUMAN	ATP synthase subunit O, mitochondrial	X	X	X
ACLY_HUMAN	ATP-citrate synthase	X	X	X
PFKAL_HUMAN	ATP-dependent 6-phosphofructokinase, liver type	X	X	X
PFKAP_HUMAN	ATP-dependent 6-phosphofructokinase, platelet type	X	X	X
DHX9_HUMAN	ATP-dependent RNA helicase A	X	X	X
DDX3X_HUMAN	ATP-dependent RNA helicase DDX3X	X	X	X
ATD3A_HUMAN	ATPase family AAA domain-containing protein 3A	X	X	X
E41L3_HUMAN	Band 4.1-like protein 3	X	X	X
PGBM_HUMAN	Basement membrane-specific heparan sulfate proteoglycan core protein	X	X	X
BASI_HUMAN	Basigin	X	X	X
SNTB2_HUMAN	Beta-2-syntrophin	X	X	X
ACTBL_HUMAN	Beta-actin-like protein 2	X	X	X
PAPS2_HUMAN	Bifunctional 3'-phosphoadenosine 5'-phosphosulfate synthase 2	X	X	X
COASY_HUMAN	Bifunctional coenzyme A synthase	X	X	X
PUR9_HUMAN	Bifunctional purine biosynthesis protein PURH	X	X	X
BASP1_HUMAN	Brain acid soluble protein 1	X	X	X
KCD12_HUMAN	BTB/POZ domain-containing protein KCTD12	X	X	X
PYR1_HUMAN	CAD protein	X	X	X
CAD13_HUMAN	Cadherin-13	X	X	X
TMCO1_HUMAN	Calcium load-activated calcium channel	X	X	X
CMC1_HUMAN	Calcium-binding mitochondrial carrier protein Aralar1	X	X	X
CMC2_HUMAN	Calcium-binding mitochondrial carrier protein Aralar2	X	X	X

SCMC1_HUMAN	Calcium-binding mitochondrial carrier protein SCaMC-1	X	X	X
CALX_HUMAN	Calnexin	X	X	X
CPNS1_HUMAN	Calpain small subunit 1	X	X	X
CAN2_HUMAN	Calpain-2 catalytic subunit	X	X	X
CALR_HUMAN	Calreticulin	X	X	X
KAP0_HUMAN	cAMP-dependent protein kinase type I-alpha regulatory subunit	X	X	X
CBR1_HUMAN	Carbonyl reductase [NADPH] 1	X	X	X
CPT1A_HUMAN	Carnitine O-palmitoyltransferase 1, liver isoform	X	X	X
CRTAP_HUMAN	Cartilage-associated protein	X	X	X
CTNA1_HUMAN	Catenin alpha-1	X	X	X
CTNB1_HUMAN	Catenin beta-1	X	X	X
CTND1_HUMAN	Catenin delta-1	X	X	X
CAV1_HUMAN	Caveolin-1	X	X	X
CD109_HUMAN	CD109 antigen	X	X	X
CD166_HUMAN	CD166 antigen	X	X	X
CD44_HUMAN	CD44 antigen	X	X	X
CD59_HUMAN	CD59 glycoprotein	X	X	X
CD81_HUMAN	CD81 antigen	X	X	X
CD9_HUMAN	CD9 antigen	X	X	X
CISD1_HUMAN	CDGSH iron-sulfur domain-containing protein 1	X	X	X
CISD2_HUMAN	CDGSH iron-sulfur domain-containing protein 2	X	X	X
CDC42_HUMAN	Cell division control protein 42 homolog	X	X	X
MUC18_HUMAN	Cell surface glycoprotein MUC18	X	X	X
CLIC1_HUMAN	Chloride intracellular channel protein 1	X	X	X
CLIC4_HUMAN	Chloride intracellular channel protein 4	X	X	X
CISY_HUMAN	Citrate synthase, mitochondrial	X	X	X
CLH1_HUMAN	Clathrin heavy chain 1	X	X	X
CLH2_HUMAN	Clathrin heavy chain 2	X	X	X

COPA_HUMAN	Coatomer subunit alpha	X	X	X
COPB2_HUMAN	Coatomer subunit beta'	X	X	X
COPD_HUMAN	Coatomer subunit delta	X	X	X
COPE_HUMAN	Coatomer subunit epsilon	X	X	X
COPG1_HUMAN	Coatomer subunit gamma-1	X	X	X
COF1_HUMAN	Cofilin-1	X	X	X
CO1A1_HUMAN	Collagen alpha-1(I) chain	X	X	X
COIA1_HUMAN	Collagen alpha-1(XVIII) chain	X	X	X
CO3_HUMAN	Complement C3	X	X	X
DAF_HUMAN	Complement decay-accelerating factor	X	X	X
CTGF_HUMAN	Connective tissue growth factor	X	X	X
CSN6_HUMAN	COP9 signalosome complex subunit 6	X	X	X
CPNE1_HUMAN	Copine-1	X	X	X
COR1C_HUMAN	Coronin-1C	X	X	X
CAND1_HUMAN	Cullin-associated NEDD8-dissociated protein 1	X	X	X
CYTB_HUMAN	Cystatin-B	X	X	X
CSRP1_HUMAN	Cysteine and glycine-rich protein 1	X	X	X
CRIP2_HUMAN	Cysteine-rich protein 2	X	X	X
QCR1_HUMAN	Cytochrome b-c1 complex subunit 1, mitochondrial	X	X	X
QCR2_HUMAN	Cytochrome b-c1 complex subunit 2, mitochondrial	X	X	X
QCR7_HUMAN	Cytochrome b-c1 complex subunit 7	X	X	X
QCR8_HUMAN	Cytochrome b-c1 complex subunit 8	X	X	X
UCRI_HUMAN	Cytochrome b-c1 complex subunit Rieske, mitochondrial	X	X	X
CYB5B_HUMAN	Cytochrome b5 type B	X	X	X
COA3_HUMAN	Cytochrome c oxidase assembly factor 3 homolog, mitochondrial	X	X	X
COX2_HUMAN	Cytochrome c oxidase subunit 2	X	X	X
COX41_HUMAN	Cytochrome c oxidase subunit 4 isoform 1, mitochondrial	X	X	X
COX6C_HUMAN	Cytochrome c oxidase subunit 6C	X	X	X

CX7A2_HUMAN	Cytochrome c oxidase subunit 7A2, mitochondrial	X	X	X
CY1_HUMAN	Cytochrome c1, heme protein, mitochondrial	X	X	X
DYHC1_HUMAN	Cytoplasmic dynein 1 heavy chain 1	X	X	X
CKAP4_HUMAN	Cytoskeleton-associated protein 4	X	X	X
BACH_HUMAN	Cytosolic acyl coenzyme A thioester hydrolase	X	X	X
SERA_HUMAN	D-3-phosphoglycerate dehydrogenase	X	X	X
P5CS_HUMAN	Delta-1-pyrroline-5-carboxylate synthase	X	X	X
DNSL1_HUMAN	Deoxyribonuclease-1-like 1	X	X	X
DSG1_HUMAN	Desmoglein-1	X	X	X
DEST_HUMAN	Destrin	X	X	X
DLDH_HUMAN	Dihydrolipoyl dehydrogenase, mitochondrial	X	X	X
ODP2_HUMAN	Dihydrolipoyllysine-residue acetyltransferase component of pyruvate dehydrogenase complex, mitochondrial	X	X	X
ODO2_HUMAN	Dihydrolipoyllysine-residue succinyltransferase component of 2-oxoglutarate dehydrogenase complex, mitochondrial	X	X	X
DPYL2_HUMAN	Dihydropyrimidinase-related protein 2	X	X	X
DPP4_HUMAN	Dipeptidyl peptidase 4	X	X	X
PRKDC_HUMAN	DNA-dependent protein kinase catalytic subunit	X	X	X
DNJB1_HUMAN	DnaJ homolog subfamily B member 1	X	X	X
DNJB4_HUMAN	DnaJ homolog subfamily B member 4	X	X	X
DJC10_HUMAN	DnaJ homolog subfamily C member 10	X	X	X
DJC13_HUMAN	DnaJ homolog subfamily C member 13	X	X	X
DPM1_HUMAN	Dolichol-phosphate mannosyltransferase subunit 1	X	X	X
OST48_HUMAN	Dolichyl-diphosphooligosaccharide--protein glycosyltransferase 48 kDa subunit	X	X	X
RPN1_HUMAN	Dolichyl-diphosphooligosaccharide--protein glycosyltransferase subunit 1	X	X	X
RPN2_HUMAN	Dolichyl-diphosphooligosaccharide--protein glycosyltransferase subunit 2	X	X	X

DAD1_HUMAN	Dolichyl-diphosphooligosaccharide--protein glycosyltransferase subunit DAD1	X	X	X
DNM1L_HUMAN	Dynamin-1-like protein	X	X	X
DYL1_HUMAN	Dynein light chain 1, cytoplasmic	X	X	X
DYSF_HUMAN	Dysferlin	X	X	X
FBLN3_HUMAN	EGF-containing fibulin-like extracellular matrix protein 1	X	X	X
EHD1_HUMAN	EH domain-containing protein 1	X	X	X
EHD2_HUMAN	EH domain-containing protein 2	X	X	X
EHD3_HUMAN	EH domain-containing protein 3	X	X	X
EHD4_HUMAN	EH domain-containing protein 4	X	X	X
GCN1_HUMAN	eIF-2-alpha kinase activator GCN1	X	X	X
ETFA_HUMAN	Electron transfer flavoprotein subunit alpha, mitochondrial	X	X	X
ETFB_HUMAN	Electron transfer flavoprotein subunit beta	X	X	X
EF1A1_HUMAN	Elongation factor 1-alpha 1	X	X	X
EF1D_HUMAN	Elongation factor 1-delta	X	X	X
EF1G_HUMAN	Elongation factor 1-gamma	X	X	X
EF2_HUMAN	Elongation factor 2	X	X	X
EFTU_HUMAN	Elongation factor Tu, mitochondrial	X	X	X
EGLN_HUMAN	Endoglin	X	X	X
ERAP1_HUMAN	Endoplasmic reticulum aminopeptidase 1	X	X	X
ERMP1_HUMAN	Endoplasmic reticulum metallopeptidase 1	X	X	X
ERP29_HUMAN	Endoplasmic reticulum resident protein 29	X	X	X
ERP44_HUMAN	Endoplasmic reticulum resident protein 44	X	X	X
ERGI1_HUMAN	Endoplasmic reticulum-Golgi intermediate compartment protein 1	X	X	X
ENPL_HUMAN	Endoplasmin	X	X	X
EPCR_HUMAN	Endothelial protein C receptor	X	X	X
ECE1_HUMAN	Endothelin-converting enzyme 1	X	X	X
ECHM_HUMAN	Enoyl-CoA hydratase, mitochondrial	X	X	X

EPHA2_HUMAN	Ephrin type-A receptor 2	X	X	X
EMC1_HUMAN	ER membrane protein complex subunit 1	X	X	X
EMC2_HUMAN	ER membrane protein complex subunit 2	X	X	X
EMC6_HUMAN	ER membrane protein complex subunit 6	X	X	X
ERLN1_HUMAN	Erlin-1	X	X	X
ERLN2_HUMAN	Erlin-2	X	X	X
ERO1A_HUMAN	ERO1-like protein alpha	X	X	X
STOM_HUMAN	Erythrocyte band 7 integral membrane protein	X	X	X
IF4A1_HUMAN	Eukaryotic initiation factor 4A-I	X	X	X
IF4A2_HUMAN	Eukaryotic initiation factor 4A-II	X	X	X
EIF3A_HUMAN	Eukaryotic translation initiation factor 3 subunit A	X	X	X
IF5A1_HUMAN	Eukaryotic translation initiation factor 5A-1	X	X	X
XPO2_HUMAN	Exportin-2	X	X	X
ESYT1_HUMAN	Extended synaptotagmin-1	X	X	X
EZRI_HUMAN	Ezrin	X	X	X
CAZA1_HUMAN	F-actin-capping protein subunit alpha-1	X	X	X
CAZA2_HUMAN	F-actin-capping protein subunit alpha-2	X	X	X
CAPZB_HUMAN	F-actin-capping protein subunit beta	X	X	X
FSCN1_HUMAN	Fascin	X	X	X
FAS_HUMAN	Fatty acid synthase	X	X	X
AL3A2_HUMAN	Fatty aldehyde dehydrogenase	X	X	X
URP2_HUMAN	Fermitin family homolog 3	X	X	X
FIBG_HUMAN	Fibrinogen gamma chain	X	X	X
FGF2_HUMAN	Fibroblast growth factor 2	X	X	X
FINC_HUMAN	Fibronectin	X	X	X
FLNA_HUMAN	Filamin-A	X	X	X
FLNB_HUMAN	Filamin-B	X	X	X
FLNC_HUMAN	Filamin-C	X	X	X

BLVRB_HUMAN	Flavin reductase (NADPH)	X	X	X
FLOT1_HUMAN	Flotillin-1	X	X	X
FLOT2_HUMAN	Flotillin-2	X	X	X
FHL2_HUMAN	Four and a half LIM domains protein 2	X	X	X
ALDOA_HUMAN	Fructose-bisphosphate aldolase A	X	X	X
ALDOC_HUMAN	Fructose-bisphosphate aldolase C	X	X	X
FUMH_HUMAN	Fumarate hydratase, mitochondrial	X	X	X
LEG1_HUMAN	Galectin-1	X	X	X
GELS_HUMAN	Gelsolin	X	X	X
G6PD_HUMAN	Glucose-6-phosphate 1-dehydrogenase	X	X	X
G6PI_HUMAN	Glucose-6-phosphate isomerase	X	X	X
GLU2B_HUMAN	Glucosidase 2 subunit beta	X	X	X
DHE3_HUMAN	Glutamate dehydrogenase 1, mitochondrial	X	X	X
DHE4_HUMAN	Glutamate dehydrogenase 2, mitochondrial	X	X	X
GFPT1_HUMAN	Glutamine--fructose-6-phosphate aminotransferase [isomerizing] 1	X	X	X
GPX1_HUMAN	Glutathione peroxidase 1	X	X	X
GSTO1_HUMAN	Glutathione S-transferase omega-1	X	X	X
GSTP1_HUMAN	Glutathione S-transferase P	X	X	X
G3P_HUMAN	Glyceraldehyde-3-phosphate dehydrogenase	X	X	X
GPDM_HUMAN	Glycerol-3-phosphate dehydrogenase, mitochondrial	X	X	X
SYG_HUMAN	Glycine--tRNA ligase	X	X	X
GSLG1_HUMAN	Golgi apparatus protein 1	X	X	X
GOGA7_HUMAN	Golgin subfamily A member 7	X	X	X
GDF15_HUMAN	Growth/differentiation factor 15	X	X	X
GRPE1_HUMAN	GrpE protein homolog 1, mitochondrial	X	X	X
RAN_HUMAN	GTP-binding nuclear protein Ran	X	X	X
SAR1A_HUMAN	GTP-binding protein SAR1a	X	X	X
SAR1B_HUMAN	GTP-binding protein SAR1b	X	X	X

RASH_HUMAN	GTPase HRas	X	X	X
RASN_HUMAN	GTPase NRas	X	X	X
GNAI2_HUMAN	Guanine nucleotide-binding protein G(i) subunit alpha-2	X	X	X
GBG12_HUMAN	Guanine nucleotide-binding protein G(I)/G(S)/G(O) subunit gamma-12	X	X	X
GBB1_HUMAN	Guanine nucleotide-binding protein G(I)/G(S)/G(T) subunit beta-1	X	X	X
GBB2_HUMAN	Guanine nucleotide-binding protein G(I)/G(S)/G(T) subunit beta-2	X	X	X
GNAS1_HUMAN	Guanine nucleotide-binding protein G(s) subunit alpha isoforms XLas	X	X	X
GNAT1_HUMAN	Guanine nucleotide-binding protein G(t) subunit alpha-1	X	X	X
GNA13_HUMAN	Guanine nucleotide-binding protein subunit alpha-13	X	X	X
GBB4_HUMAN	Guanine nucleotide-binding protein subunit beta-4	X	X	X
HS71L_HUMAN	Heat shock 70 kDa protein 1-like	X	X	X
HS12B_HUMAN	Heat shock 70 kDa protein 12B	X	X	X
HS71A_HUMAN	Heat shock 70 kDa protein 1A	X	X	X
HSP74_HUMAN	Heat shock 70 kDa protein 4	X	X	X
HSP76_HUMAN	Heat shock 70 kDa protein 6	X	X	X
HSP7C_HUMAN	Heat shock cognate 71 kDa protein	X	X	X
HS105_HUMAN	Heat shock protein 105 kDa	X	X	X
TRAP1_HUMAN	Heat shock protein 75 kDa, mitochondrial	X	X	X
HSPB1_HUMAN	Heat shock protein beta-1	X	X	X
HS90A_HUMAN	Heat shock protein HSP 90-alpha	X	X	X
HS90B_HUMAN	Heat shock protein HSP 90-beta	X	X	X
HBA_HUMAN	Hemoglobin subunit alpha	X	X	X
HNRPF_HUMAN	Heterogeneous nuclear ribonucleoprotein F	X	X	X
HNRH1_HUMAN	Heterogeneous nuclear ribonucleoprotein H	X	X	X
HNRH2_HUMAN	Heterogeneous nuclear ribonucleoprotein H2	X	X	X
HNRH3_HUMAN	Heterogeneous nuclear ribonucleoprotein H3	X	X	X
HNRPK_HUMAN	Heterogeneous nuclear ribonucleoprotein K	X	X	X
HNRPM_HUMAN	Heterogeneous nuclear ribonucleoprotein M	X	X	X

HNRPQ_HUMAN	Heterogeneous nuclear ribonucleoprotein Q	X	X	X
HNRPR_HUMAN	Heterogeneous nuclear ribonucleoprotein R	X	X	X
HNRPU_HUMAN	Heterogeneous nuclear ribonucleoprotein U	X	X	X
ROA2_HUMAN	Heterogeneous nuclear ribonucleoproteins A2/B1	X	X	X
HNRPC_HUMAN	Heterogeneous nuclear ribonucleoproteins C1/C2	X	X	X
HXK1_HUMAN	Hexokinase-1	X	X	X
H12_HUMAN	Histone H1.2	X	X	X
H14_HUMAN	Histone H1.4	X	X	X
H2A1B_HUMAN	Histone H2A type 1-B/E	X	X	X
H2A2B_HUMAN	Histone H2A type 2-B	X	X	X
H2AJ_HUMAN	Histone H2A.J	X	X	X
H2AV_HUMAN	Histone H2A.V	X	X	X
H31_HUMAN	Histone H3.1	X	X	X
H3C_HUMAN	Histone H3.3C	X	X	X
H4_HUMAN	Histone H4	X	X	X
HYOU1_HUMAN	Hypoxia up-regulated protein 1	X	X	X
IMA1_HUMAN	Importin subunit alpha-1	X	X	X
IMB1_HUMAN	Importin subunit beta-1	X	X	X
IPO7_HUMAN	Importin-7	X	X	X
IKIP_HUMAN	Inhibitor of nuclear factor kappa-B kinase-interacting protein	X	X	X
IMDH2_HUMAN	Inosine-5'-monophosphate dehydrogenase 2	X	X	X
IF2B1_HUMAN	Insulin-like growth factor 2 mRNA-binding protein 1	X	X	X
IF2B2_HUMAN	Insulin-like growth factor 2 mRNA-binding protein 2	X	X	X
IF2B3_HUMAN	Insulin-like growth factor 2 mRNA-binding protein 3	X	X	X
ITA2_HUMAN	Integrin alpha-2	X	X	X
ITA5_HUMAN	Integrin alpha-5	X	X	X
ITA6_HUMAN	Integrin alpha-6	X	X	X
ITAV_HUMAN	Integrin alpha-V	X	X	X

ITB1_HUMAN	Integrin beta-1	X	X	X
ITB3_HUMAN	Integrin beta-3	X	X	X
ILK_HUMAN	Integrin-linked protein kinase	X	X	X
ICAM2_HUMAN	Intercellular adhesion molecule 2	X	X	X
IFM1_HUMAN	Interferon-induced transmembrane protein 1	X	X	X
MMP1_HUMAN	Interstitial collagenase	X	X	X
IDH3A_HUMAN	Isocitrate dehydrogenase [NAD] subunit alpha, mitochondrial	X	X	X
SYIC_HUMAN	Isoleucine--tRNA ligase, cytoplasmic	X	X	X
PLAK_HUMAN	Junction plakoglobin	X	X	X
KINH_HUMAN	Kinesin-1 heavy chain	X	X	X
LDHA_HUMAN	L-lactate dehydrogenase A chain	X	X	X
LDHB_HUMAN	L-lactate dehydrogenase B chain	X	X	X
TRFL_HUMAN	Lactotransferrin	X	X	X
LAMB1_HUMAN	Laminin subunit beta-1	X	X	X
LAMC1_HUMAN	Laminin subunit gamma-1	X	X	X
LETM1_HUMAN	LETM1 and EF-hand domain-containing protein 1, mitochondrial	X	X	X
LPPRC_HUMAN	Leucine-rich PPR motif-containing protein, mitochondrial	X	X	X
LONM_HUMAN	Lon protease homolog, mitochondrial	X	X	X
ACSL3_HUMAN	Long-chain-fatty-acid--CoA ligase 3	X	X	X
MBOA7_HUMAN	Lysophospholipid acyltransferase 7	X	X	X
LAMP1_HUMAN	Lysosome-associated membrane glycoprotein 1	X	X	X
LYSC_HUMAN	Lysozyme C	X	X	X
MIF_HUMAN	Macrophage migration inhibitory factor	X	X	X
MVP_HUMAN	Major vault protein	X	X	X
MDHC_HUMAN	Malate dehydrogenase, cytoplasmic	X	X	X
MDHM_HUMAN	Malate dehydrogenase, mitochondrial	X	X	X
MPU1_HUMAN	Mannose-P-dolichol utilization defect 1 protein	X	X	X
MOGS_HUMAN	Mannosyl-oligosaccharide glucosidase	X	X	X

MGP_HUMAN	Matrix Gla protein	X	X	X
PGRC2_HUMAN	Membrane-associated progesterone receptor component 2	X	X	X
MANF_HUMAN	Mesencephalic astrocyte-derived neurotrophic factor	X	X	X
TIMP3_HUMAN	Metalloproteinase inhibitor 3	X	X	X
SYMC_HUMAN	Methionine--tRNA ligase, cytoplasmic	X	X	X
MIC19_HUMAN	MICOS complex subunit MIC19	X	X	X
MIC60_HUMAN	MICOS complex subunit MIC60	X	X	X
MGST3_HUMAN	Microsomal glutathione S-transferase 3	X	X	X
MACF1_HUMAN	Microtubule-actin cross-linking factor 1, isoforms 1/2/3/5	X	X	X
MAP1B_HUMAN	Microtubule-associated protein 1B	X	X	X
HM13_HUMAN	Minor histocompatibility antigen H13	X	X	X
M2OM_HUMAN	Mitochondrial 2-oxoglutarate/malate carrier protein	X	X	X
MTCH2_HUMAN	Mitochondrial carrier homolog 2	X	X	X
TIM14_HUMAN	Mitochondrial import inner membrane translocase subunit TIM14	X	X	X
TIM44_HUMAN	Mitochondrial import inner membrane translocase subunit TIM44	X	X	X
TOM22_HUMAN	Mitochondrial import receptor subunit TOM22 homolog	X	X	X
MOES_HUMAN	Moesin	X	X	X
MOT4_HUMAN	Monocarboxylate transporter 4	X	X	X
MRP1_HUMAN	Multidrug resistance-associated protein 1	X	X	X
MYADM_HUMAN	Myeloid-associated differentiation marker	X	X	X
MYDGF_HUMAN	Myeloid-derived growth factor	X	X	X
MYOF_HUMAN	Myoferlin	X	X	X
MYL6_HUMAN	Myosin light polypeptide 6	X	X	X
ML12A_HUMAN	Myosin regulatory light chain 12A	X	X	X
MYH10_HUMAN	Myosin-10	X	X	X
MYH11_HUMAN	Myosin-11	X	X	X
MYH14_HUMAN	Myosin-14 OS=Homo sapiens GN=MYH14 PE=1 SV=2	X	X	X
MYH9_HUMAN	Myosin-9	X	X	X

MAOM_HUMAN	NAD-dependent malic enzyme, mitochondrial	X	X	X
NNTM_HUMAN	NAD(P) transhydrogenase, mitochondrial	X	X	X
NDUAD_HUMAN	NADH dehydrogenase [ubiquinone] 1 alpha subcomplex subunit 13	X	X	X
NDUA2_HUMAN	NADH dehydrogenase [ubiquinone] 1 alpha subcomplex subunit 2	X	X	X
NDUA5_HUMAN	NADH dehydrogenase [ubiquinone] 1 alpha subcomplex subunit 5	X	X	X
NDUA6_HUMAN	NADH dehydrogenase [ubiquinone] 1 alpha subcomplex subunit 6	X	X	X
NDUB4_HUMAN	NADH dehydrogenase [ubiquinone] 1 beta subcomplex subunit 4	X	X	X
NDUB7_HUMAN	NADH dehydrogenase [ubiquinone] 1 beta subcomplex subunit 7	X	X	X
NDUB8_HUMAN	NADH dehydrogenase [ubiquinone] 1 beta subcomplex subunit 8, mitochondrial	X	X	X
NDUS3_HUMAN	NADH dehydrogenase [ubiquinone] iron-sulfur protein 3, mitochondrial	X	X	X
NB5R3_HUMAN	NADH-cytochrome b5 reductase 3	X	X	X
NDUS1_HUMAN	NADH-ubiquinone oxidoreductase 75 kDa subunit, mitochondrial	X	X	X
NCPR_HUMAN	NADPH--cytochrome P450 reductase	X	X	X
ADRO_HUMAN	NADPH:adrenodoxin oxidoreductase, mitochondrial	X	X	X
NEST_HUMAN	Nestin	X	X	X
AHNK_HUMAN	Neuroblast differentiation-associated protein AHNAK	X	X	X
GANAB_HUMAN	Neutral alpha-glucosidase AB	X	X	X
AAAT_HUMAN	Neutral amino acid transporter B(0)	X	X	X
NCEH1_HUMAN	Neutral cholesterol ester hydrolase 1	X	X	X
NOS3_HUMAN	Nitric oxide synthase, endothelial	X	X	X
NOMO2_HUMAN	Nodal modulator 2	X	X	X
NOMO3_HUMAN	Nodal modulator 3	X	X	X
NLTP_HUMAN	Non-specific lipid-transfer protein	X	X	X
DFNA5_HUMAN	Non-syndromic hearing impairment protein 5	X	X	X
NDK3_HUMAN	Nucleoside diphosphate kinase 3	X	X	X
NDKA_HUMAN	Nucleoside diphosphate kinase A	X	X	X

NDKB_HUMAN	Nucleoside diphosphate kinase B	X	X	X
OCAD2_HUMAN	OCIA domain-containing protein 2	X	X	X
OSTC_HUMAN	Oligosaccharyltransferase complex subunit OSTC	X	X	X
OAT_HUMAN	Ornithine aminotransferase, mitochondrial	X	X	X
PTX3_HUMAN	Pentraxin-related protein PTX3	X	X	X
PPIA_HUMAN	Peptidyl-prolyl cis-trans isomerase A	X	X	X
PPIB_HUMAN	Peptidyl-prolyl cis-trans isomerase B	X	X	X
FKB1A_HUMAN	Peptidyl-prolyl cis-trans isomerase FKBP1A	X	X	X
FKBP2_HUMAN	Peptidyl-prolyl cis-trans isomerase FKBP2	X	X	X
PTH2_HUMAN	Peptidyl-tRNA hydrolase 2, mitochondrial	X	X	X
PXDN_HUMAN	Peroxidasin homolog	X	X	X
PRDX1_HUMAN	Peroxiredoxin-1	X	X	X
PRDX2_HUMAN	Peroxiredoxin-2	X	X	X
PRDX4_HUMAN	Peroxiredoxin-4	X	X	X
PRDX5_HUMAN	Peroxiredoxin-5, mitochondrial	X	X	X
PRDX6_HUMAN	Peroxiredoxin-6	X	X	X
DHB4_HUMAN	Peroxisomal multifunctional enzyme type 2	X	X	X
SYFB_HUMAN	Phenylalanine--tRNA ligase beta subunit	X	X	X
MPCP_HUMAN	Phosphate carrier protein, mitochondrial	X	X	X
PTSS1_HUMAN	Phosphatidylserine synthase 1	X	X	X
PGK1_HUMAN	Phosphoglycerate kinase 1	X	X	X
PGAM1_HUMAN	Phosphoglycerate mutase 1	X	X	X
PLS4_HUMAN	Phospholipid scramblase 4	X	X	X
PTTG_HUMAN	Pituitary tumor-transforming gene 1 protein-interacting protein	X	X	X
AT2B3_HUMAN	Plasma membrane calcium-transporting ATPase 3	X	X	X
AT2B4_HUMAN	Plasma membrane calcium-transporting ATPase 4	X	X	X
PAI1_HUMAN	Plasminogen activator inhibitor 1	X	X	X
PLRKT_HUMAN	Plasminogen receptor (KT)	X	X	X

PLST_HUMAN	Plastin-3	X	X	X
PECA1_HUMAN	Platelet endothelial cell adhesion molecule	X	X	X
PA1B2_HUMAN	Platelet-activating factor acetylhydrolase IB subunit beta	X	X	X
PLEC_HUMAN	Plectin	X	X	X
PODXL_HUMAN	Podocalyxin	X	X	X
PCBP1_HUMAN	Poly(rC)-binding protein 1	X	X	X
PCBP2_HUMAN	Poly(rC)-binding protein 2	X	X	X
PABP1_HUMAN	Polyadenylate-binding protein 1	X	X	X
PABP4_HUMAN	Polyadenylate-binding protein 4	X	X	X
PTRF_HUMAN	Polymerase I and transcript release factor	X	X	X
UBB_HUMAN	Polyubiquitin-B	X	X	X
POTEF_HUMAN	POTE ankyrin domain family member F	X	X	X
POTEI_HUMAN	POTE ankyrin domain family member I	X	X	X
POTEJ_HUMAN	POTE ankyrin domain family member J	X	X	X
PRAF2_HUMAN	PRA1 family protein 2	X	X	X
PRAF3_HUMAN	PRA1 family protein 3	X	X	X
LMNA_HUMAN	Prelamin-A/C	X	X	X
PCYOX_HUMAN	Prenylcysteine oxidase 1	X	X	X
GT251_HUMAN	Procollagen galactosyltransferase 1	X	X	X
PLOD1_HUMAN	Procollagen-lysine,2-oxoglutarate 5-dioxygenase 1	X	X	X
PLOD2_HUMAN	Procollagen-lysine,2-oxoglutarate 5-dioxygenase 2	X	X	X
PROF1_HUMAN	Profilin-1	X	X	X
PDC6I_HUMAN	Programmed cell death 6-interacting protein	X	X	X
PHB_HUMAN	Prohibitin	X	X	X
PHB2_HUMAN	Prohibitin-2	X	X	X
P3H1_HUMAN	Prolyl 3-hydroxylase 1	X	X	X
P4HA1_HUMAN	Prolyl 4-hydroxylase subunit alpha-1	X	X	X
TEBP_HUMAN	Prostaglandin E synthase 3	X	X	X

PSA4_HUMAN	Proteasome subunit alpha type-4	X	X	X
CNPY2_HUMAN	Protein canopy homolog 2	X	X	X
CYR61_HUMAN	Protein CYR61	X	X	X
PDIA1_HUMAN	Protein disulfide-isomerase	X	X	X
PDIA3_HUMAN	Protein disulfide-isomerase A3	X	X	X
PDIA4_HUMAN	Protein disulfide-isomerase A4	X	X	X
PDIA6_HUMAN	Protein disulfide-isomerase A6	X	X	X
LMAN1_HUMAN	Protein ERGIC-53	X	X	X
F162A_HUMAN	Protein FAM162A	X	X	X
FLII_HUMAN	Protein flightless-1 homolog	X	X	X
PRDBP_HUMAN	Protein kinase C delta-binding protein	X	X	X
LYRIC_HUMAN	Protein LYRIC	X	X	X
NPS3A_HUMAN	Protein NipSnap homolog 3A	X	X	X
RER1_HUMAN	Protein RER1	X	X	X
S10AA_HUMAN	Protein S100-A10	X	X	X
S10AB_HUMAN	Protein S100-A11	X	X	X
S10A6_HUMAN	Protein S100-A6	X	X	X
SC31A_HUMAN	Protein transport protein Sec31A	X	X	X
SC61B_HUMAN	Protein transport protein Sec61 subunit beta	X	X	X
SC61G_HUMAN	Protein transport protein Sec61 subunit gamma	X	X	X
TGM2_HUMAN	Protein-glutamine gamma-glutamyltransferase 2	X	X	X
PRG4_HUMAN	Proteoglycan 4	X	X	X
PLP2_HUMAN	Proteolipid protein 2	X	X	X
PNPH_HUMAN	Purine nucleoside phosphorylase	X	X	X
PSA_HUMAN	Puromycin-sensitive aminopeptidase	X	X	X
RS26L_HUMAN	Putative 40S ribosomal protein S26-like 1	X	X	X
ACTBM_HUMAN	Putative beta-actin-like protein 3	X	X	X
NDK8_HUMAN	Putative nucleoside diphosphate kinase	X	X	X

PYC_HUMAN	Pyruvate carboxylase, mitochondrial	X	X	X
ODPA_HUMAN	Pyruvate dehydrogenase E1 component subunit alpha, somatic form, mitochondrial	X	X	X
ODPB_HUMAN	Pyruvate dehydrogenase E1 component subunit beta, mitochondrial	X	X	X
KPYM_HUMAN	Pyruvate kinase PKM	X	X	X
GDIA_HUMAN	Rab GDP dissociation inhibitor alpha	X	X	X
GDIB_HUMAN	Rab GDP dissociation inhibitor beta	X	X	X
RADI_HUMAN	Radixin	X	X	X
IQGA1_HUMAN	Ras GTPase-activating-like protein IQGAP1	X	X	X
RAIN_HUMAN	Ras-interacting protein 1	X	X	X
RAC1_HUMAN	Ras-related C3 botulinum toxin substrate 1	X	X	X
RAC2_HUMAN	Ras-related C3 botulinum toxin substrate 2	X	X	X
RRAS_HUMAN	Ras-related protein R-Ras	X	X	X
RRAS2_HUMAN	Ras-related protein R-Ras2	X	X	X
RAB10_HUMAN	Ras-related protein Rab-10	X	X	X
RB11A_HUMAN	Ras-related protein Rab-11A	X	X	X
RAB13_HUMAN	Ras-related protein Rab-13	X	X	X
RAB14_HUMAN	Ras-related protein Rab-14	X	X	X
RAB18_HUMAN	Ras-related protein Rab-18	X	X	X
RAB1A_HUMAN	Ras-related protein Rab-1A	X	X	X
RAB1B_HUMAN	Ras-related protein Rab-1B	X	X	X
RB22A_HUMAN	Ras-related protein Rab-22A	X	X	X
RAB2A_HUMAN	Ras-related protein Rab-2A	X	X	X
RAB5A_HUMAN	Ras-related protein Rab-5A	X	X	X
RAB5B_HUMAN	Ras-related protein Rab-5B	X	X	X
RAB5C_HUMAN	Ras-related protein Rab-5C	X	X	X
RAB6A_HUMAN	Ras-related protein Rab-6A	X	X	X
RAB6B_HUMAN	Ras-related protein Rab-6B	X	X	X

RAB7A_HUMAN	Ras-related protein Rab-7a	X	X	X
RAB8A_HUMAN	Ras-related protein Rab-8A	X	X	X
RAB8B_HUMAN	Ras-related protein Rab-8B	X	X	X
RALA_HUMAN	Ras-related protein Ral-A	X	X	X
RALB_HUMAN	Ras-related protein Ral-B	X	X	X
RAP1A_HUMAN	Ras-related protein Rap-1A	X	X	X
RAP1B_HUMAN	Ras-related protein Rap-1b	X	X	X
RAP2B_HUMAN	Ras-related protein Rap-2b	X	X	X
REEP5_HUMAN	Receptor expression-enhancing protein 5	X	X	X
F213A_HUMAN	Redox-regulatory protein FAM213A	X	X	X
RCN1_HUMAN	Reticulocalbin-1	X	X	X
RTN3_HUMAN	Reticulon-3	X	X	X
RTN4_HUMAN	Reticulon-4	X	X	X
RDH11_HUMAN	Retinol dehydrogenase 11	X	X	X
GDIR1_HUMAN	Rho GDP-dissociation inhibitor 1	X	X	X
RHOC_HUMAN	Rho-related GTP-binding protein RhoC	X	X	X
RHOG_HUMAN	Rho-related GTP-binding protein RhoG	X	X	X
RINI_HUMAN	Ribonuclease inhibitor	X	X	X
RUVB1_HUMAN	RuvB-like 1	X	X	X
RUVB2_HUMAN	RuvB-like 2	X	X	X
AT2A2_HUMAN	Sarcoplasmic/endoplasmic reticulum calcium ATPase 2	X	X	X
SCAM2_HUMAN	Secretory carrier-associated membrane protein 2	X	X	X
SPRE_HUMAN	Sepiapterin reductase	X	X	X
SEP11_HUMAN	Septin-11	X	X	X
SEPT2_HUMAN	Septin-2	X	X	X
SEPT7_HUMAN	Septin-7	X	X	X
GLYM_HUMAN	Serine hydroxymethyltransferase, mitochondrial	X	X	X
SRSF3_HUMAN	Serine/arginine-rich splicing factor 3	X	X	X

PP1A_HUMAN	Serine/threonine-protein phosphatase PP1-alpha catalytic subunit	X	X	X
PP1B_HUMAN	Serine/threonine-protein phosphatase PP1-beta catalytic subunit	X	X	X
PP1G_HUMAN	Serine/threonine-protein phosphatase PP1-gamma catalytic subunit	X	X	X
SERPH_HUMAN	Serpin H1	X	X	X
ALBU_HUMAN	Serum albumin	X	X	X
SDPR_HUMAN	Serum deprivation-response protein	X	X	X
PON2_HUMAN	Serum paraoxonase/arylesterase 2	X	X	X
SH3L3_HUMAN	SH3 domain-binding glutamic acid-rich-like protein 3	X	X	X
SFXN1_HUMAN	Sideroflexin-1	X	X	X
SFXN3_HUMAN	Sideroflexin-3	X	X	X
SC11A_HUMAN	Signal peptidase complex catalytic subunit SEC11A	X	X	X
SRPRB_HUMAN	Signal recognition particle receptor subunit beta	X	X	X
SSBP_HUMAN	Single-stranded DNA-binding protein, mitochondrial	X	X	X
RUXE_HUMAN	Small nuclear ribonucleoprotein E	X	X	X
RUXF_HUMAN	Small nuclear ribonucleoprotein F	X	X	X
SMD3_HUMAN	Small nuclear ribonucleoprotein Sm D3	X	X	X
AT1A1_HUMAN	Sodium/potassium-transporting ATPase subunit alpha-1	X	X	X
AT1A2_HUMAN	Sodium/potassium-transporting ATPase subunit alpha-2	X	X	X
AT1A3_HUMAN	Sodium/potassium-transporting ATPase subunit alpha-3	X	X	X
AT1B3_HUMAN	Sodium/potassium-transporting ATPase subunit beta-3	X	X	X
GTR1_HUMAN	Solute carrier family 2, facilitated glucose transporter member 1	X	X	X
SNX3_HUMAN	Sorting nexin-3	X	X	X
SPTN1_HUMAN	Spectrin alpha chain, non-erythrocytic 1	X	X	X
SPTB1_HUMAN	Spectrin beta chain, erythrocytic	X	X	X
SPTB2_HUMAN	Spectrin beta chain, non-erythrocytic 1	X	X	X
SPTN2_HUMAN	Spectrin beta chain, non-erythrocytic 2	X	X	X
SND1_HUMAN	Staphylococcal nuclease domain-containing protein 1	X	X	X
STML2_HUMAN	Stomatin-like protein 2, mitochondrial	X	X	X

GRP75_HUMAN	Stress-70 protein, mitochondrial	X	X	X
STIM1_HUMAN	Stromal interaction molecule 1	X	X	X
SDHA_HUMAN	Succinate dehydrogenase [ubiquinone] flavoprotein subunit, mitochondrial	X	X	X
SDHB_HUMAN	Succinate dehydrogenase [ubiquinone] iron-sulfur subunit, mitochondrial	X	X	X
SUCA_HUMAN	Succinate--CoA ligase [ADP/GDP-forming] subunit alpha, mitochondrial	X	X	X
SQRD_HUMAN	Sulfide:quinone oxidoreductase, mitochondrial	X	X	X
ST1A3_HUMAN	Sulfotransferase 1A3	X	X	X
SURF4_HUMAN	Surfeit locus protein 4	X	X	X
SRPX_HUMAN	Sushi repeat-containing protein SRPX	X	X	X
VAT1_HUMAN	Synaptic vesicle membrane protein VAT-1 homolog	X	X	X
SNG2_HUMAN	Synaptogyrin-2	X	X	X
SYJ2B_HUMAN	Synaptojanin-2-binding protein	X	X	X
SDCB1_HUMAN	Syntenin-1	X	X	X
TCPA_HUMAN	T-complex protein 1 subunit alpha	X	X	X
TCPB_HUMAN	T-complex protein 1 subunit beta	X	X	X
TCPD_HUMAN	T-complex protein 1 subunit delta	X	X	X
TCPE_HUMAN	T-complex protein 1 subunit epsilon	X	X	X
TCPH_HUMAN	T-complex protein 1 subunit eta	X	X	X
TCPG_HUMAN	T-complex protein 1 subunit gamma	X	X	X
TCPQ_HUMAN	T-complex protein 1 subunit theta	X	X	X
TCPZ_HUMAN	T-complex protein 1 subunit zeta	X	X	X
TLN1_HUMAN	Talin-1	X	X	X
TX1B3_HUMAN	Tax1-binding protein 3	X	X	X
TXD17_HUMAN	Thioredoxin domain-containing protein 17	X	X	X
TXND5_HUMAN	Thioredoxin domain-containing protein 5	X	X	X
PRDX3_HUMAN	Thioredoxin-dependent peroxide reductase, mitochondrial	X	X	X

TMX2_HUMAN	Thioredoxin-related transmembrane protein 2	X	X	X
SYTC_HUMAN	Threonine--tRNA ligase, cytoplasmic	X	X	X
TSP1_HUMAN	Thrombospondin-1	X	X	X
KTHY_HUMAN	Thymidylate kinase	X	X	X
TPA_HUMAN	Tissue-type plasminogen activator	X	X	X
TFR1_HUMAN	Transferrin receptor protein 1	X	X	X
BGH3_HUMAN	Transforming growth factor-beta-induced protein ig-h3	X	X	X
RHOA_HUMAN	Transforming protein RhoA	X	X	X
TAGL2_HUMAN	Transgelin-2	X	X	X
TERA_HUMAN	Transitional endoplasmic reticulum ATPase	X	X	X
TSPO_HUMAN	Translocator protein	X	X	X
SSRD_HUMAN	Translocon-associated protein subunit delta	X	X	X
SSRG_HUMAN	Translocon-associated protein subunit gamma	X	X	X
TMEDA_HUMAN	Transmembrane emp24 domain-containing protein 10	X	X	X
TMED4_HUMAN	Transmembrane emp24 domain-containing protein 4	X	X	X
TMED7_HUMAN	Transmembrane emp24 domain-containing protein 7	X	X	X
TMED9_HUMAN	Transmembrane emp24 domain-containing protein 9	X	X	X
TM109_HUMAN	Transmembrane protein 109	X	X	X
TNPO1_HUMAN	Transportin-1	X	X	X
TXTP_HUMAN	Tricarboxylate transport protein, mitochondrial	X	X	X
ECHA_HUMAN	Trifunctional enzyme subunit alpha, mitochondrial	X	X	X
ECHB_HUMAN	Trifunctional enzyme subunit beta, mitochondrial	X	X	X
PUR2_HUMAN	Trifunctional purine biosynthetic protein adenosine-3	X	X	X
TPIS_HUMAN	Triosephosphate isomerase	X	X	X
TPM4_HUMAN	Tropomyosin alpha-4 chain	X	X	X
SYWC_HUMAN	Tryptophan--tRNA ligase, cytoplasmic	X	X	X
TBA1C_HUMAN	Tubulin alpha-1C chain	X	X	X
TBA3C_HUMAN	Tubulin alpha-3C/D chain	X	X	X

TBA4A_HUMAN	Tubulin alpha-4A chain	X	X	X
TBA8_HUMAN	Tubulin alpha-8 chain	X	X	X
TBB5_HUMAN	Tubulin beta chain	X	X	X
TBB2A_HUMAN	Tubulin beta-2A chain	X	X	X
TBB3_HUMAN	Tubulin beta-3 chain	X	X	X
TBB4A_HUMAN	Tubulin beta-4A chain	X	X	X
TBB4B_HUMAN	Tubulin beta-4B chain	X	X	X
TBB6_HUMAN	Tubulin beta-6 chain	X	X	X
TBB8_HUMAN	Tubulin beta-8 chain	X	X	X
PTN1_HUMAN	Tyrosine-protein phosphatase non-receptor type 1	X	X	X
UBP5_HUMAN	Ubiquitin carboxyl-terminal hydrolase 5	X	X	X
RS27A_HUMAN	Ubiquitin-40S ribosomal protein S27a	X	X	X
UBA1_HUMAN	Ubiquitin-like modifier-activating enzyme 1	X	X	X
UGDH_HUMAN	UDP-glucose 6-dehydrogenase	X	X	X
UGGG1_HUMAN	UDP-glucose:glycoprotein glucosyltransferase 1	X	X	X
KCY_HUMAN	UMP-CMP kinase	X	X	X
MYO1C_HUMAN	Unconventional myosin-Ic	X	X	X
USMG5_HUMAN	Up-regulated during skeletal muscle growth protein 5	X	X	X
VPS35_HUMAN	Vacuolar protein sorting-associated protein 35	X	X	X
SYVC_HUMAN	Valine--tRNA ligase	X	X	X
ACADV_HUMAN	Very long-chain specific acyl-CoA dehydrogenase, mitochondrial	X	X	X
HACD3_HUMAN	Very-long-chain (3R)-3-hydroxyacyl-CoA dehydratase 3	X	X	X
DHB12_HUMAN	Very-long-chain 3-oxoacyl-CoA reductase	X	X	X
GOT1B_HUMAN	Vesicle transport protein GOT1B	X	X	X
VAMP3_HUMAN	Vesicle-associated membrane protein 3	X	X	X
VAMP5_HUMAN	Vesicle-associated membrane protein 5	X	X	X
SC22B_HUMAN	Vesicle-trafficking protein SEC22b	X	X	X
VIME_HUMAN	Vimentin	X	X	X

VINC_HUMAN	Vinculin	X	X	X
VKORL_HUMAN	Vitamin K epoxide reductase complex subunit 1-like protein 1	X	X	X
VDAC1_HUMAN	Voltage-dependent anion-selective channel protein 1	X	X	X
VDAC2_HUMAN	Voltage-dependent anion-selective channel protein 2	X	X	X
VDAC3_HUMAN	Voltage-dependent anion-selective channel protein 3	X	X	X
CA2D1_HUMAN	Voltage-dependent calcium channel subunit alpha-2/delta-1	X	X	X
STRUM_HUMAN	WASH complex subunit strumpellin	X	X	X
WDR1_HUMAN	WD repeat-containing protein 1	X	X	X
XRCC6_HUMAN	X-ray repair cross-complementing protein 6	X	X	X
PDP1_HUMAN	[Pyruvate dehydrogenase [acetyl-transferring]]-phosphatase 1, mitochondrial	X	X	
U5S1_HUMAN	116 kDa U5 small nuclear ribonucleoprotein component	X	X	
DECR_HUMAN	2,4-dienoyl-CoA reductase, mitochondrial	X	X	
PRS6B_HUMAN	26S protease regulatory subunit 6B	X	X	
PRS7_HUMAN	26S protease regulatory subunit 7	X	X	
PSD12_HUMAN	26S proteasome non-ATPase regulatory subunit 12	X	X	
PSMD5_HUMAN	26S proteasome non-ATPase regulatory subunit 5	X	X	
PSMD6_HUMAN	26S proteasome non-ATPase regulatory subunit 6	X	X	
RT14_HUMAN	28S ribosomal protein S14, mitochondrial	X	X	
RT17_HUMAN	28S ribosomal protein S17, mitochondrial	X	X	
HCD2_HUMAN	3-hydroxyacyl-CoA dehydrogenase type-2	X	X	
3HIDH_HUMAN	3-hydroxyisobutyrate dehydrogenase, mitochondrial	X	X	
HIBCH_HUMAN	3-hydroxyisobutyryl-CoA hydrolase, mitochondrial	X	X	
RM23_HUMAN	39S ribosomal protein L23, mitochondrial	X	X	
RM44_HUMAN	39S ribosomal protein L44, mitochondrial	X	X	
RM49_HUMAN	39S ribosomal protein L49, mitochondrial	X	X	
RS15_HUMAN	40S ribosomal protein S15	X	X	

RS28_HUMAN	40S ribosomal protein S28	X	X	
6PGD_HUMAN	6-phosphogluconate dehydrogenase, decarboxylating	X	X	
RL10A_HUMAN	60S ribosomal protein L10a	X	X	
RL13_HUMAN	60S ribosomal protein L13	X	X	
RL27_HUMAN	60S ribosomal protein L27	X	X	
RL32_HUMAN	60S ribosomal protein L32	X	X	
RL35_HUMAN	60S ribosomal protein L35	X	X	
RL8_HUMAN	60S ribosomal protein L8	X	X	
RL9_HUMAN	60S ribosomal protein L9	X	X	
ILVBL_HUMAN	Acetolactate synthase-like protein	X	X	
ACON_HUMAN	Aconitate hydratase, mitochondrial	X	X	
ABLM3_HUMAN	Actin-binding LIM protein 3	X	X	
FAHD1_HUMAN	Acylpyruvase FAHD1, mitochondrial	X	X	
KAD4_HUMAN	Adenylate kinase 4, mitochondrial	X	X	
ADAS_HUMAN	Alkyldihydroxyacetonephosphate synthase, peroxisomal	X	X	
RETST_HUMAN	All-trans-retinol 13,14-reductase	X	X	
AL7A1_HUMAN	Alpha-aminoadipic semialdehyde dehydrogenase	X	X	
ANXA7_HUMAN	Annexin A7	X	X	
AP2B1_HUMAN	AP-2 complex subunit beta	X	X	
AP3B1_HUMAN	AP-3 complex subunit beta-1	X	X	
AP3S1_HUMAN	AP-3 complex subunit sigma-1	X	X	
CLPP_HUMAN	ATP-dependent Clp protease proteolytic subunit, mitochondrial	X	X	
BAP31_HUMAN	B-cell receptor-associated protein 31	X	X	
BAG3_HUMAN	BAG family molecular chaperone regulator 3	X	X	
BAF_HUMAN	Barrier-to-autointegration factor	X	X	
B2CL1_HUMAN	Bcl-2-like protein 1	X	X	
SYEP_HUMAN	Bifunctional glutamate/proline--tRNA ligase	X	X	
CADH5_HUMAN	Cadherin-5	X	X	

CHP1_HUMAN	Calcineurin B homologous protein 1	X	X	
KCC2D_HUMAN	Calcium/calmodulin-dependent protein kinase type II subunit delta	X	X	
CYBP_HUMAN	Calcyclin-binding protein	X	X	
CALD1_HUMAN	Caldesmon	X	X	
CALU_HUMAN	Calumenin	X	X	
KAP2_HUMAN	cAMP-dependent protein kinase type II-alpha regulatory subunit	X	X	
NTPCR_HUMAN	Cancer-related nucleoside-triphosphatase	X	X	
CSK21_HUMAN	Casein kinase II subunit alpha	X	X	
CSK23_HUMAN	Casein kinase II subunit alpha 3	X	X	
CATA_HUMAN	Catalase	X	X	
COMT_HUMAN	Catechol O-methyltransferase	X	X	
CATB_HUMAN	Cathepsin B	X	X	
CATD_HUMAN	Cathepsin D	X	X	
COPB_HUMAN	Coatomer subunit beta	X	X	
COPZ1_HUMAN	Coatomer subunit zeta-1	X	X	
COF2_HUMAN	Cofilin-2	X	X	
CCD47_HUMAN	Coiled-coil domain-containing protein 47	X	X	
C1QBP_HUMAN	Complement component 1 Q subcomponent-binding protein, mitochondrial	X	X	
CNTP1_HUMAN	Contactin-associated protein 1	X	X	
CSN3_HUMAN	COP9 signalosome complex subunit 3	X	X	
CSN8_HUMAN	COP9 signalosome complex subunit 8	X	X	
CPNE2_HUMAN	Copine-2	X	X	
CPNE3_HUMAN	Copine-3	X	X	
H2AY_HUMAN	Core histone macro-H2A.1	X	X	
CDK5_HUMAN	Cyclin-dependent-like kinase 5	X	X	
QCR6_HUMAN	Cytochrome b-c1 complex subunit 6, mitochondrial	X	X	
CYC_HUMAN	Cytochrome c	X	X	

ACOC_HUMAN	Cytoplasmic aconitate hydratase	X	X	
AMPL_HUMAN	Cytosol aminopeptidase	X	X	
DHRS7_HUMAN	Dehydrogenase/reductase SDR family member 7	X	X	
ECH1_HUMAN	Delta(3,5)-Delta(2,4)-dienoyl-CoA isomerase, mitochondrial	X	X	
DESM_HUMAN	Desmin	X	X	
DESP_HUMAN	Desmoplakin	X	X	
DNJA1_HUMAN	DnaJ homolog subfamily A member 1	X	X	
DJB11_HUMAN	DnaJ homolog subfamily B member 11	X	X	
DNJC3_HUMAN	DnaJ homolog subfamily C member 3	X	X	
STT3A_HUMAN	Dolichyl-diphosphooligosaccharide--protein glycosyltransferase subunit STT3A	X	X	
STT3B_HUMAN	Dolichyl-diphosphooligosaccharide--protein glycosyltransferase subunit STT3B	X	X	
DREB_HUMAN	Drebrin	X	X	
DYN2_HUMAN	Dynamin-2	X	X	
RN213_HUMAN	E3 ubiquitin-protein ligase RNF213	X	X	
ELAV1_HUMAN	ELAV-like protein 1	X	X	
ENDD1_HUMAN	Endonuclease domain-containing 1 protein	X	X	
SHLB1_HUMAN	Endophilin-B1	X	X	
ESAM_HUMAN	Endothelial cell-selective adhesion molecule	X	X	
ECI1_HUMAN	Enoyl-CoA delta isomerase 1, mitochondrial	X	X	
ES1_HUMAN	ES1 protein homolog, mitochondrial	X	X	
EIF3C_HUMAN	Eukaryotic translation initiation factor 3 subunit C	X	X	
EIF3E_HUMAN	Eukaryotic translation initiation factor 3 subunit E	X	X	
EIF3M_HUMAN	Eukaryotic translation initiation factor 3 subunit M	X	X	
IF4G1_HUMAN	Eukaryotic translation initiation factor 4 gamma 1	X	X	
IF4G2_HUMAN	Eukaryotic translation initiation factor 4 gamma 2	X	X	
FAF2_HUMAN	FAS-associated factor 2	X	X	

FILA2_HUMAN	Filaggrin-2	X	X	
IF16_HUMAN	Gamma-interferon-inducible protein 16	X	X	
GDN_HUMAN	Glia-derived nexin	X	X	
GSH0_HUMAN	Glutamate--cysteine ligase regulatory subunit	X	X	
GSTK1_HUMAN	Glutathione S-transferase kappa 1	X	X	
GSTM3_HUMAN	Glutathione S-transferase Mu 3	X	X	
GAPR1_HUMAN	Golgi-associated plant pathogenesis-related protein 1	X	X	
PIGS_HUMAN	GPI transamidase component PIG-S	X	X	
GIMA1_HUMAN	GTPase IMAP family member 1	X	X	
GNAI3_HUMAN	Guanine nucleotide-binding protein G(k) subunit alpha	X	X	
H1BP3_HUMAN	HCLS1-binding protein 3	X	X	
ROAA_HUMAN	Heterogeneous nuclear ribonucleoprotein A/B	X	X	
HNRPD_HUMAN	Heterogeneous nuclear ribonucleoprotein D0	X	X	
HNRL2_HUMAN	Heterogeneous nuclear ribonucleoprotein U-like protein 2	X	X	
HIG1A_HUMAN	HIG1 domain family member 1A, mitochondrial	X	X	
HINT2_HUMAN	Histidine triad nucleotide-binding protein 2, mitochondrial	X	X	
HORN_HUMAN	Hornerin	X	X	
CDC37_HUMAN	Hsp90 co-chaperone Cdc37	X	X	
IPO5_HUMAN	Importin-5	X	X	
ITPR3_HUMAN	Inositol 1,4,5-trisphosphate receptor type 3	X	X	
ILF2_HUMAN	Interleukin enhancer-binding factor 2	X	X	
IDH3B_HUMAN	Isocitrate dehydrogenase [NAD] subunit beta, mitochondrial	X	X	
IDH3G_HUMAN	Isocitrate dehydrogenase [NAD] subunit gamma, mitochondrial	X	X	
IDHP_HUMAN	Isocitrate dehydrogenase [NADP], mitochondrial	X	X	
SYIM_HUMAN	Isoleucine--tRNA ligase, mitochondrial	X	X	
KDEL2_HUMAN	KDEL motif-containing protein 2	X	X	
DCXR_HUMAN	L-xylulose reductase	X	X	
LAMA5_HUMAN	Laminin subunit alpha-5	X	X	

LTBP1_HUMAN	Latent-transforming growth factor beta-binding protein 1	X	X	
LTBP2_HUMAN	Latent-transforming growth factor beta-binding protein 2	X	X	
SYLC_HUMAN	Leucine--tRNA ligase, cytoplasmic	X	X	
LRC59_HUMAN	Leucine-rich repeat-containing protein 59	X	X	
LASP1_HUMAN	LIM and SH3 domain protein 1	X	X	
ODB2_HUMAN	Lipoamide acyltransferase component of branched-chain alpha-keto acid dehydrogenase complex, mitochondrial	X	X	
LYAG_HUMAN	Lysosomal alpha-glucosidase	X	X	
MA2B1_HUMAN	Lysosomal alpha-mannosidase	X	X	
SCRB2_HUMAN	Lysosome membrane protein 2	X	X	
MMGT1_HUMAN	Membrane magnesium transporter 1	X	X	
PGRC1_HUMAN	Membrane-associated progesterone receptor component 1	X	X	
MTX1_HUMAN	Metaxin-1	X	X	
MIC26_HUMAN	MICOS complex subunit MIC26	X	X	
BCS1_HUMAN	Mitochondrial chaperone BCS1	X	X	
FIS1_HUMAN	Mitochondrial fission 1 protein	X	X	
GHC1_HUMAN	Mitochondrial glutamate carrier 1	X	X	
TOM40_HUMAN	Mitochondrial import receptor subunit TOM40 homolog	X	X	
TOM70_HUMAN	Mitochondrial import receptor subunit TOM70	X	X	
MIRO1_HUMAN	Mitochondrial Rho GTPase 1	X	X	
MK03_HUMAN	Mitogen-activated protein kinase 3	X	X	
TR112_HUMAN	Multifunctional methyltransferase subunit TRM112-like protein	X	X	
MMRN1_HUMAN	Multimerin-1	X	X	
NAGK_HUMAN	N-acetyl-D-glucosamine kinase	X	X	
NQO1_HUMAN	NAD(P)H dehydrogenase [quinone] 1	X	X	
NDUA7_HUMAN	NADH dehydrogenase [ubiquinone] 1 alpha subcomplex subunit 7	X	X	
NDUB9_HUMAN	NADH dehydrogenase [ubiquinone] 1 beta subcomplex subunit 9	X	X	
NDUV1_HUMAN	NADH dehydrogenase [ubiquinone] flavoprotein 1, mitochondrial	X	X	

NDUV2_HUMAN	NADH dehydrogenase [ubiquinone] flavoprotein 2, mitochondrial	X	X	
NDUS7_HUMAN	NADH dehydrogenase [ubiquinone] iron-sulfur protein 7, mitochondrial	X	X	
NB5R1_HUMAN	NADH-cytochrome b5 reductase 1	X	X	
NACAM_HUMAN	Nascent polypeptide-associated complex subunit alpha, muscle-specific form	X	X	
PLPL6_HUMAN	Neuropathy target esterase	X	X	
NH2L1_HUMAN	NHP2-like protein 1	X	X	
NIBL1_HUMAN	Niban-like protein 1	X	X	
NCLN_HUMAN	Nicalin	X	X	
NICA_HUMAN	Nicastrin	X	X	
NONO_HUMAN	Non-POU domain-containing octamer-binding protein	X	X	
NU155_HUMAN	Nuclear pore complex protein Nup155	X	X	
NOP56_HUMAN	Nucleolar protein 56	X	X	
NOP58_HUMAN	Nucleolar protein 58	X	X	
NUCL_HUMAN	Nucleolin	X	X	
NPM_HUMAN	Nucleophosmin	X	X	
NP1L1_HUMAN	Nucleosome assembly protein 1-like 1	X	X	
OLA1_HUMAN	Obg-like ATPase 1	X	X	
OCAD1_HUMAN	OCIA domain-containing protein 1	X	X	
OSBL8_HUMAN	Oxysterol-binding protein-related protein 8	X	X	
FKB10_HUMAN	Peptidyl-prolyl cis-trans isomerase FKBP10	X	X	
FKB11_HUMAN	Peptidyl-prolyl cis-trans isomerase FKBP11	X	X	
FKBP4_HUMAN	Peptidyl-prolyl cis-trans isomerase FKBP4	X	X	
PERI_HUMAN	Peripherin	X	X	
ETHE1_HUMAN	Persulfide dioxygenase ETHE1, mitochondrial	X	X	
PICAL_HUMAN	Phosphatidylinositol-binding clathrin assembly protein	X	X	
PLTP_HUMAN	Phospholipid transfer protein	X	X	

PMVK_HUMAN	Phosphomevalonate kinase	X	X	
PVR_HUMAN	Poliovirus receptor	X	X	
PAP1L_HUMAN	Polyadenylate-binding protein 1-like	X	X	
PTBP1_HUMAN	Polypyrimidine tract-binding protein 1	X	X	
PRP8_HUMAN	Pre-mRNA-processing-splicing factor 8	X	X	
PCYXL_HUMAN	Prenylcysteine oxidase-like	X	X	
DDX17_HUMAN	Probable ATP-dependent RNA helicase DDX17	X	X	
DDX5_HUMAN	Probable ATP-dependent RNA helicase DDX5	X	X	
DDX6_HUMAN	Probable ATP-dependent RNA helicase DDX6	X	X	
PLOD3_HUMAN	Procollagen-lysine,2-oxoglutarate 5-dioxygenase 3	X	X	
PDCD6_HUMAN	Programmed cell death protein 6	X	X	
P4HA2_HUMAN	Prolyl 4-hydroxylase subunit alpha-2	X	X	
SAP_HUMAN	Prosaposin	X	X	
PARK7_HUMAN	Protein deglycase DJ-1	X	X	
NDRG1_HUMAN	Protein NDRG1	X	X	
NIPS2_HUMAN	Protein NipSnap homolog 2	X	X	
PML_HUMAN	Protein PML	X	X	
SC23A_HUMAN	Protein transport protein Sec23A	X	X	
LYOX_HUMAN	Protein-lysine 6-oxidase	X	X	
H90B3_HUMAN	Putative heat shock protein HSP 90-beta-3	X	X	
P5CR1_HUMAN	Pyrroline-5-carboxylate reductase 1, mitochondrial	X	X	
P5CR2_HUMAN	Pyrroline-5-carboxylate reductase 2	X	X	
QOR_HUMAN	Quinone oxidoreductase	X	X	
RFIP5_HUMAN	Rab11 family-interacting protein 5	X	X	
LTOR3_HUMAN	Ragulator complex protein LAMTOR3	X	X	
RAB21_HUMAN	Ras-related protein Rab-21	X	X	
RAB6C_HUMAN	Ras-related protein Rab-6C	X	X	
ROMO1_HUMAN	Reactive oxygen species modulator 1	X	X	

RACK1_HUMAN	Receptor of activated protein C kinase 1	X	X	
RENT1_HUMAN	Regulator of nonsense transcripts 1	X	X	
RENR_HUMAN	Renin receptor	X	X	
RDH14_HUMAN	Retinol dehydrogenase 14	X	X	
GDIR2_HUMAN	Rho GDP-dissociation inhibitor 2	X	X	
RHG01_HUMAN	Rho GTPase-activating protein 1	X	X	
RRBP1_HUMAN	Ribosome-binding protein 1	X	X	
RTCA_HUMAN	RNA 3'-terminal phosphate cyclase	X	X	
RALY_HUMAN	RNA-binding protein Raly	X	X	
AT2A1_HUMAN	Sarcoplasmic/endoplasmic reticulum calcium ATPase 1	X	X	
SCRN1_HUMAN	Secernin-1	X	X	
SQSTM_HUMAN	Sequestosome-1	X	X	
PRS23_HUMAN	Serine protease 23	X	X	
SYSC_HUMAN	Serine--tRNA ligase, cytoplasmic	X	X	
SRSF7_HUMAN	Serine/arginine-rich splicing factor 7	X	X	
2AAA_HUMAN	Serine/threonine-protein phosphatase 2A 65 kDa regulatory subunit A alpha isoform	X	X	
SPB6_HUMAN	Serpin B6	X	X	
SPCS2_HUMAN	Signal peptidase complex subunit 2	X	X	
STAT3_HUMAN	Signal transducer and activator of transcription 3	X	X	
SMD2_HUMAN	Small nuclear ribonucleoprotein Sm D2	X	X	
RSMB_HUMAN	Small nuclear ribonucleoprotein-associated proteins B and B'	X	X	
SAM50_HUMAN	Sorting and assembly machinery component 50 homolog	X	X	
SNX6_HUMAN	Sorting nexin-6	X	X	
SPRC_HUMAN	SPARC	X	X	
DX39B_HUMAN	Spliceosome RNA helicase DDX39B	X	X	
SF3B3_HUMAN	Splicing factor 3B subunit 3	X	X	
SFPQ_HUMAN	Splicing factor, proline- and glutamine-rich	X	X	

SLIRP_HUMAN	SRA stem-loop-interacting RNA-binding protein, mitochondrial	X	X	
NSDHL_HUMAN	Sterol-4-alpha-carboxylate 3-dehydrogenase, decarboxylating	X	X	
SCOT1_HUMAN	Succinyl-CoA:3-ketoacid coenzyme A transferase 1, mitochondrial	X	X	
QSOX1_HUMAN	Sulfhydryl oxidase 1	X	X	
SYNPO_HUMAN	Synaptopodin	X	X	
SNP23_HUMAN	Synaptosomal-associated protein 23	X	X	
RIC8A_HUMAN	Synembryn-A	X	X	
STX12_HUMAN	Syntaxin-12	X	X	
TADBP_HUMAN	TAR DNA-binding protein 43	X	X	
THIO_HUMAN	Thioredoxin	X	X	
TRXR1_HUMAN	Thioredoxin reductase 1, cytoplasmic	X	X	
TOIP1_HUMAN	Torsin-1A-interacting protein 1	X	X	
TPPC5_HUMAN	Trafficking protein particle complex subunit 5	X	X	
TKT_HUMAN	Transketolase	X	X	
TMTC3_HUMAN	Transmembrane and TPR repeat-containing protein 3	X	X	
TMED5_HUMAN	Transmembrane emp24 domain-containing protein 5	X	X	
TMM11_HUMAN	Transmembrane protein 11, mitochondrial	X	X	
T126A_HUMAN	Transmembrane protein 126A	X	X	
TM256_HUMAN	Transmembrane protein 256	X	X	
TMM65_HUMAN	Transmembrane protein 65	X	X	
RTCB_HUMAN	tRNA-splicing ligase RtcB homolog	X	X	
TMOD3_HUMAN	Tropomodulin-3	X	X	
TPM3_HUMAN	Tropomyosin alpha-3 chain	X	X	
SYYM_HUMAN	Tyrosine--tRNA ligase, mitochondrial	X	X	
LSM2_HUMAN	U6 snRNA-associated Sm-like protein LSm2	X	X	
UCHL1_HUMAN	Ubiquitin carboxyl-terminal hydrolase isozyme L1	X	X	
UMPS_HUMAN	Uridine 5'-monophosphate synthase	X	X	
VATA_HUMAN	V-type proton ATPase catalytic subunit A	X	X	

VATE1_HUMAN	V-type proton ATPase subunit E 1	X	X	
VAPA_HUMAN	Vesicle-associated membrane protein-associated protein A	X	X	
LMAN2_HUMAN	Vesicular integral-membrane protein VIP36	X	X	
XRCC5_HUMAN	X-ray repair cross-complementing protein 5	X	X	
ZYX_HUMAN	Zyxin	X	X	
AINX_HUMAN	Alpha-internexin	X		X
PARVB_HUMAN	Beta-parvin	X		X
CAN1_HUMAN	Calpain-1 catalytic subunit	X		X
IGJ_HUMAN	Immunoglobulin J chain	X		X
IVD_HUMAN	Isovaleryl-CoA dehydrogenase, mitochondrial	X		X
TIM16_HUMAN	Mitochondrial import inner membrane translocase subunit TIM16	X		X
NCKP1_HUMAN	Nck-associated protein 1	X		X
S10A8_HUMAN	Protein S100-A8	X		X
TLN2_HUMAN	Talin-2	X		X
GLGB_HUMAN	1,4-alpha-glucan-branching enzyme	X		
CN37_HUMAN	2',3'-cyclic-nucleotide 3'-phosphodiesterase	X		
RL36_HUMAN	60S ribosomal protein L36	X		
MMP2_HUMAN	72 kDa type IV collagenase	X		
LYPA1_HUMAN	Acyl-protein thioesterase 1	X		
ADPGK_HUMAN	ADP-dependent glucokinase	X		
AGRIN_HUMAN	Agrin	X		
MGAT1_HUMAN	Alpha-1,3-mannosyl-glycoprotein 2-beta-N-acetylglucosaminyltransferase	X		
YMEL1_HUMAN	ATP-dependent zinc metalloprotease	X		
BET1_HUMAN	BET1 homolog	X		
B2MG_HUMAN	Beta-2-microglobulin	X		

BID_HUMAN	BH3-interacting domain death agonist	X		
DPYL3_HUMAN	Dihydropyrimidinase-related protein 3	X		
DPM3_HUMAN	Dolichol-phosphate mannosyltransferase subunit 3	X		
MP2K1_HUMAN	Dual specificity mitogen-activated protein kinase kinase 1	X		
DUS3_HUMAN	Dual specificity protein phosphatase 3	X		
ERH_HUMAN	Enhancer of rudimentary homolog	X		
IF2G_HUMAN	Eukaryotic translation initiation factor 2 subunit 3	X		
ECSIT_HUMAN	Evolutionarily conserved signalling intermediate in Toll pathway, mitochondrial	X		
FRIL_HUMAN	Ferritin light chain	X		
GALK1_HUMAN	Galactokinase	X		
GNA1_HUMAN	Glucosamine 6-phosphate N-acetyltransferase	X		
GLSK_HUMAN	Glutaminase kidney isoform, mitochondrial	X		
GLRX5_HUMAN	Glutaredoxin-related protein 5, mitochondrial	X		
GNAI1_HUMAN	Guanine nucleotide-binding protein G(i) subunit alpha-1	X		
GNAT3_HUMAN	Guanine nucleotide-binding protein G(t) subunit alpha-3	X		
NOP10_HUMAN	H/ACA ribonucleoprotein complex subunit 3	X		
HBB_HUMAN	Hemoglobin subunit beta	X		
ROA1_HUMAN	Heterogeneous nuclear ribonucleoprotein A1	X		
ROA3_HUMAN	Heterogeneous nuclear ribonucleoprotein A3	X		
HCDH_HUMAN	Hydroxyacyl-coenzyme A dehydrogenase, mitochondrial	X		
ISOC2_HUMAN	Isochorismatase domain-containing protein 2	X		
LPCT4_HUMAN	Lysophospholipid acyltransferase LPCAT4	X		
PCP_HUMAN	Lysosomal Pro-X carboxypeptidase	X		
MMP14_HUMAN	Matrix metalloproteinase-14	X		
MOT1_HUMAN	Monocarboxylate transporter 1	X		
MGLL_HUMAN	Monoglyceride lipase	X		
NDUBB_HUMAN	NADH dehydrogenase [ubiquinone] 1 beta subcomplex subunit 11,	X		

	mitochondrial			
NDUS8_HUMAN	NADH dehydrogenase [ubiquinone] iron-sulfur protein 8, mitochondrial	X		
NFM_HUMAN	Neurofilament medium polypeptide	X		
NPM3_HUMAN	Nucleoplasmin-3	X		
OSTF1_HUMAN	Osteoclast-stimulating factor 1	X		
SYFA_HUMAN	Phenylalanine--tRNA ligase alpha subunit	X		
PEBP1_HUMAN	Phosphatidylethanolamine-binding protein 1	X		
GPX4_HUMAN	Phospholipid hydroperoxide glutathione peroxidase, mitochondrial	X		
AT12A_HUMAN	Potassium-transporting ATPase alpha chain 2	X		
SCRIB_HUMAN	Protein scribble homolog	X		
RUXGL_HUMAN	Putative small nuclear ribonucleoprotein G-like protein 15	X		
LTOR1_HUMAN	Ragulator complex protein LAMTOR1	X		
LTOR2_HUMAN	Ragulator complex protein LAMTOR2	X		
RAB43_HUMAN	Ras-related protein Rab-43	X		
RMD3_HUMAN	Regulator of microtubule dynamics protein 3	X		
AL1A1_HUMAN	Retinal dehydrogenase 1	X		
SIAS_HUMAN	Sialic acid synthase	X		
SRP14_HUMAN	Signal recognition particle 14 kDa protein	X		
AT1B1_HUMAN	Sodium/potassium-transporting ATPase subunit beta-1	X		
SF3B6_HUMAN	Splicing factor 3B subunit 6	X		
SODC_HUMAN	Superoxide dismutase [Cu-Zn]	X		
SODM_HUMAN	Superoxide dismutase [Mn], mitochondrial	X		
TMX1_HUMAN	Thioredoxin-related transmembrane protein 1	X		
TPPC3_HUMAN	Trafficking protein particle complex subunit 3	X		
TMM33_HUMAN	Transmembrane protein 33	X		
TMM43_HUMAN	Transmembrane protein 43	X		
OTUB1_HUMAN	Ubiquitin thioesterase OTUB1	X		

UGPA_HUMAN	UTP--glucose-1-phosphate uridylyltransferase	X		
VPS29_HUMAN	Vacuolar protein sorting-associated protein 29	X		
AGRL4_HUMAN	Adhesion G protein-coupled receptor L4		X	X
CBR3_HUMAN	Carbonyl reductase [NADPH] 3		X	X
ECI2_HUMAN	Enoyl-CoA delta isomerase 2, mitochondrial		X	X
JAM1_HUMAN	Junctional adhesion molecule A		X	X
LCAP_HUMAN	Leucyl-cystinyl aminopeptidase		X	X
NDUAC_HUMAN	NADH dehydrogenase [ubiquinone] 1 alpha subcomplex subunit 12		X	X
NDUC2_HUMAN	NADH dehydrogenase [ubiquinone] 1 subunit C2		X	X
KPCA_HUMAN	Protein kinase C alpha type		X	X
RAB2B_HUMAN	Ras-related protein Rab-2B		X	X
RAB35_HUMAN	Ras-related protein Rab-35		X	X
SEPT9_HUMAN	Septin-9		X	X
FYN_HUMAN	Tyrosine-protein kinase Fyn		X	X
VA0D1_HUMAN	V-type proton ATPase subunit d 1		X	X
RM01_HUMAN	39S ribosomal protein L1, mitochondrial		X	
RL21_HUMAN	60S ribosomal protein L21		X	
RL28_HUMAN	60S ribosomal protein L28		X	
ARC1B_HUMAN	Actin-related protein 2/3 complex subunit 1B		X	
ARL8B_HUMAN	ADP-ribosylation factor-like protein 8B		X	
ANGL4_HUMAN	Angiopoietin-related protein 4		X	
RAI14_HUMAN	Ankycorbin		X	
AP3D1_HUMAN	AP-3 complex subunit delta-1		X	
ATP5H_HUMAN	ATP synthase subunit d, mitochondrial		X	
DX39A_HUMAN	ATP-dependent RNA helicase DDX39A		X	
BOLA2_HUMAN	BolA-like protein 2		X	

CSK2B_HUMAN	Casein kinase II subunit beta		X	
CTNA2_HUMAN	Catenin alpha-2		X	
CLIC3_HUMAN	Chloride intracellular channel protein 3		X	
MMAB_HUMAN	Cob(I)yrinic acid a,c-diamide adenosyltransferase, mitochondrial		X	
CO4A2_HUMAN	Collagen alpha-2(IV) chain		X	
CPNE5_HUMAN	Copine-5		X	
CDK12_HUMAN	Cyclin-dependent kinase 12		X	
CDK17_HUMAN	Cyclin-dependent kinase 17		X	
CCNY_HUMAN	Cyclin-Y		X	
CYFP1_HUMAN	Cytoplasmic FMR1-interacting protein 1		X	
ADAM9_HUMAN	Disintegrin and metalloproteinase domain-containing protein 9		X	
DNJA3_HUMAN	DnaJ homolog subfamily A member 3, mitochondrial		X	
UBR4_HUMAN	E3 ubiquitin-protein ligase UBR4		X	
EFTS_HUMAN	Elongation factor Ts, mitochondrial		X	
EPHB2_HUMAN	Ephrin type-B receptor 2		X	
HYEP_HUMAN	Epoxide hydrolase 1		X	
EMC3_HUMAN	ER membrane protein complex subunit 3		X	
EIF3D_HUMAN	Eukaryotic translation initiation factor 3 subunit D		X	
EIF3I_HUMAN	Eukaryotic translation initiation factor 3 subunit I		X	
EXOC2_HUMAN	Exocyst complex component 2		X	
EXOC4_HUMAN	Exocyst complex component 4		X	
XPOT_HUMAN	Exportin-T		X	
FGFR4_HUMAN	Fibroblast growth factor receptor 4		X	
TIGAR_HUMAN	Fructose-2,6-bisphosphatase TIGAR		X	
CCND1_HUMAN	G1/S-specific cyclin-D1		X	
OFUT1_HUMAN	GDP-fucose protein O-fucosyltransferase 1		X	
GFPT2_HUMAN	Glutamine--fructose-6-phosphate aminotransferase [isomerizing] 2		X	
PYGB_HUMAN	Glycogen phosphorylase, brain form		X	

GLTP_HUMAN	Glycolipid transfer protein		X	
HHIP_HUMAN	Hedgehog-interacting protein		X	
HMOX2_HUMAN	Heme oxygenase 2		X	
HNRPL_HUMAN	Heterogeneous nuclear ribonucleoprotein L		X	
HPCL1_HUMAN	Hippocalcin-like protein 1		X	
HMGCL_HUMAN	Hydroxymethylglutaryl-CoA lyase, mitochondrial		X	
IPO4_HUMAN	Importin-4		X	
ITPR2_HUMAN	Inositol 1,4,5-trisphosphate receptor type 2		X	
IL18_HUMAN	Interleukin-18		X	
LAMB2_HUMAN	Laminin subunit beta-2		X	
MAGT1_HUMAN	Magnesium transporter protein 1		X	
MIC13_HUMAN	MICOS complex subunit MIC13		X	
TIM50_HUMAN	Mitochondrial import inner membrane translocase subunit TIM50		X	
MPPB_HUMAN	Mitochondrial-processing peptidase subunit beta		X	
MK01_HUMAN	Mitogen-activated protein kinase 1		X	
MMRN2_HUMAN	Multimerin-2		X	
NDUA9_HUMAN	NADH dehydrogenase [ubiquinone] 1 alpha subcomplex subunit 9, mitochondrial		X	
NDUB1_HUMAN	NADH dehydrogenase [ubiquinone] 1 beta subcomplex subunit 1		X	
NDUBA_HUMAN	NADH dehydrogenase [ubiquinone] 1 beta subcomplex subunit 10		X	
HPCA_HUMAN	Neuron-specific calcium-binding protein hippocalcin		X	
NPC1_HUMAN	Niemann-Pick C1 protein		X	
NU160_HUMAN	Nuclear pore complex protein Nup160		X	
NU205_HUMAN	Nuclear pore complex protein Nup205		X	
PDLI7_HUMAN	PDZ and LIM domain protein 7		X	
PPIC_HUMAN	Peptidyl-prolyl cis-trans isomerase C		X	
CDS2_HUMAN	Phosphatidate cytidylyltransferase 2		X	
SAC1_HUMAN	Phosphatidylinositide phosphatase SAC1		X	

PARP1_HUMAN	Poly [ADP-ribose] polymerase 1		X	
PABP3_HUMAN	Polyadenylate-binding protein 3		X	
DHX15_HUMAN	Pre-mRNA-splicing factor ATP-dependent RNA helicase DHX15		X	
PZP_HUMAN	Pregnancy zone protein		X	
PREP_HUMAN	Presequence protease, mitochondrial		X	
GPX8_HUMAN	Probable glutathione peroxidase 8		X	
PROSC_HUMAN	Proline synthase co-transcribed bacterial homolog protein		X	
PSME3_HUMAN	Proteasome activator complex subunit 3		X	
PSB3_HUMAN	Proteasome subunit beta type-3		X	
KPCG_HUMAN	Protein kinase C gamma type		X	
SE1L1_HUMAN	Protein sel-1 homolog 1		X	
SRC_HUMAN	Proto-oncogene tyrosine-protein kinase Src		X	
TI23B_HUMAN	Putative mitochondrial import inner membrane translocase subunit Tim23B		X	
RAB31_HUMAN	Ras-related protein Rab-31		X	
RAB3D_HUMAN	Ras-related protein Rab-3D		X	
RCN3_HUMAN	Reticulocalbin-3		X	
RL1D1_HUMAN	Ribosomal L1 domain-containing protein 1		X	
FBRL_HUMAN	rRNA 2'-O-methyltransferase fibrillarin		X	
SCPDL_HUMAN	Saccharopine dehydrogenase-like oxidoreductase		X	
SCAM3_HUMAN	Secretory carrier-associated membrane protein 3		X	
SEPT8_HUMAN	Septin-8		X	
PAK1_HUMAN	Serine/threonine-protein kinase PAK 1		X	
SPCS3_HUMAN	Signal peptidase complex subunit 3		X	
SPEE_HUMAN	Spermidine synthase		X	
STING_HUMAN	Stimulator of interferon genes protein		X	
SUCB2_HUMAN	Succinate--CoA ligase [GDP-forming] subunit beta, mitochondrial		X	
TTC37_HUMAN	Tetratricopeptide repeat protein 37		X	

TXD12_HUMAN	Thioredoxin domain-containing protein 12		X	
TIF1B_HUMAN	Transcription intermediary factor 1-beta		X	
TAGL_HUMAN	Transgelin		X	
SSRA_HUMAN	Translocon-associated protein subunit alpha		X	
TM9S3_HUMAN	Transmembrane 9 superfamily member 3		X	
TM9S4_HUMAN	Transmembrane 9 superfamily member 4		X	
TINAL_HUMAN	Tubulointerstitial nephritis antigen-like		X	
YES_HUMAN	Tyrosine-protein kinase Yes		X	
RU2A_HUMAN	U2 small nuclear ribonucleoprotein A'		X	
U520_HUMAN	U5 small nuclear ribonucleoprotein 200 kDa helicase		X	
MYO1B_HUMAN	Unconventional myosin-Ib		X	
MYO6_HUMAN	Unconventional myosin-VI		X	
UPAR_HUMAN	Urokinase plasminogen activator surface receptor		X	
UTRO_HUMAN	Utrophin		X	
VPP1_HUMAN	V-type proton ATPase 116 kDa subunit a isoform 1		X	
VP26A_HUMAN	Vacuolar protein sorting-associated protein 26A		X	
VIGLN_HUMAN	Vigilin		X	
SAHH_HUMAN	Adenosylhomocysteinase			X
ARF6_HUMAN	ADP-ribosylation factor 6			X
ASNA_HUMAN	ATPase ASNA1			X
C1TC_HUMAN	C-1-tetrahydrofolate synthase, cytoplasmic			X
CDIPT_HUMAN	CDP-diacylglycerol--inositol 3-phosphatidyltransferase			X
CERU_HUMAN	Ceruloplasmin			X
CC127_HUMAN	Coiled-coil domain-containing protein 127			X
EDIL3_HUMAN	EGF-like repeat and discoidin I-like domain-containing protein 3			X
HNRC1_HUMAN	Heterogeneous nuclear ribonucleoprotein C-like 1			X
ITA3_HUMAN	Integrin alpha-3			X

TMX3_HUMAN	Protein disulfide-isomerase TMX3			X
S61A1_HUMAN	Protein transport protein Sec61 subunit alpha isoform 1			X
SVIP_HUMAN	Small VCP/p97-interacting protein			X
TRPV2_HUMAN	Transient receptor potential cation channel subfamily V member 2			X
TPBG_HUMAN	Trophoblast glycoprotein			X

Table 4: ClueGO Functional Analysis of eMPs^{HG} -Exclusive Proteins.

GO Groups	GO Term	Ontology Source	Term PValue Corrected with Benjamini-Hochberg	Group P-Value Corrected with Benjamini-Hochberg	# of Proteins
Group 00	Carboxylic Acid Metabolic Process	GO_BiologicalProcess-GOA_23.02.2017_10h01	1.1E-3	830.0E-6	13.00
Group 01	Protein Localization to Membrane	GO_BiologicalProcess-GOA_23.02.2017_10h01	9.0E-3	8.3E-3	7.00
Group 02	Response to Bacterium	GO_BiologicalProcess-GOA_23.02.2017_10h01	14.0E-3	14.0E-3	7.00
	Response to Lipopolysaccharide	GO_BiologicalProcess-GOA_23.02.2017_10h01	14.0E-3	14.0E-3	5.00
Group 03	Single-Organism Catabolic Process	GO_BiologicalProcess-GOA_23.02.2017_10h01	4.5E-3	4.5E-3	11.00
	Small Molecule Catabolic Process	GO_BiologicalProcess-GOA_23.02.2017_10h01	24.0E-3	4.5E-3	5.00
Group 04	Protein Complex Assembly	GO_BiologicalProcess-GOA_23.02.2017_10h01	870.0E-6	350.0E-6	17.00
	Protein Oligomerization	GO_BiologicalProcess-GOA_23.02.2017_10h01	1.3E-3	350.0E-6	9.00
Group 05	Degradation of the Extracellular Matrix	REACTOME_Pathways_01.03.2017	9.4E-3	31.0E-3	5.00
	Extracellular Matrix Organization	REACTOME_Pathways_01.03.2017	9.4E-3	31.0E-3	5.00
	Extracellular Matrix Organization	GO_BiologicalProcess-GOA_23.02.2017_10h01	14.0E-3	31.0E-3	5.00
Group 06	Neutrophil Degranulation	REACTOME_Pathways_01.03.2017	2.2E-3	3.4E-3	8.00
	Regulated Exocytosis	GO_BiologicalProcess-GOA_23.02.2017_10h01	2.8E-3	3.4E-3	10.00
	Neutrophil Degranulation	GO_BiologicalProcess-	2.8E-3	3.4E-3	8.00

		GOA_23.02.2017_10h01			
Group 07	Biosynthesis of the N-glycan Precursor (Dolichol Lipid-Linked Oligosaccharide, LLO) and Transfer to a Nascent Protein	REACTOME_Pathways_01.03.2017	2.8E-3	3.3E-3	6.00
	Asparagine N-Linked Glycosylation	REACTOME_Pathways_01.03.2017	2.8E-3	3.3E-3	6.00
	Synthesis of Substrates in N-Glycan Biosythesis	REACTOME_Pathways_01.03.2017	2.8E-3	3.3E-3	6.00
	GDP-Fucose Biosynthesis	REACTOME_Pathways_01.03.2017	2.8E-3	3.3E-3	6.00
Group 08	Hexose Transport	REACTOME_Pathways_01.03.2017	1.8E-3	600.0E-6	12.00
	Transmembrane Transport of Small Molecules	REACTOME_Pathways_01.03.2017	1.8E-3	600.0E-6	12.00
	SLC-Mediated Transmembrane Transport	REACTOME_Pathways_01.03.2017	1.8E-3	600.0E-6	12.00
	Metabolism of Carbohydrates	REACTOME_Pathways_01.03.2017	1.8E-3	600.0E-6	12.00
	Carbohydrate Metabolic Process	GO_BiologicalProcess-GOA_23.02.2017_10h01	2.4E-3	600.0E-6	9.00
	Generation of Precursor Metabolites and Energy	GO_BiologicalProcess-GOA_23.02.2017_10h01	1.6E-3	600.0E-6	8.00
	carbohydrate derivative metabolic process	GO_BiologicalProcess-GOA_23.02.2017_10h01	1.3E-3	600.0E-6	15.00
	single-organism carbohydrate metabolic process	GO_BiologicalProcess-GOA_23.02.2017_10h01	6.7E-3	600.0E-6	7.00
Group 09	Cell Surface Interactions at the Vascular Wall	REACTOME_Pathways_01.03.2017	3.5E-3	3.8E-3	5.00
	Regulation by c-FLIP	REACTOME_Pathways_01.03.2017	3.5E-3	3.8E-3	5.00
	RIPK1-Mediated Regulated Necrosis	REACTOME_Pathways_01.03.2017	3.5E-3	3.8E-3	5.00
	Regulated Necrosis	REACTOME_Pathways_01.03.2017	3.5E-3	3.8E-3	5.00
	CASP8 Activity is Inhibited	REACTOME_Pathways_01.03.2017	3.5E-3	3.8E-3	5.00

	TP53 Regulates Transcription of Cell Death Genes	REACTOME_Pathways_01.03.2017	3.5E-3	3.8E-3	5.00
	Regulation of Necroptotic Cell Death	REACTOME_Pathways_01.03.2017	3.5E-3	3.8E-3	5.00
	TP53 Regulates Transcription of Death Receptors and Ligands	REACTOME_Pathways_01.03.2017	3.5E-3	3.8E-3	5.00
	Dimerization of Procaspase-8	REACTOME_Pathways_01.03.2017	3.5E-3	3.8E-3	5.00
	Death Receptor Signalling	REACTOME_Pathways_01.03.2017	3.5E-3	3.8E-3	5.00
	TRAIL signalling	REACTOME_Pathways_01.03.2017	3.5E-3	3.8E-3	5.00
Group 10	Carbohydrate Metabolic Process	GO_BiologicalProcess-GOA_23.02.2017_10h01	2.4E-3	140.0E-6	9.00
	Generation of Precursor Metabolites and Energy	GO_BiologicalProcess-GOA_23.02.2017_10h01	1.6E-3	140.0E-6	8.00
	Oxidation-Reduction Process	GO_BiologicalProcess-GOA_23.02.2017_10h01	780.0E-6	140.0E-6	15.00
	Carbohydrate Derivative Metabolic Process	GO_BiologicalProcess-GOA_23.02.2017_10h01	1.3E-3	140.0E-6	15.00
	Energy Derivation by Oxidation of Organic Compounds	GO_BiologicalProcess-GOA_23.02.2017_10h01	2.7E-3	140.0E-6	6.00
	Organophosphate Metabolic Process	GO_BiologicalProcess-GOA_23.02.2017_10h01	1.9E-3	140.0E-6	15.00
	Single-organism Carbohydrate Metabolic Process	GO_BiologicalProcess-GOA_23.02.2017_10h01	6.7E-3	140.0E-6	7.00
	Nucleotide Metabolic Process	GO_BiologicalProcess-GOA_23.02.2017_10h01	2.4E-3	140.0E-6	10.00
	Nucleoside Monophosphate Metabolic Process	GO_BiologicalProcess-GOA_23.02.2017_10h01	1.5E-3	140.0E-6	7.00
	Nucleoside Triphosphate Metabolic Process	GO_BiologicalProcess-GOA_23.02.2017_10h01	3.3E-3	140.0E-6	6.00
	Purine Nucleotide Metabolic Process	GO_BiologicalProcess-GOA_23.02.2017_10h01	14.0E-3	140.0E-6	7.00
	Ribonucleotide Metabolic Process	GO_BiologicalProcess-	14.0E-3	140.0E-6	7.00

		GOA_23.02.2017_10h01			
Group 11	Hemostasis	REACTOME_Pathways_01.03.2017	2.2E-3	8.4E-3	13.00
	Translocation of GLUT4 to the Plasma Membrane	REACTOME_Pathways_01.03.2017	2.2E-3	8.4E-3	13.00
	Gap Junction Trafficking and Regulation	REACTOME_Pathways_01.03.2017	2.2E-3	8.4E-3	13.00
	Gap junction trafficking	REACTOME_Pathways_01.03.2017	2.2E-3	8.4E-3	13.00
	Microtubule-dependent Trafficking of Connexons from Golgi to the Plasma Membrane	REACTOME_Pathways_01.03.2017	2.2E-3	8.4E-3	13.00
	Gap Junction Assembly	REACTOME_Pathways_01.03.2017	2.2E-3	8.4E-3	13.00
	Transport of Connexons to the Plasma Membrane	REACTOME_Pathways_01.03.2017	2.2E-3	8.4E-3	13.00
	ER to Golgi Anterograde Transport	REACTOME_Pathways_01.03.2017	2.2E-3	8.4E-3	13.00
	MHC Class II Antigen Presentation	REACTOME_Pathways_01.03.2017	2.2E-3	8.4E-3	13.00
	Resolution of Sister Chromatid Cohesion	REACTOME_Pathways_01.03.2017	2.2E-3	8.4E-3	13.00
	Recruitment of Mitotic Centrosome Proteins and Complexes	REACTOME_Pathways_01.03.2017	2.2E-3	8.4E-3	13.00
	Centrosome Maturation	REACTOME_Pathways_01.03.2017	2.2E-3	8.4E-3	13.00
	Recruitment of NuMA to Mitotic Centrosomes	REACTOME_Pathways_01.03.2017	2.2E-3	8.4E-3	13.00
	Cooperation of Prefoldin and TriC/CCT in Actin and Tubulin Folding	REACTOME_Pathways_01.03.2017	2.2E-3	8.4E-3	13.00
	Formation of Tubulin Folding Intermediates by CCT/TriC	REACTOME_Pathways_01.03.2017	2.2E-3	8.4E-3	13.00
	Post-chaperonin Tubulin Folding Pathway	REACTOME_Pathways_01.03.2017	2.2E-3	8.4E-3	13.00

	Chaperonin-mediated Protein Folding	REACTOME_Pathways_01.03.2017	2.2E-3	8.4E-3	13.00
	Protein Folding	REACTOME_Pathways_01.03.2017	2.2E-3	8.4E-3	13.00
	RHO GTPases Activate IQGAPs	REACTOME_Pathways_01.03.2017	2.2E-3	8.4E-3	13.00
	RHO GTPases Activate Formins	REACTOME_Pathways_01.03.2017	2.2E-3	8.4E-3	13.00
	COPI-mediated Anterograde Transport	REACTOME_Pathways_01.03.2017	2.2E-3	8.4E-3	13.00
	COPI-independent Golgi-to-ER Retrograde Traffic	REACTOME_Pathways_01.03.2017	2.2E-3	8.4E-3	13.00
	Mitotic Prometaphase	REACTOME_Pathways_01.03.2017	2.2E-3	8.4E-3	13.00
	Transport to the Golgi and Subsequent Modification	REACTOME_Pathways_01.03.2017	2.2E-3	8.4E-3	13.00
	Kinesins	REACTOME_Pathways_01.03.2017	2.2E-3	8.4E-3	13.00
	Factors Involved in Megakaryocyte Development and Platelet Production	REACTOME_Pathways_01.03.2017	2.2E-3	8.4E-3	13.00
	Blood Circulation	GO_BiologicalProcess-GOA_23.02.2017_10h01	24.0E-3	8.4E-3	6.00

6.0. References

1. Canadian Diabetes Association. Diabetes in Canada [Internet]. 2016. Available from: http://www.stridemagazine.com/2003_05 May/article03/article03.htm

2. Zhou B, Lu Y, Hajifathalian K, Bentham J, Di Cesare M, Danaei G, Bixby H, Cowan MJ, Ali MK, Taddei C, Lo WC, Reis-Santos B, Stevens GA, Riley LM, Miranda JJ, Bjerregaard P, Rivera JA, Fouad HM, Ma G, Mbanya JCN, McGarvey ST, Mohan V, Onat A, Pilav A, Ramachandran A, Ben Romdhane H, Paciorek CJ, Bennett JE, Ezzati M, Abdeen ZA, Kadir KA, Abu-Rmeileh NM, Acosta-Cazares B, Adams R, Aekplakorn W, Aguilar-Salinas CA, Agyemang C, Ahmadvand A, Al-Othman AR, Alkerwi A, Amouyel P, Amuzu A, Bo Andersen L, Anderssen SA, Anjana RM, Aounallah-Skhiri H, Aris T, Arlappa N, Arveiler D, Assah FK, Avdicov?? M, Azizi F, Balakrishna N, Bandosz P, Barbagallo CM, Barcel?? A, Batieha AM, Baur LA, Benet M, Bernabe-Ortiz A, Bharadwaj S, Bhargava SK, Bi Y, Bjertness E, Bjertness MB, Bj??rkelund C, Blokstra A, Bo S, Boehm BO, Boissonnet CP, Bovet P, Brajkovich I, Breckenkamp J, Brenner H, Brewster LM, Brian GR, Bruno G, Bugge A, De Le??n AC, Can G, C??ndido APC, Capuano V, Carlsson AC, Carvalho MJ, Casanueva FF, Casas JP, Caserta CA, Castetbon K, Chamukuttan S, Chaturvedi N, Chen CJ, Chen F, Chen S, Cheng CY, Chetrit A, Chiou ST, Cho Y, Chudek J, et al. Worldwide trends in diabetes since 1980: A pooled analysis of 751 population-based studies with 4.4 million participants. *Lancet* [Internet]. 2016;387:1513–1530. Available from: http://dx.doi.org/10.1016/S0140-6736(16)00618-8

3. World Health Organization. Global Report on Diabetes [Internet]. 2016. Available from: http://www.who.int/about/licensing/%5Cnhttp://apps.who.int/iris/bitstream/10665/204871/1/9789241565257_eng.pdf

4. Centers for Disease Control and Prevention. National Diabetes Statistics Report , 2014 Estimates of Diabetes and Its Burden in the Epidemiologic estimation methods. 2014.

5. Holman R, Sanjoy P, Bethel A, Matthews D, Neil A. 10-Year Follow-up of Intensive Glucose Control in Type 2 Diabetes. *N Engl J Med*. 2008;359:1577–89.

6. Paz NG, Amore PAD. Arterial versus venous endothelial cells. 2004;335:5–16.

7. Cines DB, Pollak ES, Buck CA, Loscalzo J, Zimmerman GA, McEver RP, Pober JS, Wick TM, Konkle BA, Schwartz BS, Barnathan ES, McCrae KR, Hug BA, Schmidt AM, Stern DM. Endothelial cells in physiology and in the pathophysiology of vascular disorders. *Blood*. 1998;91:3527–3561.

8. Kawashima S. The two faces of endothelial nitric oxide synthase in the pathophysiology of atherosclerosis. *Endothelium*. 2004;11:99–107.

9. Endemann DH, Schiffrin EL. Endothelial dysfunction. *J Am Soc Nephrol*. 2004;15:1983–1992.

10. Furchgott RF, Zawadzki J V. The obligatory role of endothelial cells in the relaxation of arterial smooth muscle by acetylcholine. *Nature*. 1980;288:373–376.

11. De Mey JG, Claeys M, Vanhoutte PM. Endothelium-dependent inhibitory effects of acetylcholine, adenosine triphosphate, thrombin and arachidonic acid in the canine femoral artery. *J Pharmacol Exp Ther* [Internet]. 1982;222:166 LP-173. Available from: http://jpet.aspetjournals.org/content/222/1/166.abstract

12. Kim F, Pham M, Maloney E, Rizzo NO, Morton GJ, Wisse BE, Kirk EA, Chait A, Schwartz MW. Vascular inflammation, insulin resistance, and reduced nitric oxide production precede the onset of peripheral insulin resistance. *Arterioscler Thromb Vasc Biol*. 2008;28:1982–1988.

13. Majed BH, Khalil RA. Molecular mechanisms regulating the vascular prostacyclin pathways and their adaptation during pregnancy and in the newborn. *Pharmacol Rev* [Internet]. 2012;64:540–82. Available from: http://www.ncbi.nlm.nih.gov/pubmed/22679221%5Cnhttp://www.pubmedcentral.nih.gov/articlerender.fcgi?artid=PMC3400831

14. Flammer AJ, Anderson T, Celermajer DS, Mark A, Deanfield J, Ganz P, Hamburg N, Thomas F, Shechter M, Taddei S, Vita J a. The Assessment of Endothelial Function - From Research into Clinical Practice. *Circulation*. 2012;126:753–767.

15. Rizzoni D, Porteri E, De Ciuceis C, Boari GEM, Zani F, Miclini M, Paiardi S, Tiberio GAM, Giulini SM, Muiesan ML, Castellano M, Rosei EA. Lack of prognostic role of endothelial dysfunction in subcutaneous small resistance arteries of hypertensive patients. *J Hypertens*. 2006;24:867–873.

16. Drexler H. Endothelial dysfunction: Clinical implications. *Prog Cardiovasc Dis*. 1997;39:287–324.

17. Chhabra N. Endothelial dysfunction : A predictor of atherosclerosis. *Interent J Med Updat*. 2009;4:33–41.

18. Hirase T, Node K. Endothelial dysfunction as a cellular mechanism for vascular failure. *Am J Physiol Heart Circ Physiol* [Internet]. 2012;302:H499-505. Available from: http://www.ncbi.nlm.nih.gov/pubmed/22081698

19. Birben E, Murat U, Md S, Sackesen C, Erzurum S, Kalayci O. Oxidative Stress and Antioxidant Defense. *WAO J*. 2012;5:9–19.

20. Chiarugi P, Pani G, Giannoni E, Taddei L, Colavitti R, Raugei G, Symons M, Borrello S, Galeotti T, Ramponi G. Reactive oxygen species as essential mediators of cell adhesion: The oxidative inhibition of a FAK tyrosine phosphatase is required for cell adhesion. *J Cell Biol*. 2003;161:933–944.

21. Giugliano D, Ceriello A, Paolisso G. Oxidative stress and diabetic vascular complications. *Diabetes Care* [Internet]. 1996;19:257—267. Available from: https://doi.org/10.2337/diacare.19.3.257

22. Kamata H, Honda S, Maeda S, Chang L, Hirata H, Karin M. Reactive Oxygen Species Promote TNF alpha-Induced Death and Sustained JNK Activation by Inhibiting MAP Kinase Phosphatases. *Cell* [Internet]. 2017;120:649–661. Available from: http://dx.doi.org/10.1016/j.cell.2004.12.041

23. Simon H-U, Haj-Yehia A, Levi-Schaffer F. Role of reactive oxygen species (ROS) in apoptosis induction. *Apoptosis* [Internet]. 2000;5:415–418. Available from: http://dx.doi.org/10.1023/A:1009616228304

24. Levi M, van der Poll T. Inflammation and coagulation. *Crit Care Med* [Internet]. 2010;38:S26-34. Available from: http://content.wkhealth.com/linkback/openurl?sid=WKPTLP:landingpage&an=00003246-201002001-00005%5Cnhttp://www.ncbi.nlm.nih.gov/pubmed/20083910

25. Esmon CT. The interactions between inflammation and coagulation. Br. J. Haematol. 2005;131:417–430.

26. Schalkwijk CG, Stehouwer CD. Vascular complications in diabetes mellitus: the role of endothelial dysfunction. *Clin Sci* [Internet]. 2005;109:143–159. Available from: http://www.ncbi.nlm.nih.gov/pubmed/16033329

27. Simsek S, Van Den Oever IAM, Raterman HG, Nurmohamed MT. Endothelial dysfunction, inflammation, and apoptosis in diabetes mellitus. *Mediators Inflamm*. 2010;2010.

28. Edelman D, Olsen MK, Dudley TK, Harris AC, Oddone EZ. Utility of hemoglobin A1c in predicting diabetes risk. *J Gen Intern Med*. 2004;19:1175–1180.

29. Andersson C, Van Gaal L, Caterson ID, Weeke P, James WPT, Couthino W, Finer N, Sharma AM, Maggioni AP, Torp-Pedersen C. Relationship between HbA 1c levels and risk of cardiovascular adverse outcomes and all-cause mortality in overweight and obese cardiovascular high-risk women and men with type 2 diabetes. *Diabetologia*. 2012;55:2348–2355.

30. Kaiser N, Sasson S, Feener EP, Boukobza-Vardi N, Higashi S, Moller DE, Davidheiser S, Przybylski RJ, King GL. Differential Regulation of Glucose Transport and Transporters by Glucose in Vascular Endothelial and Smooth Muscle Cells. *Diabetes* [Internet]. 1993;42:80 LP-89. Available from: http://diabetes.diabetesjournals.org/content/42/1/80.abstract

31. Eelen G, Zeeuw P de, Simons M, Carmeliet P. Endothelial cell metabolism in normal and diseased vasculature. 2016;116:1231–1244.

32. Wautier M, Chappey O, Corda S, Stern DM, Schmidt AM, Wautier J. Activation of NADPH oxidase by AGE links oxidant stress to altered gene expression via RAGE. *Am J Physiol Endocrinol Metab*. 2001;280:E685-94.

33. Esposito K, Nappo F, Marfella R, Giugliano G, Giugliano F, Ciotola M, Quagliaro L, Ceriello A, Giugliano D. Inflammatory cytokine concentrations are acutely increased by hyperglycemia in humans: Role of oxidative stress. *Circulation*. 2002;106:2067–2072.

34. Stentz FB, Umpierrez GE, Cuervo R, Kitabchi AE. Proinflammatory Cytocines, Markers of cardiovascular risks, oxidative stress, and lipid peroxidation in patients with hyperglycemic crises. *Diabetes*. 2004;1:2079–2086.

35. Rodríguez-Mañas L, Angulo J, Peiró C, Llergo JL, Sánchez-Ferrer A, López-Dóriga P, Sánchez-Ferrer CF. Endothelial dysfunction and metabolic control in streptozotocin-

induced diabetic rats. *Br J Pharmacol*. 1998;123:1495–502.

36. Skyler JS, Bergenstal R, Bonow RO, Buse J, Deedwania P, Gale EAM, Howard B V, Kirkman MS, Kosiborod M, Reaven P, Sherwin RS. Intensive glycemic control and the prevention of cardiovascular events: implications of the ACCORD, ADVANCE, and VA diabetes trials: a position statement of the American Diabetes Association and a scientific statement of the American College of Cardiology. *Circulation*. 2009;119:351–357.

37. Lasser C, Alikhani VS, Ekstrom K, Eldh M, Paredes PT, Bossios A, Sjostrand M, Gabrielsson S, Lotvall J, Valadi H. Human saliva, plasma and breast milk exosomes contain RNA: uptake by macrophages. *J Transl Med*. 2011;9:9.

38. Jimenez CR, Knol JC, Meijer GA, Fijneman RJA. Proteomics of colorectal cancer: overview of discovery studies and identification of commonly identified cancer-associated proteins and candidate CRC serum markers. *J Proteomics*. 2010;73:1873–1895.

39. Grigor'eva AE, Tamkovich SN, Eremina A V, Tupikin AE, Kabilov MR, Chernykh V V, Vlassov V V, Laktionov PP, Ryabchikova EI. Characteristics of exosomes and microparticles discovered in human tears. *Biomed Khim*. 2016;62:99–106.

40. Laske C, Stellos K, Kempter I, Stransky E, Maetzler W, Fleming I, Randriamboavonjy V. Increased cerebrospinal fluid calpain activity and microparticle levels in Alzheimer's disease. *Alzheimers Dement*. 2015;11:465–474.

41. Burger D, Thibodeau J-F, Holterman CE, Burns KD, Touyz RM, Kennedy CRJ. Urinary podocyte microparticles identify prealbuminuric diabetic glomerular injury. *J Am Soc Nephrol*. 2014;25:1401–1407.

42. Connor DE, Exner T, Ma DD, Joseph JE. Detection of the procoagulant activity of microparticle-associated phosphatidylserine using XACT. *Blood Coagul Fibrinolysis* [Internet]. 2009;20:558–564. Available from: http://content.wkhealth.com/linkback/openurl?sid=WKPTLP:landingpage&an=00001721-200910000-00012

43. Lötvall J, Hill AF, Hochberg F, Buzás EI, Di Vizio D, Gardiner C, Gho YS, Kurochkin I V, Mathivanan S, Quesenberry P, Sahoo S, Tahara H, Wauben MH, Witwer KW, Théry C. Minimal experimental requirements for definition of extracellular vesicles and their functions: a position statement from the International Society for Extracellular Vesicles. *J Extracell vesicles* [Internet]. 2014;3:26913. Available from: http://www.pubmedcentral.nih.gov/articlerender.fcgi?artid=4275645&tool=pmcentrez&rendertype=abstract

44. Witwer KWW, Buzás EII, Bemis LTT, Bora A, Lässer C, Lötvall J, Nolte-'t Hoen ENN, Piper MGG, Sivaraman S, Skog J, Théry C, Wauben MHH, Hochberg F. Standardization of sample collection, isolation and analysis methods in extracellular vesicle research. *J Extracell vesicles* [Internet]. 2013;2:1–25. Available from: http://www.pubmedcentral.nih.gov/articlerender.fcgi?artid=3760646&tool=pmcentrez&rendertype=abstract

45. Akers JC, Gonda D, Kim R, Carter BS, Chen CC. Biogenesis of extracellular vesicles (EV): Exosomes, microvesicles, retrovirus-like vesicles, and apoptotic bodies. *J*

Neurooncol. 2013;113:1–11.

46. Burger D, Schock S, Thompson CS, Montezano AC, Hakim AM, Touyz RM. Microparticles: biomarkers and beyond. *Clin Sci (Lond)*. 2013;124:423–441.

47. Denzer K, Kleijmeer MJ, Heijnen HF, Stoorvogel W, Geuze HJ, Advani RJ, Yang B, Prekeris R, Lee KC, Klumperman J, Scheller RH, Albert ML, Sauter B, Bhardwaj N, Amigorena S, Webster P, Drake J, Newcomb J, Cresswell P, Mellman I, Angelisova P, Hilgert I, Horejsi V, Arnold PY, Mannie MD, Bakke O, Nordeng TW, Berditchevski F, Tolias KF, Wong K, Carpenter CL, Hemler ME, Bock JB, Scheller RH, Callahan GN, Ferrone S, Poulik MD, Reisfeld RA, Klein J, Casciola-Rosen L, Rosen A, Petri M, Schlissel M, Davis JQ, Dansereau D, Johnstone RM, Bennett V, Denzer K, Eijk M van, Kleijmeer MJ, Jakobson E, Groot C de, Geuze HJ, Emerson SG, Cone RE, Emerson SG, Cone RE, Escola JM, Kleijmeer MJ, Stoorvogel W, Griffith JM, Yoshie O, Geuze HJ, Faigle W, Raposo G, Tenza D, Pinet V, Vogt AB, Kropshofer H, Fischer A, Saint-Basile G de, Amigorena S, Felder S, Miller K, Moehren G, Ullrich A, Schlessinger J, Hopkins CR, Fernandez-Borja M, Wubbolts R, Calafat J, Janssen H, Divecha N, Dusseljee S, Neefjes J, Fitter S, Sincock PM, Jolliffe CN, Ashman LK, Flamand V, Sornasse T, Thielemans K, Demanet C, Bakkus M, Bazin H, Tielemans F, Leo O, Urbain J, et al. Exosome: from internal vesicle of the multivesicular body to intercellular signaling device. *J Cell Sci* [Internet]. 2000;113 Pt 19:3365–74. Available from: http://www.ncbi.nlm.nih.gov/pubmed/10984428

48. van Balkom BWM, de Jong OG, Smits M, Brummelman J, den Ouden K, de Bree PM, van Eijndhoven MAJ, Pegtel DM, Stoorvogel W, Wurdinger T, Verhaar MC. Endothelial cells require miR-214 to secrete exosomes that suppress senescence and induce angiogenesis in human and mouse endothelial cells. *Blood*. 2013;121:3997–4006, S1-15.

49. Sheldon H, Heikamp E, Turley H, Dragovic R, Thomas P, Oon CE, Leek R, Edelmann M, Kessler B, Sainson RCA, Sargent I, Li J-L, Harris AL. New mechanism for Notch signaling to endothelium at a distance by Delta-like 4 incorporation into exosomes. *Blood*. 2010;116:2385–2394.

50. Feng B, Chen Y, Luo Y, Chen M, Li X, Ni Y. Circulating level of microparticles and their correlation with arterial elasticity and endothelium-dependent dilation in patients with type 2 diabetes mellitus. *Atherosclerosis*. 2010;208:264–269.

51. Morel O, Jesel L, Freyssinet JM, Toti F. Cellular mechanisms underlying the formation of circulating microparticles. *Arterioscler Thromb Vasc Biol*. 2011;31:15–26.

52. Amabile N, Heiss C, Real WM, Minasi P, McGlothlin D, Rame EJ, Grossman W, De Marco T, Yeghiazarians Y. Circulating endothelial microparticle levels predict hemodynamic severity of pulmonary hypertension. *Am J Respir Crit Care Med*. 2008;177:1268–1275.

53. Amabile N, Guérin AP, Tedgui A, Boulanger CM, London GM. Predictive value of circulating endothelial microparticles for cardiovascular mortality in end-stage renal failure: a pilot study. *Nephrol Dial Transplant*. 2012;27:1873–80.

54. Yeung T, Gilbert GE, Shi J, Silvius J, Kapus A, Grinstein S. Membrane

Phosphatidylserine Regulates Surface Charge and Protein Localization. *Science (80-)* [Internet]. 2008;319:210–213. Available from: http://science.sciencemag.org/content/319/5860/210

55. Meziani F, Tesse A, Andriantsitohaina R. Microparticles are vectors of paradoxical information in vascular cells including the endothelium: Role in health and diseases. *Pharmacol Reports*. 2008;60:75–84.

56. Jimenez JJ, Jy W, Mauro LM, Soderland C, Horstman LL, Ahn YS. Endothelial cells release phenotypically and quantitatively distinct microparticles in activation and apoptosis. *Thromb Res*. 2003;109:175–180.

57. Alexandru N, Badila E, Weiss E, Cochior D, St??pie?? E, Georgescu A. Vascular complications in diabetes: Microparticles and microparticle associated microRNAs as active players. *Biochem Biophys Res Commun*. 2016;472:1–10.

58. Peterson DB, Sander T, Kaul S, Wakim BT, Halligan B, Twigger S, Pritchard KA, Oldham KT, Ou J-S. Comparative proteomic analysis of PAI-1 and TNF-alpha-derived endothelial microparticles. *Proteomics* [Internet]. 2008;8:2430–2446. Available from: http://dx.doi.org/10.1002/pmic.200701029

59. Wolf P. The Nature and Significance of Platelet Products in Human Plasma. *Br J Haematol* [Internet]. 1967;13:269–288. Available from: http://dx.doi.org/10.1111/j.1365-2141.1967.tb08741.x

60. Hargett L a, Bauer NN. On the origin of microparticles: From "platelet dust" to mediators of intercellular communication. *Pulm Circ* [Internet]. 2013;3:329–340. Available from: http://www.pubmedcentral.nih.gov/articlerender.fcgi?artid=3757826&tool=pmcentrez&rendertype=abstract

61. Barry OP, Kazanietz MG, Praticò D, Fitzgerald GA, Pratico D. CELL BIOLOGY AND METABOLISM : Arachidonic Acid in Platelet Microparticles Prostaglandin Formation via a Protein Kinase C / Mitogen-activated Protein Kinase-dependent Pathway Arachidonic Acid in Platelet Microparticles Up-regulates Cyclooxygenase-2-depende. 1999;274:7545–7556.

62. Burger D, Turner M, Munkonda MNMN, Touyz RMRM. Endothelial Microparticle-Derived Reactive Oxygen Species: Role in Endothelial Signaling and Vascular Function. *Oxid Med Cell Longev*. 2016;2016:12–15.

63. Sabatier F, Roux V, Anfosso F, Camoin L, Sampol J, Dignat-George F. Interaction of endothelial microparticles with monocytic cells in vitro induces tissue factor-dependent procoagulant activity. *Blood*. 2002;99:3962–3970.

64. Rozmyslowicz T, Majka M, Kijowski J, Murphy SL, Conover DO, Poncz M, Ratajczak J, Gaulton GN, Ratajczak MZ. Platelet- and megakaryocyte-derived microparticles transfer CXCR4 receptor to CXCR4-null cells and make them susceptible to infection by X4-HIV. *AIDS*. 2003;17:33–42.

65. Burger D, Montezano ACAC, Nishigaki N, He Y, Carter A, Touyz RMRM. Endothelial Microparticle Formation by Angiotensin II Is Mediated via Ang II Receptor Type

I/NADPH Oxidase/ Rho Kinase Pathways Targeted to Lipid Rafts. *Arterioscler Thromb Vasc Biol*. 2011;31:1898–1907.

66. Jansen F, Yang X, Franklin BS, Hoelscher M, Schmitz T, Bedorf J, Nickenig G, Werner N. High glucose condition increases NADPH oxidase activity in endothelial microparticles that promote vascular inflammation. *Cardiovasc Res*. 2013;98:94–106.

67. Kay JG, Grinstein S. Sensing phosphatidylserine in cellular membranes. Sensors. 2011;11:1744–1755.

68. He Z, Zhang Y, Cao M, Ma R, Meng H, Yao Z, Zhao L, Liu Y, Wu X, Deng R, Dong Z, Bi Y, Kou J, Novakovic V, Shi J, Hao L. Increased phosphatidylserine-exposing microparticles and their originating cells are associated with the coagulation process in patients with IgA nephropathy. *Nephrol Dial Transplant*. 2016;31:747–759.

69. Santilli F, Marchisio M, Lanuti P, Boccatonda A, Miscia S, Davl G. Microparticles as new markers of cardiovascular risk in diabetes and beyond. *Thromb Haemost* [Internet]. 2016;116:220–234. Available from: http://www.embase.com/search/results?subaction=viewrecord&from=export&id=L611437229%0Ahttp://dx.doi.org/10.1160/TH16-03-0176%0Ahttp://rug.on.worldcat.org/atoztitles/link/?sid=EMBASE&issn=03406245&id=doi:10.1160%2FTH16-03-0176&atitle=Microparticles+as+new+

70. Nomura S, Ozaki Y, Ikeda Y. Function and role of microparticles in various clinical settings. *Thromb Res* [Internet]. 2008;123:8–23. Available from: http://dx.doi.org/10.1016/j.thromres.2008.06.006

71. Mallat Z, Benamer H, Hugel B, Benessiano J, Steg PG, Tedgui A. Elevated Levels of Shed Membrane Microparticles With Procoagulant Potential in the Peripheral Circulating Blood of Patients With Acute Coronary Syndromes. 2000;841–843.

72. Boulanger CM, Scoazec A, Ebrahimian T, Henry P, Mathieu E, Tedgui A, Mallat Z. Circulating microparticles from patients with myocardial infarction cause endothelial dysfunction. *Circulation* [Internet]. 2001;104:2649–2652. Available from: http://circ.ahajournals.org/cgi/doi/10.1161/hc4701.100516

73. Werner N, Wassmann S, Ahlers P, Kosiol S, Nickenig G. Circulating CD31+/annexin V+ apoptotic microparticles correlate with coronary endothelial function in patients with coronary artery disease. *Arterioscler Thromb Vasc Biol*. 2006;26:112–116.

74. Agouni A, Lagrue-Lak-Hal AH, Ducluzeau PH, Mostefai HA, Draunet-Busson C, Leftheriotis G, Heymes C, Martinez MC, Andriantsitohaina R. Endothelial dysfunction caused by circulating microparticles from patients with metabolic syndrome. *Am J Pathol* [Internet]. 2008;173:1210–9. Available from: http://www.pubmedcentral.nih.gov/articlerender.fcgi?artid=2543087&tool=pmcentrez&rendertype=abstract

75. Sabatier F, Darmon P, Hugel B, Combes V, Sanmarco M, Velut JG, Arnoux D, Charpiot P, Freyssinet JM, Oliver C, Sampol J, Dignat-George F. Type 1 and type 2 diabetic patients display different patterns of cellular microparticles. *Diabetes*. 2002;51:2840–2845.

76. Nozaki T, Sugiyama S, Koga H. Significance of a Multiple Biomarkers Strategy Including Endothelial Dysfunction to Improve Risk Stratification for Cardiovascular Events in Patients at High Risk for Coronary Heart Disease. *JAC* [Internet]. 2009;54:601–608. Available from: http://dx.doi.org/10.1016/j.jacc.2009.05.022

77. Zu L, Niu C, Li J, Shan L, Li L, Zhang D, Willard B, Zheng L. Proteomic research of high-glucose-activated endothelial microparticles and related proteins to Alzheimer's disease. *Diabetes Vasc Dis Res* [Internet]. 2015;12:467–470. Available from: http://journals.sagepub.com/doi/10.1177/1479164115597865

78. Klein CL, Kohler H, Bittinger F, Wagner M, Hermanns I, Grant K, Lewis JC, Kirkpatrick CJ. Comparative studies on vascular endothelium in vitro. I. Cytokine effects on the expression of adhesion molecules by human umbilical vein, saphenous vein and femoral artery endothelial cells. *Pathobiology*. 1994;62:199–208.

79. Burger D, Turner M, Xiao F, Munkonda MN, Akbari S, Burns KD. High glucose increases the formation and pro-oxidative activity of endothelial microparticles. *Diabetalogia*. 2017;

80. Yuana Y, Bo AN, Grootemaat AE, Pol E Van Der, Hau CM, Cizmar P, Buhr E, Sturk A, Nieuwland R. Handling and storage of human body fluids for analysis of extracellular vesicles. 2015;1:1–12.

81. Zhou H, Yuen PST, Pisitkun T, Gonzales PA, Yasuda H, Dear W, Gross P, Knepper MA, Star RA. Collection, storage, preservation and normalizationg of human urinary exosomes for biomarker discovery. 2008;69:1471–1476.

82. Trummer A, De Rop C, Tiede A, Ganser A, Eisert R. Recovery and composition of microparticles after snap-freezing depends on thawing temperature. *Blood Coagul Fibrinolysis*. 2009;20:52–56.

83. Szatanek R, Baran J, Siedlar M, Baj-Krzyworzeka M. Isolation of extracellular vesicles: Determining the correct approach (Review). *Int J Mol Med*. 2015;36:11–7.

84. Mehdiani A, Maier A, Pinto A, Barth M, Akhyari P, Lichtenberg A. An innovative method for exosome quantification and size measurement. *J Vis Exp*. 2015;50974.

85. Williams DB, Carter CB. Transmission Electron Microscopy: A Textbook for Materials Science [Internet]. 2009. Available from: http://www.loc.gov/catdir/enhancements/fy0820/96028435-d.html

86. Burger D, Kwart DG, Montezano AC, Read NC, Kennedy CRJCRJ, Thompson CS, Touyz RM. Microparticles Induce Cell Cycle Arrest Through Redox-Sensitive Processes in Endothelial Cells: Implications in Vascular Senescence. *J Am Heart Assoc*. 2012;1:e001842.

87. Bindea G, Mlecnik B, Hackl H, Charoentong P, Tosolini M, Kirilovsky A, Fridman WH, Pagès F, Trajanoski Z, Galon J. ClueGO: A Cytoscape plug-in to decipher functionally grouped gene ontology and pathway annotation networks. *Bioinformatics*. 2009;25:1091–1093.

88. Shannon, Paul; Markiel, Andrew; Ozier, Owen; Baliga, Nitin; Wang, Jonathan; Ramage,

Daniel; Amin, Nada; Schwikowski, Benno; Ideker T. Cytoscape: a software environment for integrated models of biomolecular interaction networks. *Genome Res*. 2003;

89. Laurindo FRM, Fernandes DC, Santos CXC. Assessment of superoxide production and NADPH oxidase activity by HPLC analysis of dihydroethidium oxidation products. *Methods Enzymol*. 2008;441:237–60.

90. Fernandes DC, Wosniak J, Pescatore L a, Bertoline M a, Liberman M, Laurindo FRM, Santos CXC. Analysis of DHE-derived oxidation products by HPLC in the assessment of superoxide production and NADPH oxidase activity in vascular systems. *Am J Physiol Cell Physiol*. 2007;292:C413–C422.

91. Briones AM, Cat AND, Callera GE, Yogi A, Burger D, He Y, Corrêa JW, Gagnon AM, Gomez-Sanchez CE, Gomez-Sanchez EP, Sorisky A, Ooi TC, Ruzicka M, Burns KD, Touyz RM. Adipocytes produce aldosterone through calcineurin-dependent signaling pathways: Implications in diabetes mellitus-associated obesity and vascular dysfunction. *Hypertension*. 2012;59:1069–1078.

92. Spiers A, Padmanabhan N. A guide to wire myography. *Methods Mol Med*. 2005;108:91–104.

93. Mulvany M. Contractile properties of small arterial resistance vessels in spontaneously hypertensive and normotensive rats.pdf. *Circ Res* [Internet]. 1977;41:19–26. Available from: http://www.ncbi.nlm.nih.gov/pubmed/?term=862138

94. Boulanger CM. ATVB in Focus The Many Faces of Endothelial Microparticles Franc. 2010;

95. Chen YY, Lin YJ, Chong E, Chen PC, Chao TF, Chen SA, Chien KL. The impact of diabetes mellitus and corresponding HbA1c levels on the future risks of cardiovascular disease and mortality: A representative cohort study in Taiwan. *PLoS One*. 2015;10:1–12.

96. Verma S, Buchanan MR, Anderson TJ. Endothelial Function Testing as a Biomarker of Vascular Disease. *Circulation*. 2003;108:2054–2059.

97. Ettelaie C, Su S, Li C, Collier MEW. Tissue factor-containing microparticles released from mesangial cells in response to high glucose and AGE induce tube formation in microvascular cells. *Microvasc Res* [Internet]. 2008;76:152–160. Available from: http://dx.doi.org/10.1016/j.mvr.2008.07.007

98. Abstract Book: ISEV 2017. *J Extracell vesicles*. 2017;

99. González-Quintero VH, Smarkusky LP, Jiménez JJ, Mauro LM, Jy W, Hortsman LL, O'Sullivan MJ, Ahn YS. Elevated plasma endothelial microparticles: Preeclampsia versus gestational hypertension. *Am J Obstet Gynecol*. 2004;191:1418–1424.

100. Redman CWG, Tannetta DS, Dragovic RA, Gardiner C, Southcombe JH, Collett GP, Sargent IL. Review : Does size matter ? Placental debris and the pathophysiology of pre-eclampsia. *Placenta* [Internet]. 2012;33:S48–S54. Available from: http://dx.doi.org/10.1016/j.placenta.2011.12.006

101. Baran J, Baj-Krzyworzeka M, Weglarczyk K, Szatanek R, Zembela M, Barbasz J,

Czupryna A, Szczepanik A, Zembala M. Circulating tumour-derived microvesicles in plasma of gastric cancer patients. *Cancer Immunol Immunother*. 2010;59:841–850.

102. Rupert DLM, Claudio V, Lässer C, Bally M. Methods for the physical characterization and quantification of extracellular vesicles in biological samples. *Biochim Biophys Acta - Gen Subj* [Internet]. 2017;1861:3164–3179. Available from: http://linkinghub.elsevier.com/retrieve/pii/S0304416516302756

103. Akagi T, Kato K, Hanamura N, Kobayashi M, Ichiki T. Evaluation of desialylation effect on zeta potential of extracellular vesicles secreted from human prostate cancer cells by on-chip microcapillary electrophoresis Evaluation of desialylation effect on zeta potential of extracellular vesicles secreted from. *Jpn J Appl Phys*. 2014;1:06JL01-4.

104. Janša R, Šuštar V, Frank M, Sušanj P, Bešter J, Manček-Keber M, Kržan M, Iglič A. Number of microvesicles in peripheral blood and ability of plasma to induce adhesion between phospholipid membranes in 19 patients with gastrointestinal diseases. *Blood Cells, Mol Dis*. 2008;41:124–132.

105. Ramakrishnan D, Hajj-Ali R, Chen Y, Silverstein R. Extracellular vesicles activate a CD36 dependent signaling pathway to inhibit microvascular endothelial cell migration and tube formation. *Arter Thromb Vasc Biol*. 2016;36:534–544.

106. Ghosh A, Li W, Febbraio M, Espinola RG, Mccrae KR, Cockrell E, Silverstein RL. Platelet CD36 mediates interactions with endothelial cell – derived microparticles and contributes to thrombosis in mice. 2008;118.

107. Deng F, Wang S, Zhang L. Endothelial Microparticles Act as Novel Diagnostic and Therapeutic Biomarkers of Diabetes and Its Complications: A Literature Review. *Biomed Res Int*. 2016;2016.

108. Bulut D, Maier K, Bulut-Streich N, Börgel J, Hanefeld C, Mügge A. Circulating Endothelial Microparticles Correlate Inversely With Endothelial Function in Patients With Ischemic Left Ventricular Dysfunction. *J Card Fail*. 2008;14:336–340.

109. Koga H, Sugiyama S, Kugiyama K, Watanabe K, Fukushima H, Tanaka T, Sakamoto T, Yoshimura M, Jinnouchi H, Ogawa H. Elevated levels of VE-cadherin-positive endothelial microparticles in patients with type 2 diabetes mellitus and coronary artery disease. *J Am Coll Cardiol* [Internet]. 2005;45:1622–1630. Available from: http://dx.doi.org/10.1016/j.jacc.2005.02.047

7.0. Copyright Release

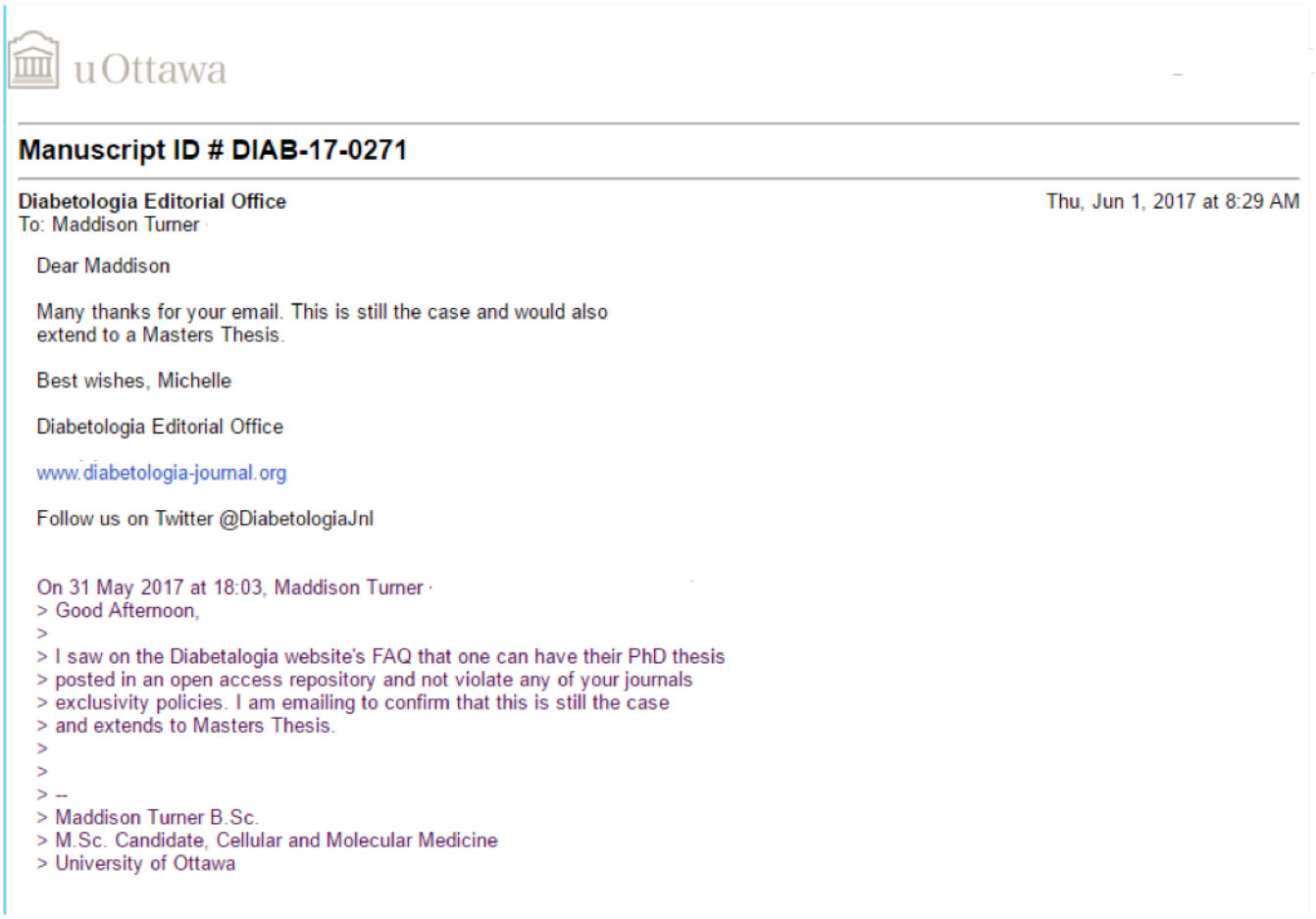

uOttawa

Manuscript ID # DIAB-17-0271

Diabetologia Editorial Office Thu, Jun 1, 2017 at 8:29 AM
To: Maddison Turner

Dear Maddison

Many thanks for your email. This is still the case and would also extend to a Masters Thesis.

Best wishes, Michelle

Diabetologia Editorial Office

www.diabetologia-journal.org

Follow us on Twitter @DiabetologiaJnl

On 31 May 2017 at 18:03, Maddison Turner
> Good Afternoon,
>
> I saw on the Diabetalogia website's FAQ that one can have their PhD thesis
> posted in an open access repository and not violate any of your journals
> exclusivity policies. I am emailing to confirm that this is still the case
> and extends to Masters Thesis.
>
>
> --
> Maddison Turner B.Sc.
> M.Sc. Candidate, Cellular and Molecular Medicine
> University of Ottawa

8.0. Curriculum Vitae

MADDISON E. M. TURNER

EDUCATION:

September 2015 – 2017	M.Sc. Candidate in Cellular & Molecular Medicine Supervisors: Dr. Dylan Burger & Dr. Chris Kennedy University of Ottawa, ON, Canada
September 2011 – 2015	Honours B.Sc. in Neuroscience and Mental Health Minor in Psychology Carleton University, Ottawa, ON, Canada

RESEARCH EXPERIENCE:

July 2013 –August 2015	Undergraduate Research Assistant Kidney Research Centre, Ottawa
June & July 2013	Undergraduate Research Volunteer Bruyère Research Institute

TEACHING ASSISTANT/PROCTORING:

April 2016	Anatomy Lab Proctor
January – April 2016	Introduction to Biochemistry Teaching Assistant
December 2015	Genetics Final Exam Proctor
November 2015	Anatomy & Physiology Midterm 2 Proctor

HONOURS & AWARDS:

2016	Canadian Diabetes Association Travel Award. Canadian Diabetes Association.
2016	Augostino Monteduro Endowement Fund. Kidney Foundation of Canada.
2015	Graduated on Dean's Honor List. Carleton University.
2014	Canadian Hypertension Congress Travel Award. Hypertension Canada.
2012	Varsity Athlete Scholarship. Carleton University.
2012	Ed Ireland Bursary Fund. Ed Ireland.
2011	Undergraduate Entrance Scholarship. Carleton University.

PUBLICATIONS

1. Burger D, **Turner M,** Xiao F, Munkonda MN, Akbari S, Burns K. "High glucose increases the formation and pro-oxidative activity of endothelial microparticles." *Diabetalogia.* (doi: 10.1007/s00125-017-4331-2. 2015 Impact Factor: 6.21).
2. Burger D, **Turner M**, Touyz R (2015) "Endothelial microparticle-derived reactive oxygen species: role in endothelial signaling and vascular function" *Oxidative Medicine and Cellular Longevity* (Manuscript ID: 5047954, 2016 Impact Factor: 4.49).

Submitted Manuscripts

1. Munkonda MN, Akbari S, Turner M, Holterman CE, Nasrallah R, Hébert RL, Kennedy CRJ, Burger, D (2017) "Podocyte-derived Microparticles Promotes Proximal Tubule Fibrotic Signaling Via p38 MAPK and CD36". In revision with *The Journal of Extracellular Vesicles.* (MS#: ZJEV-2017-0029)
2. Nash L, McFall E, Perozzo A, **Turner M**, Poulin K, De Repentigny Y, Burns J, McMillin H, Chardon J, Burger D, Kothary R, Parks R. "Survival Motor Neuron Protein is Released from Cells in Exosomes: A Potential Biomarker for Spinal Muscular Atrophy." Submitted to *Scientific Reports* (SREP-17-23995).

PRESENTED ABSTRACTS

Oral Presentations

1. **Turner M*,** Munkonda MN, Akbari S, Burger D (2016) "Effects of high glucose on endothelial microparticle formation, composition and activity". *Canadian Diabetes Association Meeting.* (October 2016, Ottawa ON. Canada).
2. **Turner M*,** Munkonda MN, Akbari S, Burger D (2016) "Effects of high glucose on endothelial microparticle formation, composition and activity". *Canadian Hypertension Congress.* (October 2016, Montreal QC. Canada).
3. **Turner M*,** Munkonda MN, Akbari S, Burger D (2016) "Effects of high glucose on endothelial microparticle formation, composition and activity". *International Society of Hypertension Scientific Meeting*. (September 2016, Seoul, South Korea) .

Poster Presentations

1. Munkonda MN, Akbari S, **Turner M**, Burger D* (2017). "Podocyte-derived microparticles induce pro-fibrotic responses in cultured human proximal tubule epithelial cells through CD36". *Canadian Society of Nephrology.* (May 2017, Montreal QC. Canada).
2. **Turner M,** Thibodeau JF, Holterman CE, Kennedy CRJ, Burger D*(2017). "Effect of a diabetic microenvironment on circulating microparticle protein composition". *Canadian Society of Nephrology.* (May 2017, Montreal QC. Canada).

3. **Turner M**, Thibodeau JF, Holterman CE, Kennedy CRJ, Burger D* (2017). "The diabetic microenvironment alters circulating microparticle protein composition". *International Society of Extracellular Vesicles*. (May 2017, Toronto ON. Canada).
4. **Turner M***, Munkonda MN, Akbari S, Burger D (2016). "Thrombospondin-1 and Its Glycocalyx Binding Partners Are Enriched in Endothelial Microparticles Formed under High Glucose Conditions". *American Society of Nephrology Kidney Week* (November 2016, Chicago IL. USA). Abstract published in *Journal of American Society of Nephrology. l* 27, 2016: TH-PO312.
5. Munkonda MN, Akbari S, **Turner M**, Burger D* (2016). "Podocyte-derived Microparticles Induce Pro-fibrotic Responses in Cultured Human Promote Proximal Epithelial Cells". *Canadian Diabetes Association/Canadian Society for Endocrinology and Metabolism Annual Meeting* (October 2016, Ottawa ON. Canada)
6. **Turner M*,** Munkonda MN, Akbari S, Burger D (2015) "Effects of high glucose on endothelial microparticle formation, composition and activity" *Canadian Institute of Health Research* (February 2016, Ottawa ON. Canada).
7. **Turner M*,** Munkonda MN, Akbari S, Burger D (2015) "Effects of high glucose on endothelial microparticle formation, composition and activity" *OHRI Research Day* (November 2015, Ottawa ON. Canada)
8. **Turner M*,** Munkonda MN, Akbari S, Burger D (2015) "Effects of high glucose on endothelial microparticle formation, composition and activity" *Cellular & Molecular Medicine Research Day* (October 2015, Ottawa ON. Canada)
9. Akbari S, **Turner M**, Munkonda MN, Burger D* "Proteomic analysis of microparticles derived from human endothelial cells and podocytes" *Canadian Hypertension Congress* (October, 2015, Toronto ON. Canada).
10. Akbari S, **Turner M**, Burger D* (2014) "Podocyte microparticles induce p38 activation and reactive oxygen species production in human cultured proximal tubule cells". *Joint Meeting of the European Society of Hypertension (ESH) and International Society of Hypertension (ISH)* (June 2014, Athenes Greece). Abstract published in the *Journal of Hypertension.*
11. Munkonda MN, Akbari S, **Turner M**, Burger D* (2015) "Microparticles-derived from human podocytes induce pro-fibrotic signaling in cultured human proximal tubule epithelial cells" *International Society for Extracellular Vesicles* (April 2015 Washington DC, USA)
12. Burger D*, Akbari S, **Turner M** (2014) "Podocyte microparticles: mechanisms of formation and downstream effects on proximal tubule epithelial cells" *American Society of Nephrology* (November 2014, San Diego CA. USA)
13. **Turner M**,* Akbari S, Burger D (2014) "De novo production of reactive oxygen species by endothelial microparticles". *Canadian Hypertension Congress.* (October 2014, Gatineau QC. Canada).
14. Akbari S*, **Turner M**, Burger D (2014) "Effects of podocyte microparticles on cultured human proximal tubule cells". *Canadian Hypertension Congress* (October 2014, Gatineau QC. Canada)

15. Akbari S, **Turner M**, Burger D* (2014) "Podocyte Microparticles Stimulate Reactive Oxygen Species Production and Induce p38 Activation in Cultured Human Proximal Tubule Cells". *Canadian Society of Nephrology* (April 2014, Vancouver).

UNIVERSITY VOLUNTEER EXPERIENCE

December 2016 – Present	The Ottawa Hospital Rehabilitation Center Volunteer
September 2016 – Present	Mentor for 4th year honour students writing their thesis
April 2016	Science Travels Volunteer (Outreach Science Trip to Kenora ON.)
September 2016 – Present	Let's Talk Science Volunteer
September 2016 – Present	Cellular & Molecular Medicine Student Council Representative
2014 – 2015	Neuroscience 4th year Mentor & Society Member
March 10 2015	Society for Neuroscience Brain Awareness Week Ambassador
June & July 2013	Undergraduate Research Volunteer (Bruyère Research Institute)
2011 – 2012	Carleton Science Student Success Centre First Year Representative